REVIEW ARTICLE

Remote thermometry with thermographic phosphors: Instrumentation and applications

S. W. Allison[a)]
Engineering Technology Division, Oak Ridge National Laboratory, Oak Ridge, Tennessee 37831-7280

G. T. Gillies[b)]
Department of Mechanical, Aerospace, and Nuclear Engineering, University of Virginia, Charlottesville, Virginia 22901

(Received 12 July 1996; accepted for publication 8 April 1997)

The temperature-dependent characteristics of fluorescence of several rare-earth-doped ceramic phosphors has made these materials the focus of a major effort in the field of noncontact thermometry over the past few decades. These ''thermographic phosphors,'' e.g., Y_2O_3:Eu, have been used for remote measurements of the temperatures of both static and moving surfaces, and have performed many other tasks that standard sensors (thermocouples, thermistors, etc.) cannot. The range of usefulness of this class of materials extends from cryogenic temperatures to those approaching 2000 °C. The instrumentation needed for this type of thermometry has followed many different lines of development, and this evolution has produced a wide variety of both field- and laboratory-grade systems that are now described in the literature. In general, the technique offers high sensitivity ($\approx$0.05 °C), robustness (e.g., stability of the sensor sample in harsh environments), and NIST traceability. In addition, such systems have been successfully adapted to make remotely sensed measurements of pressure, heat flux, shear stress, and strain. In this review, we summarize the physical mechanisms that form the basis for the technique, and then catalog and discuss the instrumentation-related aspects of several different remote thermometry systems that employ thermographic phosphors as the sensors.
[S0034-6748(97)01407-X]

I. INTRODUCTION

The measurement of temperature is a virtually ubiquitous requirement in all of the experimental and/or applied fields of science, engineering, and medicine. Moreover, the accelerating proliferation of technology in these areas has led to an ever-increasing variety of situations that requires knowledge of the temperature of some specimen, component, system or process. As a result, new approaches to the measurement of temperature are often called for, and this has led to the development of novel instrumentation systems aimed at meeting these needs.

One thermometric technique that is adaptable to the needs of a wide variety of situations is based on fluorescing materials, many of them phosphors. The thermal dependence of phosphor fluorescence may be exploited to provide for a noncontact, emissivity-independent, optical alternative to other more conventional techniques, e.g., those employing pyrometry, thermocouples, or thermistors. In fact, as discussed below, there are certain situations in which the advantages fluorescence-based thermometry has over other methods make it the only useful approach.

The general goal of this article is to review the methods of thermometry that are based on fluorescence, with emphasis on those employing a special class of materials known as thermographic phosphors. We shall concentrate on that class of techniques which is noncontact in nature, but extend the discussion to include the relevant features of contact-based devices when appropriate. The latter class of instrumentation consists largely of phosphor-tipped fiberoptic probes, the design principles and performance characteristics of which have been described in detail by Grattan and Zhang.[1]

We begin with an historical background that outlines the nature of phosphors and describes the evolution of phosphor-based thermometry from the 1940s to the 1980s, when the first commercial instruments appeared. Section II also includes some discussion of the various technical advances that have driven the developmental work in this area and a survey of the physical principles underlying the prototypical fluorescence thermometer. Following this, in Sec. III the practicalities of selecting a phosphor and bonding it onto the surface of interest are addressed. Section IV presents a description of the instrumentation needed to formulate the generic phosphor thermometry system and it then goes on to discuss the pertinent calibration methodologies. Thereafter, we catalog the characteristics of several different experimental arrangements, provide an overview of the many applications for this technique in Sec. V, and discuss its use in the sensing of quantities other than temperature in Sec. VI. Section VII compares the performance of phosphor thermometry with that of competing methods and ends with some sugges-

[a)]Electronic mail: s1a@ornl.gov
[b)]Also with Dept. of Biomedical Engineering, Health Sciences Center, University of Virginia, Charlottesville, VA 22908 and Div. of Neurosurgery, Medical College of Virginia, Virginia Commonwealth University, Richmond, VA 23298-0631.

TABLE I. Early phosphor thermometry systems and the applications for which they were used, from about 1950 to 1980.

Author(s)	Application	Phosphor/method	Design features	Range/uncertainty	(Year/Ref.)
Bradley	Measurement of temperature distributions on a flat plate in supersonic flow	ZnCdS:Ag,Cu (New Jersey Zinc Co.), intensity shift	Excitation at 365 nm, with fluorescence signal passed through a Wratten 2A filter	$\approx 8-25$ °C $\Delta T = \pm 0.2$ °C	1953; 15
Gross *et al.*	Development of phosphor-based detectors of thermal radiation	ZnS:Ag:Cl, CdS:Ag, intensity change and wavelength shift	Spectrometer used to monitor intensity variations and wavelength shift of heated target	$\approx 10-40$ °C No error estimate presented by author	1960; 38, 39
Czysz and Dixon	Thermal mapping of models in wind tunnels for heat transfer measurements	Radel in phosphors (U.S. Radium Co.), intensity shift	Surface thermocouple heat transfer gauges used to eliminate the absolute intensity measurements	Range unspecified $\Delta T \approx 0.2$ °C	1966; 21, 22, 23
Brenner	Measurement of collector junction temperatures in power transistors	Radel in No. 2090 (U.S. Radium Co.), intensity shift	ASA 400 B&W film used to sense fluorescence intensities with readout via microdensitometry	170–210 °C $\Delta T = 2.0$ °C	1971; 40
Fry	Integrated circuit	Radel in No. 3251	Fiberoptic conveys fluorescence from the IC to the detector	60–100 °C	1971; 41
Kusama *et al.*	Determination of the temperature of color television screens	Y_2O_2S:Eu, line shift of the $^5D_0 \rightarrow {}^7F_2$ transition	Sony Trinitron™ color CRT used, with beam currents varied from 100 μA to 1 mA per RGB channel	$\approx 25-50$ °C $\Delta T = 1.0$ °C	1976; 29
Pattison	Measurement of surface temperatures on rotating turbogenerators	Levy West W800 in transparent lacquer, intensity shift	Fiberoptic cables used to convey excitation and emission signals through the generator housing	No specific range or error estimate presented by author	1977; 42
Wickersheim and Alves	Measurements requiring isolation from or immunity to electromagnetic fields	Eu^{3+}-doped, rare-earth oxysulfides, line-intensity ratios	Prefiltration of UV excitation radiation by reflection from series of dichroic mirrors	9–250 °C Noise equivalent temp. = 0.025 °C	1979; 13
Sholes and Small	Thermal dosimetry during rf-hyperthermia treatments of malignant tumors	$Al_2O_3:Cr^{3+}$ (0.05%), decay lifetime of R lines	Mechanical shutter exposes the ruby sample to the excitation source for 10 ms intervals	35–46 °C (Partial range) $\Delta T = 0.3$ °C	1980; 17
Samulski and Shrivastava	Thermal dosimetry during rf-hyperthermia treatments of malignant tumors	Calcium and zinc–cadmium sulfides, integrated response	0.75 ms pulses from xenon lamp used as excitation; data were taken at 1 min intervals	20–50 °C Probe resolution = 0.3–0.4 °C	1980; 35, 36
McCormack	Measurements requiring electrically insulating and chemically inert probes	BaClF:Sm^{2+} decay lifetime of the $^5D_0 \rightarrow {}^7F_0$ transition	Plastic-clad silica fiber with NA = 0.25 was used to maximize the optical power collected	$\approx 25-200$ °C $\Delta T = \pm 5$ °C	1981; 37

tions for additional research aimed at extending the scope and precision of the technique.

II. BACKGROUND

A. The nature of phosphorescent materials

Prior to discussing those properties of phosphors important to thermometry, some relevant terminology should be introduced. Luminescence refers to the absorption of energy by a material, with the subsequent emission of light. This is a phenomenon distinct from blackbody radiation, incandescence, or other such effects that cause materials to glow at high temperature. Fluorescence refers to the same process as luminescence, but with the qualification that the emission is usually in the visible band and has a duration of typically $10^{-9}-10^{-3}$ s. Phosphorescence is a type of luminescence of greater duration, $\approx 10^{-3}-10^{3}$ s. Emission, luminescence, phosphorescence, and fluorescence are closely related terms and sometimes are used interchangeably.[2]

A phosphor is a fine white, or slightly colored, powder designed to fluoresce very efficiently. Color television and cathode-ray tube (CRT) displays employ phosphor screens that emit visible light then seen by the viewer. The source of energy that excites this fluorescence is a beam of electrons. Other examples of phosphor uses are in fluorescent spray paints, fluorescent lighting, photocopy lamps, scintillators and x-ray conversion screens. For the last, a beam of x rays provides the excitation. Other excitation sources are neutrons, gamma rays, ultraviolet (UV) light and, in some cases, visible light. Many different phosphors are manufactured for these and other applications. The lighting and display industries have provided the impetus for the study of thousands of phosphor materials over the last several decades, and much is known about them.[3–5]

In terms of their composition, phosphors may be divided into two classes: organic and inorganic. It is the latter that have primarily but not exclusively found use in thermometry. Inorganic phosphors consist of two components: a host inorganic compound and an activator (or doping agent) from which the light is emitted. Such materials do not have to be in the powdered form to be useful. Some phosphors are fabricated into macroscopic pieces of crystal or glass. In this form, certain of them are useful as solid-state laser media, and can be thought of as phosphors having a singular particle size and number density.[6–9] In this article, this more-generalized meaning of the term ''phosphor,'' including such macroscopic solids, is intended and used.

B. History of the technique

Research on luminescing materials was largely the domain of academia until the introduction of the fluorescent lamp in 1938.[4] After this, industrial laboratories were spurred into action by the growing need for commercial and domestic lighting, and also by the need for improved cathode

ray tubes. The degradation of luminescent output with increasing temperature can be a detriment in lamp applications. Therefore, thermal characterization was an important task for those studying phosphors. Neubert suggested phosphor use for thermometry as early as 1937.[10] Urbach[11,12] contributed to early phosphor thermometry approaches and applications. Table I surveys some of the developments important to phosphor thermometry from that time through the early 1980s.

In 1950, magnesium fluorogermanate was synthesized and used widely as a lamp phosphor.[3] Eventually, in the 1980s, it became the basis of commercial phosphor thermometry products.[13,14] One of the first thermometric applications of a phosphor known to us was by Bradley[15] who, in 1952, measured the temperature distribution on a flat wedge in a supersonic flow field using a phosphor provided by Urbach. Fluorescence thermometry in the 1950s is surveyed in a paper by Byler and Hays[16] of U.S. Radium Corporation (now USR Optonix, Inc.) which marketed the phosphors identified by Urbach. In 1960, Maiman invented the ruby laser, making use of the efficient fluorescence of ruby, in which Cr^{3+} is the activator in an Al_2O_3 host. Its temperature-dependent fluorescence properties have also been used for thermometry.[17–19] Trivalent rare-earth activators are now widely used, particularly Tb^{3+}, Eu^{3+}, and Dy^{3+}, in a variety of hosts. Interestingly, their use as laser media predates their use in television picture tubes. For example, Chang[20] operated a Y_2O_3:Eu laser in 1963. Renowned for its relative insensitivity to temperature changes, we shall describe below situations wherein this material has nevertheless found use in practical high temperature ($>600\ ^\circ C$) thermometry systems. Also in the 1960s, Czysz *et al.*[21–23] carried out phosphor thermometry on models in wind tunnels at the Arnold Engineering Development Center (AEDC), and this work has continued up to the present at this facility. They use phosphors originally investigated by Urbach. Wickersheim and colleagues[24–28] explored the possible use of rare-earth activated materials in a variety of applications, including lasers, scintillators, neutron detectors, x-ray detectors, etc. Their efforts at determining the temperature sensitivity of phosphors were fruitful, and this work eventually led to the commercialization of thermometry systems based on fluorescence. In 1977, Kusama *et al.*[29] exploited the thermal dependence of cathode ray tube phosphors to study electron-beam heating effects in color television applications.

It was not until the 1970s that the technological tools became generally available for exploiting the thermal properties of phosphor emission in a broader range of applications. For instance, high quality optical fibers capable of ultraviolet transmission appeared at that time. A group led by Leroux developed approaches based on utilizing the temperature dependence of fluorescence intensity and temporal response[30–33] for surface thermometry purposes. By applying phosphor to the tip of an optical fiber, Wickersheim and Alves[13] produced the optical analog of a thermocouple. In 1979, James *et al.*[34] mentioned several methods for extracting temperature from phosphor fluorescence measurements, including phosphor time decay determination. Also pursuing this approach were Samulski and colleagues[35,36] in 1980 and McCormack[37] in 1981.

Also, from the beginning, lasers have been useful in studying and characterizing phosphors. In many situations, a laser is the most appropriate source of illumination for phosphor-based thermography, even over relatively large surfaces. Moreover, the introduction of new types of lasers makes possible new classes of thermal phosphor applications. For instance, significant advances in phosphor thermometry in the 1980s were made possible by the advent of short-pulse UV lasers.

Finally, over the past 15 years, the many advances in electro-optics and solid state electronics have enabled measurements of fluorescence decay times at the nanosecond level. Prior to this, the capture and analysis of such fast pulses lay mostly in the domain of experimental nuclear and particle physics and required expensive, sophisticated instrumentation.

Histories and reviews of phosphor-based thermometry have been written by Dowell[43] and Baumann.[33] Thorough bibliographies of the literature covering the research on thermographic phosphors carried out in the 1980s have been assembled[44,45] and described[46] elsewhere; the present review seeks to provide additional citations to the more recent work.

C. Physical principles of fluorescence thermometry

It has long been generally known that the brightness or energy-to-light conversion efficiency of phosphorescent materials is temperature dependent. There are several ways this temperature dependence is manifested. Since a number of factors underlies the intrinsic nature of the fluorescence process, we begin with an overview of it.

1. The fluorescence process

The fundamental aspects of the fluorescence of solid materials are well understood. Prior to excitation, the material's electronic levels are populated in the ground state. A means to deposit energy in the material is required in order to excite a higher electronic state. This may be accomplished by exposure to electromagnetic radiation (visible or ultraviolet light, or x or gamma rays), particle beams (electrons, neutrons, or ions), or, as is the case for semiconductors, electrical current. The atomic configuration will not typically remain permanently excited but will either return to its ground state or assume an intermediate level. Conservation principles dictate that the amount of energy absorbed must also be released. This may be manifested by emission of a photon with energy equal to that of the energy-level difference, by transfer of energy via quantized vibrational (phonon) exchange in the material, or by other more complicated energy exchange mechanisms. Generally the lifetime of the excited state is short, on the order of only a few milliseconds. Neither the longer lived phosphorescent states nor the electron traps that may be present in some phosphors to varying degrees have typically been utilized for fluorescence thermometry. (The thesis of Peatman[47] presents additional discussion of the processes involved in these phenomena.)

Many of the materials that fluoresce efficiently and that have been found useful for a variety of laser, display, lighting, fluorographic, and thermographic applications are those for which the luminescence originates from a deliberately

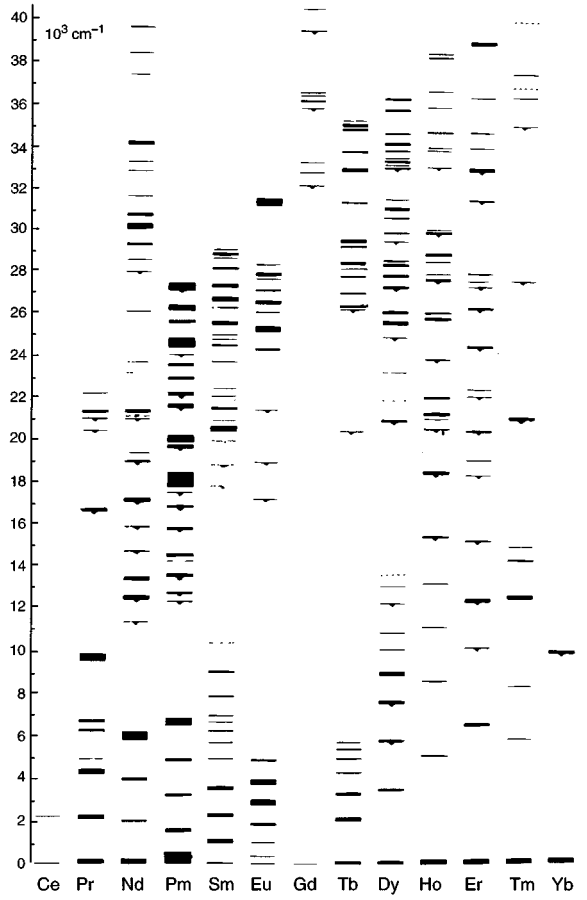

FIG. 1. The energy-level diagrams for various well-known states of some rare earths that are commonly used as the luminescent center in a thermometry application (after Ref. 48).

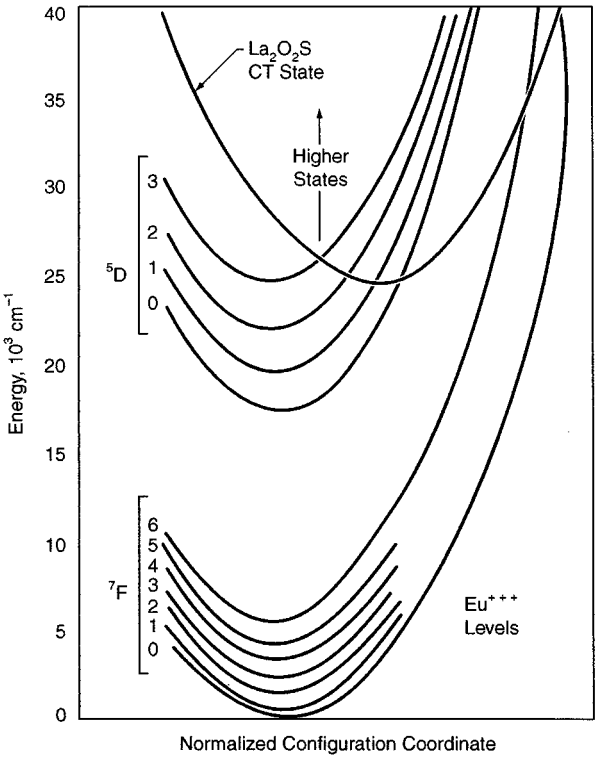

FIG. 2. The configuration coordinate diagram for La_2O_2S:Eu (after Ref. 49).

added impurity. As an example, a host material such as Al_2O_3 is transparent and nonfluorescent until Cr^{3+} is added. It then becomes red and fluoresces with properties that make it useful in the design of lasers and thermometry systems. The dopant concentration is usually a few percent or less so that nonradiative deexcitation exchange is minimized between the atoms (i.e., the luminescent centers are said to be isolated).

Fluorescence as referred to here is the emission occurring from electronic transitions and is usually in the visible region of the spectrum, but may also be in the near infrared (IR), as from Nd, or in the UV, as is typical for Gd. Figure 1 presents the energy-level diagrams for various well-known states of some rare earths that are commonly used as the luminescent center in a thermometry application.[48]

It is generally true that the fluorescence spectral properties of any material will change with temperature. This is so in part because the Boltzmann distribution governs the partitioning of the populations in the various participating vibrational levels of the ground, excited, and emitting states. A change in intensity distribution (including width and position of spectral lines) results since individual oscillator strengths vary in accordance with the selection rules and the Franck–Condon principle. Kusama *et al.*[29] explored this for Y_2O_2S:Eu. They measured the temperatures of a commercially available CRT using cathode ray stimulation and subsequent observation of the line shifts.

The temperature dependence of these processes can be striking when there is competition with states which contend for nonradiative deexcitation pathways. The rate of change of the population of an emitting state, 2, to a ground state, 1, is the sum of a constant, purely radiative spontaneous emission, $A_{1,2}$, and a nonradiative component, $W_{1,2}$, which is temperature dependent.

$$\kappa = 1/\tau = A_{1,2} + W_{1,2}. \tag{1}$$

The measured lifetime, τ, is the reciprocal of the decay rate, κ. One model for temperature dependence for some fluorescence materials used for thermometry is based on thermal promotion to a nonemitting electronic state followed by nonradiative relaxation. For europium phosphors, this is cited as a charge transfer state (CTS). This is illustrated in Fig. 2 which shows an energy level diagram based on the model that Fonger and Struck used to describe the thermal quenching of oxysulfides.[49,50] The excited electronic states of this atom are designated by ^5D_j where $j=0$, 1, 2, and 3. Once the particular ^5D_j state is excited, by whatever means, its population may be increased or decreased via several energy transfer pathways. A radiative transition to the ground state is possible with a probability rate of a_j. Note that this is the reciprocal of the spontaneous, unquenched lifetime. Depending on the temperature, the vibrational distribution in the excited state will be given by a Boltzmann distribution. At low temperature, states in resonance with the CTS seen in Fig. 2 are improbable. However, at higher temperature a significant fraction of the distribution will be at energies corresponding to the CTS and the transition to the CTS becomes

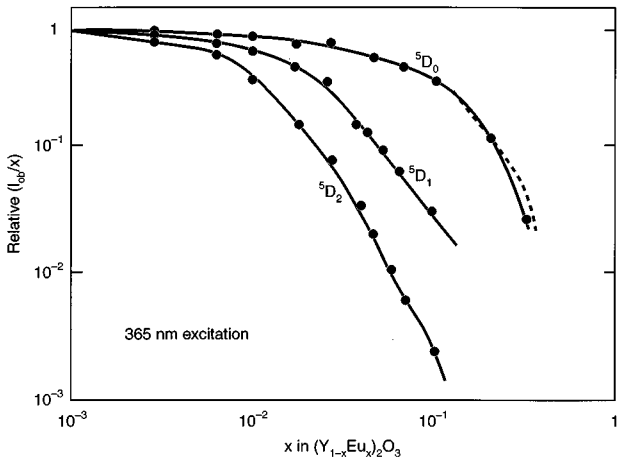

FIG. 3. Fluorescence intensity vs dopant concentration for Eu in a host of Y_2O_3 (after Ref. 57).

likely. The rate is therefore proportional to $e^{(-\Delta E/kT)}$ where ΔE is the energy difference between the ^5D_j and the CT states and the constant of proportionality is $a_{\mathrm{CTS},j}$. Feeding from the CTS down to the ^5D_j is possible. Deactivation from the CTS is nonradiative with a rate of a_{CTS}. The rates to and from the CTS, according to Fonger and Struck[49,50] are about $10^{11}-10^{12}$ s^{-1}, i.e., on the order of a lattice vibration rate. For continuous illumination, they note that the intensity is given by

$$I(T)=[a_j+a_j\cdot A\ \exp(-\Delta E/kT)]^{-1}, \tag{2}$$

where A is related to a_{CTS} and $a_{\mathrm{CTS},j}$, T is temperature, E is energy, and k is the Boltzmann constant. Other models for some phosphors have a similar dependence.

For some materials, a temperature-dependent deexcitation pathway based on multiphonon emission[51] exists. The multiphonon decay rate is

$$W_m=G[(1-e^{(h\nu/kT)})^{-N}\cdot e^{(-\gamma\cdot\Delta E)}], \tag{3}$$

where N is the number of photons required to reach the energy of the transition ΔE, and G and γ are characteristics of the material. This explanation has been applied to YAG hosts,[52–56] among others. If the energy difference between the ground and emitting states is four to five times the highest vibrational frequency of the surrounding lattice, then at sufficiently high temperatures a multiphonon transition is allowed and the transition probability is temperature dependent.

2. Factors influencing the fluorescence process

a. Dopant concentration. The parameters describing the luminescence characteristics of any given phosphor are dependent on the concentration of the activating impurity. Overall intensity, relative spectral distribution, decay time, rise time, and response to temperature are all affected to some degree. It is standard practice when characterizing the thermal response of a given phosphor to measure its brightness as a function of dopant concentration. A representative case[57] is shown in Fig. 3. These data illustrate that a high dopant concentration of Eu in a host of Y_2O_3 results in most of the luminescence being concentrated into the $^5D_0$ emission line (at 611 nm) that is of importance to color televisions. They further illustrate that the more activator centers there are in a phosphor, the more it will fluoresce, up to a point. However, when the concentration levels reach a certain point, another nonradiative deexcitation pathway becomes important. As the activator density is increased, the probability that an excited activator will transfer energy nonradiatively to a neighboring dopant ion increases. The arrival at a cutoff in this process is usually referred to as concentration quenching. For other dopants, even when in the same host, the concentration that produces the maximum brightness will be different. For example, the optimum concentration[4,58] of Sm or Dy in Y_2O_3 is 0.5%.

Generally, one seeks to maximize the brightness of the phosphor. With respect to thermometry applications, however, there are other considerations that may warrant the use of different strategies. For instance, at high concentrations the fluorescence decay profile may not be that of simple single-exponential decay. This is important for decay-time-based approaches since multiexponential and nonexponential decay profiles are more difficult to model. (Multiexponential decay is not necessarily a problem if measurements based on continuous line intensities are being made though.) These more complex wave forms can make calibration and data analysis difficult but not intractable. An example of this phenomenon arises in the use of YAG:Tb, which is a good phosphor for high temperature thermometry. At low concentrations, about 5/6 of the excitation energy drives the $^5D_3$ states (blue bands between 350 and 450 nm) while the remainder excites the $^5D_4$ states (blue-green and green bands at 488 and 544 nm). At sufficiently high dopant levels, there is an energy transfer from the higher to the lower states. Whereas the latter states exhibit exponential decay at up to 3% dopant concentration, the former appear to follow the Förster model,[59,60] the decay function for which is

$$x(t)/x(0)=\exp[-t/\tau-N/N_0(\pi t/\tau)^{1/2}], \tag{4}$$

where $N_0=3/(4\pi R_0^3)$ with R_0 being the critical distance for energy transfer ($\geqslant 1$ nm), N is the dopant concentration in number of atoms per cm^3, and τ is the unquenched spontaneous lifetime. The implications and role of the Förster model with respect to fluorescence thermometry are discussed by Dowell.[60,61] The spectral emission distribution can be a sensitive function of dopant concentration. An example of this[62] is illustrated in Fig. 4 for Y_2O_2S:Eu. At low Eu concentrations, the shorter wavelength lines are stronger than they are at higher concentrations. Kusama *et al.*[29] noted that this is particularly important for intensity based thermometry. They indicate that the $^5D_2$ emission of Y_2O_2S:Eu is especially sensitive to Eu concentrations. In comparing temperature dependent ratios of this line to a $^5D_0$ emission line, a difference of 0.1 mol % between samples will vary the ratio by about 5% and lead to an estimated error of 15 °C.

Finally, rise times are affected by dopant levels. This occurs especially when one level feeds another as noted by Hellier[63] and Rys-Williams and Fuller.[64] Table II contains the results of measurements of rise time versus Eu concentration in Y_2O_3.

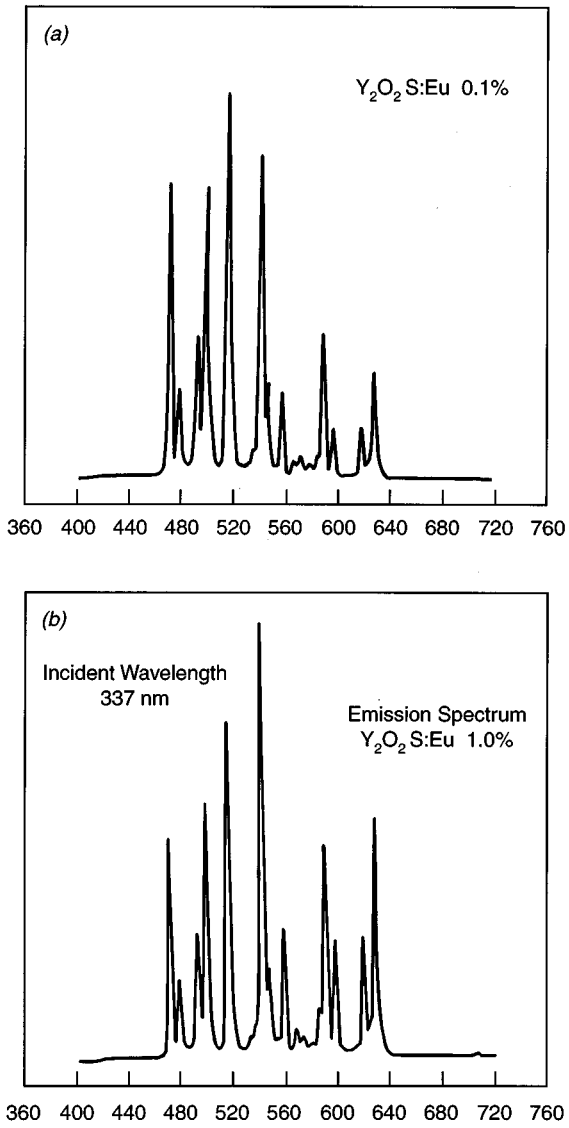

FIG. 4. Spectral emission distribution for Y_2O_2S:Eu at dopant concentrations of (a) 0.1% and (b) 1.0%.

b. Saturation effects. Saturation effects on YAG:Tb, another phosphor of interest in thermometry, are discussed by de Leeuw and 't Hooft.[65] A survey of the study of saturation effects is given there.

High incident fluxes, whether from laser, particle beam, or any other excitation source, can lead to luminescence saturation effects. When this occurs, phosphor efficiency changes as a function of the incident flux. In typical applications, this would manifest itself as a spurious temperature change if the flux were to increase to the point of causing saturation. An illustrative example arises in the description of saturation of Y_2O_3S:Eu by Imanaga *et al.*[66] where the relative dopant concentrations were 0.1% and 4%. A nitrogen laser (337 nm) focused to a spot size of about 1 mm^2 was used for short-duration (4 ns) photon excitation. For cathode ray excitation, a 10 kV electron beam of 5 μs duration was used and a number of effects were noted. With the latter form of excitation, the spectral distribution changed as a function of input fluence beginning at about 0.1 $\mu A/cm^2$. The effect was more pronounced at higher concentrations. Above a certain threshold value, overall intensity decreases, but for the lower concentration, this threshold value itself is lower and the rate of decrease is faster than at higher concentrations. Increasing the beam voltage, independently of beam current, will degrade the saturation of this phosphor according to Yamamoto and Kano.[67] Conversely, the situation may improve for some phosphors over a certain range, as observed in the case of ZnS and Zn_2SiO_4 by Dowling and Sewell.[68] For short-pulse excitation via nitrogen laser, the saturation effects are even more complex. Moreover, saturation is itself a temperature-dependent phenomenon. Generally, for all concentrations, the saturation thresholds are lower at higher temperatures. Saturation is enhanced at higher concentrations, but the rates will be different from one emission line to another.

There is evidence for a decrease in fluorescence decay time with increasing laser fluence. Imanaga *et al.*[66] suggest several possible mechanisms that may cause luminescence-saturation behavior in this case. Beam-induced temperature rise was ruled out as a possible cause since saturation was less pronounced for the most temperature-dependent emission lines, as well as for other reasons,[66] although this might be the dominant mechanism at work in other cases. Thermodynamic considerations, coupled with experimental studies, can help determine if beam-related effects will be a problem in a given situation. The results found by Imanaga *et al.*[66] may likely be due to the increased probability of having two excited dopant atoms in close proximity to each other. Evidently, when this occurs, an additional nonradiative de-excitation path is allowed. For instance, one of the excited atoms might transfer its energy to its neighbor, thus creating a doubly excited atom which nonetheless can emit only one fluorescence photon rather than two, thus decreasing the emission rate.

In most applications, one does not have the opportunity to deliver a surfeit of laser excitation due to the necessity for transporting beams long distances, usually over optical fibers which have limited fluence-handling capacity (see the discussion on the design of fiberoptic-based systems below). Saturation becomes a relatively important problem during laboratory calibrations, however, when a more nearly ideal optical arrangement is employed, i.e., one having higher available laser power and finer focusing.

Finally, we note that Raue *et al.*[69] have studied saturation effects in Tb-doped phosphors excited by cathode ray beams. They have developed a model that is consistent with the results of excited state absorption experiments carried out on a variety of these materials.

TABLE II. The dependence of the rise time of the $^5D_0 \rightarrow {}^7F_2$ transition on the concentration of Eu^{3+} in Y_2O_3:Eu^{3+} (after Ref. 64).

Eu^{3+} (mol %)	Rise time (ms)
0.27	0.320
1.00	0.267
2.20	0.189
3.30	0.130
5.56	0.060
11.10	0.020

c. Impurities. There are inevitably small amounts of undesired species in solid solution in the host material, and these change the atomic electronic environment experienced by the activators so as to either augment or hinder phosphor performance. For instance, at concentrations greater than 1 ppm, transition metal impurities will decrease phosphor brightness. This is because they absorb at wavelengths similar to those of the typical activators, thus effectively stealing excitation energy and decreasing the number of excited fluorescence centers. Moreover, nonradiative energy transfer from an excited activator to such impurities is efficient, thus increasing the decay rate and quenching the emission.

Even so, it is possible to mix powdered phosphors with a great variety of substances, from epoxies to inorganic binders, without affecting emission characteristics. In fact, ceramic binders can be flame sprayed, plasma sprayed, etc., as long as the result is a suspension of mixed materials. Properly chosen additives can also play a positive role. For example, addition of small amounts of Dy and Tb or Pr to Y_2O_3:Eu has the effect of decreasing the lifetime by as much as a factor of 3 with little or no change in quantum efficiency.[70] Having a faster response can be important when using phosphor thermometry to interrogate, e.g., a high speed rotating shaft that has a ''viewing time'' that is limited[71,72] (see Sec. IV C).

d. Sensitizers. A sensitizer is a material that, when added to a phosphor, increases the fluorescence output. Weber,[9] in a survey of rare-earth laser research, formulated a table of rare-earth ions that have been used as active laser media, and included in it the corresponding rare earths used as sensitizers for each. The sensitizing dopant will absorb energy and, rather than emitting fluorescence, it transfers its energy to the main dopant from which an optical transition occurs. For example, he notes that erbium has been found to be a sensitizer for dysprosium, while gadolinium is a sensitizer for terbium. A prospective sensitizer must exhibit no absorption at the emission wavelength of interest. It must also have absorption bands that do not steal excitation energy from the activator. Finally, it must have energy levels that are above the fluorescing line which feed the activator but which do not quench it.[73]

e. Quantum efficiency. Quantum efficiency, Q_E, is a parameter often used to help scale a phosphor's ability to produce bright light. Knowledge of the approximate quantum efficiency of a phosphor can aid in determining expected signal levels. Numerically, the quantum efficiency is the ratio of the number of photons absorbed by the phosphor to the number that are emitted. If $Q_E \geqslant 0.8$, a material is considered to be an efficient phosphor. Q_E is not as dominant a criterion for fluorescence thermometry as it is for lighting and display applications. Figure 5 presents the emission intensities for a variety of activators[4] in YVO_4. With Eu as an activator, the resulting phosphor is most efficient and useful in thermometry only above the quenching temperature of ≈ 500 °C. On the other hand, a Dy activator in this host will produce decay times that make the phosphor[62] useful in the range from 300 to 500 °C. (The ratio of two emitting lines in this case can also be used to make measurements at somewhat lower temperatures.) It is interesting to note that YVO_4:Nd is being used as a laser medium despite its low efficiency. For YVO_4:Eu, $Q_E = 68\%$ at the optimum concentration of 0.05 mol % (253.7 nm excitation) whereas $Q_E = 88\%$ for YVO_4:Dy at a concentration of 0.003 mol %. The latter is clearly a more efficient phosphor, except for the fact that the concentration dependence is more pronounced.

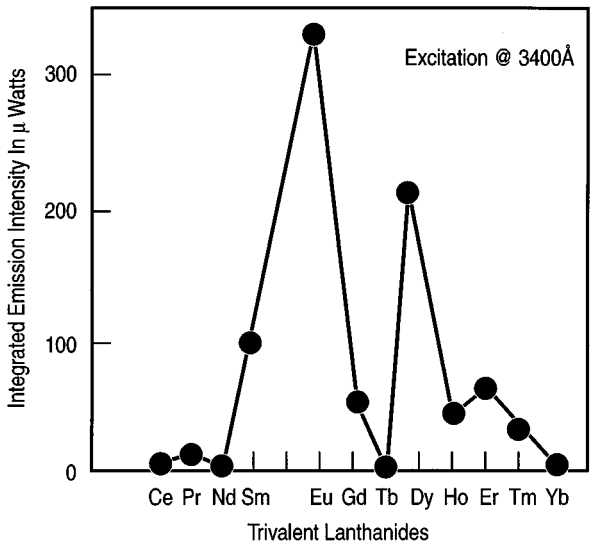

FIG. 5. The emission intensities for various rare-earth activators in YVO_4 (reprinted from R. C. Ropp, *Luminescence and the Solid State* (Elsevier Science, Amsterdam, 1991), p. 438, with the kind permission of Elsevier Science, Amsterdam.

Efficiency is a wavelength-dependent phenomenon. Therefore, if, e.g., instrumentation availability prevents the use of mid-UV excitation with a phosphor that happens to be efficient in that band, then a substitute material better suited to the wavelength of the excitation source should be used instead.

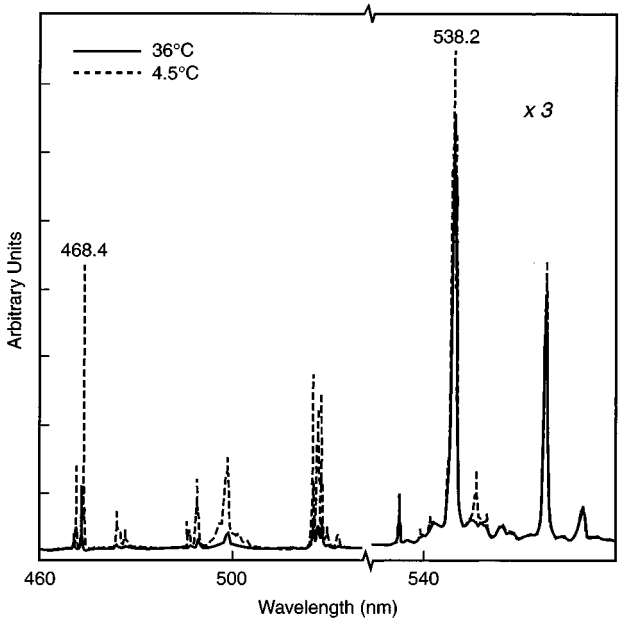

FIG. 6. Temperature dependence of La_2O_2S:Eu spectra.

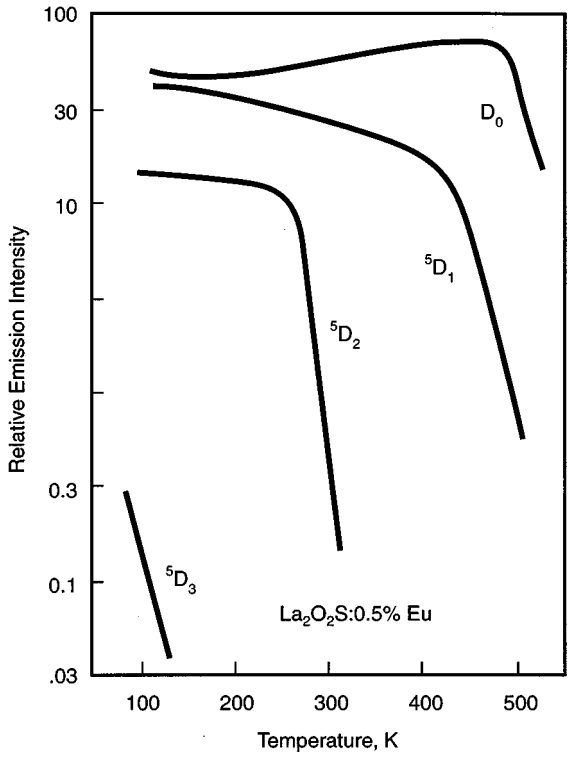

FIG. 7. Emission intensity vs temperature for La_2O_2S:Eu (after Ref. 49).

3. Fluorescence intensity

A comparison of the two spectra of La_2O_2S:Eu presented in Fig. 6 shows that the relative intensities of the lines near 465 and 512 nm are temperature dependent. In fact, it is generally the case that certain of the lines in these phosphors get weaker, i.e., become less bright, as the temperature of the material is increased. A plot of intensity versus temperature is shown in Fig. 7. Clearly, for this material, there is a region where the selected emission line is no longer sensitive to temperature change. At a particular value, viz., the ''quenching temperature'' (as discussed above), the strength of the emission line falls off drastically. The quenching temperatures and the slopes of the temperature dependencies usually differ for each type of phosphor and for each of the emission lines within the spectrum of a given phosphor. In some cases there may be an increase in intensity with temperature over a given range of temperatures, although the opposite is more typical.

4. Fluorescence lifetime

When a phosphor is excited by a pulsed source, the persistence of the resulting fluorescence can be observed providing that the length of the source pulse is much shorter than the persistence time of the phosphor's fluorescence. This is illustrated in Fig. 8 for the 514 nm line of La_2O_2S:Eu monitored at two different temperatures. The luminescence intensity decays exponentially in this case, according to the relation:

$$I = I_0 e^{-t/\tau}, \tag{5}$$

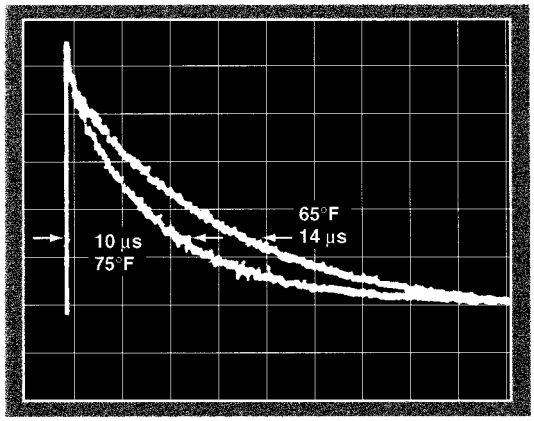

FIG. 8. Phosphor decay characteristics at 65 and 75 F (La_2O_2S:Eu at 514 nm).

where τ (the lifetime or decay time) is the standard $1/e$ ($\approx 37\%$) folding time for the fluorescence. The decay time is often a very sensitive function of temperature and, therefore, a determination of its value constitutes a very useful method of thermometry. A portion of a calibration curve for La_2O_2S:Eu is shown in Fig. 9 for three of its emission lines.

5. Fluorescence line shift

Each emission line is characterized by a wavelength for which the intensity is maximum. Its value may change slightly with temperature, and this is termed a line shift. Also, an emission line has a finite width, called the linewidth, which is often designated by the spectral width at half the maximum line intensity. Linewidth and line shift changes as a function of temperature are generally small, and are not often used in fluorescence thermometry. However, as previously mentioned, Kusama *et al.*[29] utilized this approach for cathode-ray-tube thermometry. As shown in Fig. 10, they

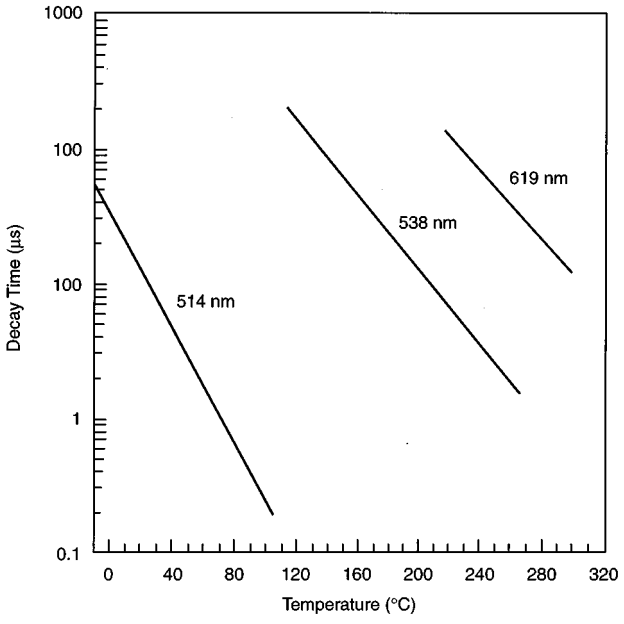

FIG. 9. Fluorescence decay time vs temperature for La_2O_2S:Eu.

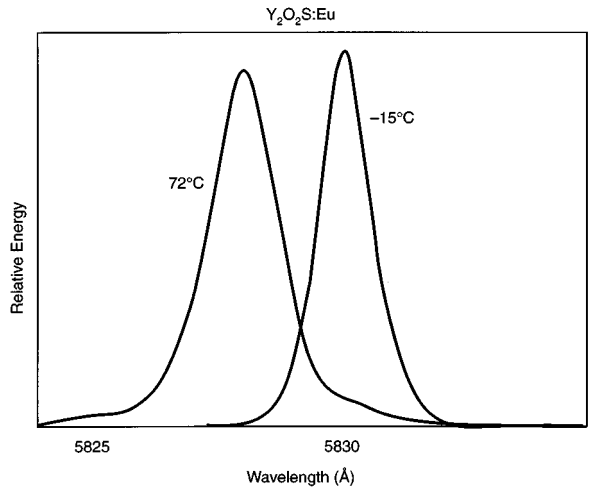

FIG. 10. Linewidth and line position at −15 and 72 °C for Y_2O_2S:Eu (after Ref. 29).

observed a shift to the blue of about 0.2 nm in going from −15 to 72 °C. The data they presented indicate that the line shift has an approximately quadratic dependence on frequency.

6. Absorption band and excitation spectra temperature dependence

The absorption spectra of many phosphors consist of a relatively broad band at the blue or ultraviolet end of the spectrum, along with sharper absorption features in the visible and near-IR. The sharper features are often due to atomic transitions of the dopant atom and, as noted above, exhibit some temperature sensitivity. The broad absorption band, however, since it results from direct interaction with the host, may show a more marked temperature dependence.

Bugos[74] studied the temperature-dependent excitation spectra of a number of thermographic phosphors. The results were very instructive, because an excitation spectrum provides an alternate means of determining the position and strength of absorption features in a material. Whereas absorption spectra are obtained by measuring the amount of light transmitted through a specimen as a function of wavelength, an excitation spectrum is determined by monitoring the intensity of an emission line while the excitation wavelength is varied. An example is shown in Fig. 11, which presents the temperature-dependent excitation spectra[75] of Y_2O_3:Eu. Within the resolution of the Perkin-Elmer model 650-10S spectrometer ($\approx$1 nm) used in that work, no discernible change was found in the atomic-transition bandwidths. Even so, the charge-transfer band is seen to move toward the red end of the spectrum by about 30 nm per 50 °C (i.e., 0.6 nm/°C.) The peak of the absorption for this material increases up to about 400 °C. (At this point, the heat generated by the oven placed inside the spectrometer could begin to affect the measurement.) We note that at room temperature this phosphor is not excited efficiently by standard sources such as a nitrogen laser (337 nm), a tripled YAG laser (355 nm), or a long-wavelength mercury vapor lamp (365 nm). Even so, these particular sources are efficiently absorbed at higher temperatures and are quite useful in that regime.

The temperature dependence of the absorption was exploited by Turley *et al.*[76] to infer the energy of a CO_2 laser by its heating of a phosphor sample. For this, constant excitation was applied to a YVO_4:Dy phosphor by a flashlamp that was filtered to illuminate at 365 nm. This wavelength is weakly absorbed by the phosphor at room temperature. When the 100 ns laser pulse heated the sample, the absorption and the resulting (detected) fluorescence increased in proportion to the incident laser energy. The associated tem-

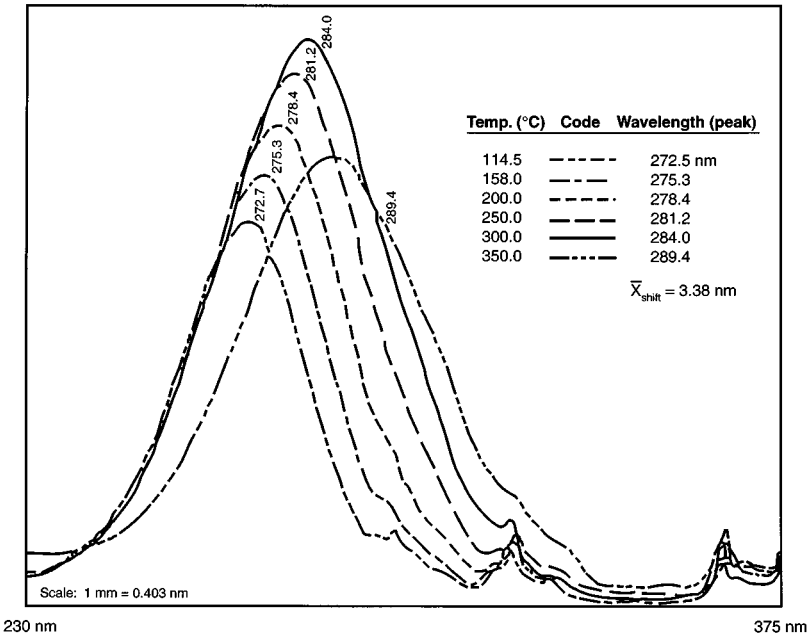

FIG. 11. The temperature-dependent excitation spectra of Y_2O_3:Eu, as measured with a Perkin-Elmer model 650-10S spectrometer with a resolution of approximately 1 nm.

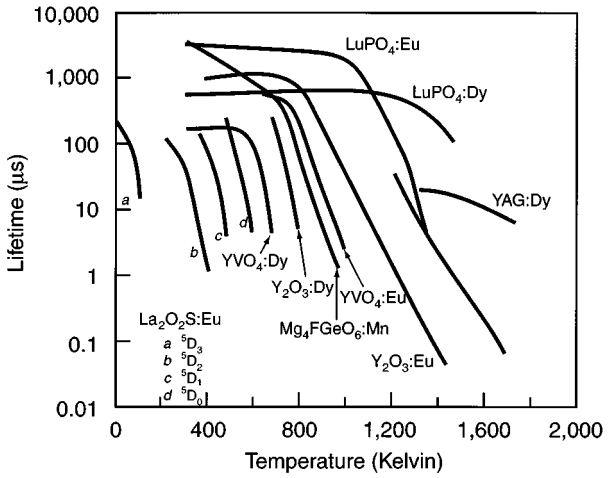

FIG. 12. Lifetime vs temperature of selected phosphors.

perature rise did not exceed the quenching temperature of the phosphor.

III. PRACTICAL DESIGN CONSIDERATIONS

A. Choice of phosphor

Figure 12 shows lifetime versus temperature for several materials that have been tested at Oak Ridge National Laboratory (ORNL) and collaborating institutions.[77] The choice of phosphor for a given application will clearly depend on the temperature range that must be spanned. However, there are additional considerations: chemical compatibility between phosphor, substrate and the surrounding environment, for instance, is one such concern. Fortunately, many of the most efficiently fluorescing materials are very inert; in fact, some are ceramics. As another example, the optical background in a given situation may make the wavelength of the phosphor emission an important consideration. In response, however, we note that one can select from among phosphors that emit anywhere between the infrared and the ultraviolet. Figure 13 shows blackbody emission curves for temperatures of 800, 1200, and 1600 K and prominent emission lines from Eu (611 nm) and Dy (488 nm). The blackbody emission at the latter wavelength is more than an order of magnitude less.

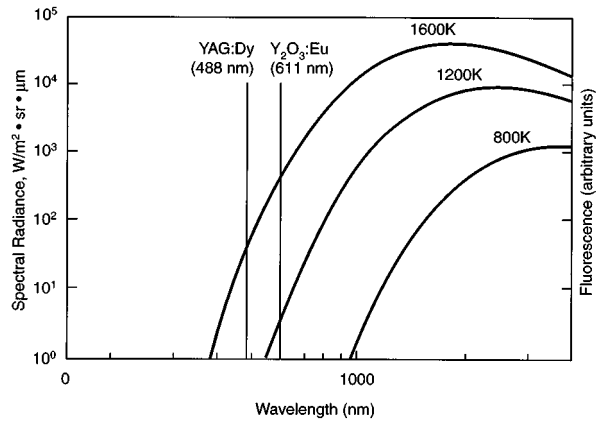

FIG. 13. The blackbody emission curves for temperatures of 800, 1200, and 1600 K along with prominent emission lines from phosphors containing Eu (611 nm) and Dy (488 nm).

It is sometimes convenient or even necessary to use a phosphor that emits several lines, each with differing thermal characteristics. As an example, YVO_4:Dy (the commercial lamp phosphor discussed above) exhibits bright bands centered at 575 and 484 nm. These lines have nearly identical lifetimes and both quench at $\approx 300\,^{\circ}C$. The intensities of both of these bands decrease slightly with temperature but another weak band (at ambient) at 453 nm grows instead.[62] We have found that where the temperatures were $<300\,^{\circ}C$, the intensity ratio of the 453 and 484 nm lines provides the means for making measurements down to room temperature if not below. Above that, the lifetime approach must be used.

B. Bonding techniques

In some critical applications, the most important technical problem encountered is that of bonding (i.e., securing adhesion of) the phosphor material to the surface undergoing thermography.[78] In what follows, we discuss the considerations that typically underlie the choice of a bonding method, describe the various phosphor bonding processes, and examine the techniques used to evaluate and test bonding strengths.

1. Selection criteria

There are several criteria to consider in choosing a bonding method. (1) The temperature range of interest will narrow the field of potential phosphors that might be used in a particular application, and it is a primary consideration in selecting a bonding method. As discussed below, some of the high-temperature bonding processes cannot be used with certain of the more chemically and thermally sensitive phosphors, thus further restricting the choice. (2) The heat flux through the measurement surface and the surface-to-air temperature differential may be important. The phosphor coating must be thin enough to approximate isothermal conditions across the layer. On the other hand, through careful design, a nonisothermal condition may be established in a two-phosphor layer, thus creating a heat-flux gauge as a result. The realization of one such gauge will be discussed later in the article. A thin coating is also a necessity when fast thermal transients must be measured. (3) Any thermal cycling of the surface and the temperature range of such cycles must be taken into account. The larger the temperature excursion, the more important it is to choose, test, and verify the appropriate adhesion method since cracking and breakup of the coating may otherwise result from repeated cycling. (4) The sample's physical environment can be a cause for concern. For example, if the measurement must be made in a high-temperature reducing or oxidizing atmosphere, the phosphor must be synthesized from chemically compatible materials. If erosion is perceived as a potential problem due to gas and particles impinging at high Mach numbers, then a smooth and physically durable coating is required. (5) The substrate characteristics must be such that neither contamination of the phosphor nor chemical reactions with it will occur. In addi-

tion, any substantial mismatch between the thermal expansion coefficients of the phosphor and the substrate becomes important, especially if rapid changes of temperature are expected. (6) The size of the surface to be thermographically characterized and/or its location will determine whether the coating must be applied in the laboratory with special equipment or whether it can be done on-site with appropriate portable equipment (a discussion of the various approaches follows below).

For the least critical applications, the coating process can be relatively straightforward. Typically, a slurry of phosphor is mixed with an available epoxy, paint, glue, or other binding agent and then brushed or daubed onto the surface. If the viscosity of the mixture is low enough, an air brush may also be used. The binder may have to be suitably transparent to ultraviolet light to achieve satisfactory excitation of the phosphor. Some surfaces have enough porosity or coarseness to even allow sufficient bonding with just the rubbing of the phosphor onto them. In general, however, one seeks to obtain a very robust coating and approaches more specialized than these are needed.

2. Surface preparation

Especially when adhesion is critical, surface cleanliness and roughness are important concerns. In such cases, an abrasive-blast spray (e.g., sand blasting) can both clean and appropriately roughen the surface. A certain degree of roughness is required to provide a ''tooth'' to which the phosphor/binder can adhere, since it is sometimes difficult to obtain adhesion to a surface that is too smooth. Even so, blast cleaning should proceed only until, e.g., the mirrorlike sheen of metallic surfaces is lost; pitting or other damage to the substrate should be avoided. Ultrasonic cleaning may be used as an alternative, as well as immersion or wiping with conventional solvents such as acetone. Scrubbing with nonabrasive brushes to remove grit may be beneficial, as is clean air blasting or spray. Last, the piece may be oven dried to minimize oxide formation and the absorption of water, and to bake off other contaminants.

3. Chemical bonding

When phosphor thickness is not an issue, chemicals with adhesive properties can be mixed and applied to the surface. Epoxies are typically useful to about 350 °C. Above this, a variety of binder materials, some based, e.g., on silicates, silicones and silicates, water-mix refractories, cellulosic mix, etc., can be used, possibly in excess of 1200 °C. Borella[79] summarizes some of the possibilities and issues with regard to their use. Sperex™M VHT-1 is representative of a variety of such binders that have been tested and put in use. With it, a cure time of 1 h each at 200, 400, and 600 °C in succession is recommended. In situations where this is not possible or practical, a room temperature cure may suffice if there is no exposure to solvents.

4. Electron-beam vapor deposition

Electron-beam (e-beam) vapor deposition produces thin yet durable coatings. The phosphor must be either cold or hot pressed into a disk shape and mounted in the deposition system's vacuum chamber. Instrumentation typical of this approach was assembled by Turley *et al.*[80] and consisted of a 61 cm (24 in.) vacuum chamber evacuated to 3×10^{-8} Pa (4×10^{-6} Torr), with the beam set to $\approx$40–50 mA at 6 kV. Deposition rates vary from about 0.2 to 2 μm/h. For e-beam deposition of phosphor films, significant increases in phosphor efficiency can be achieved by postprocess annealing. Among the advantages of this approach to bonding are the fine degree of film-thickness control that is obtainable, and the fact that there is no chemical binding agent present. The latter can absorb and scatter excitation light and generally decrease efficiency. The high temperatures generated at the e-beam point of impact irreversibly break down some phosphors, such as the oxysulfides, and postannealing in this case offers no benefit.

5. Radio frequency sputtering

The radio-frequency (rf) sputtering process is functionally similar to e-beam deposition of phosphors, and it has been investigated as a bonding method in a wide variety of situations.[81,82] In this technique, the target achieves the vapor phase by momentum exchange, a mechanical process. A postbonding anneal should also be carried out once the film is deposited to the proper thickness. In one carefully planned test of instrumentation designed to make temperature measurements in turbine engines, samples of three phosphors were prepared by the rf sputtering, e-beam, and chemical binder approaches. After annealing and exposure to 8 h in a turbine-simulating burner rig, the fluorescence efficiency of all specimens was compared to the pure phosphor powder. The results, presented in Table III, from Turley *et al.*,[80] showed a spread in the efficiencies that ranged from 30% to 60%. Since rf sputtering is a technique that is quite similar to e-beam deposition, there is not likely to be a general distinction or advantage of one approach over the other in terms of bonding performance.

6. Laser ablation

Laser-ablation deposition is a proven method for producing high temperature superconducting thin films.[83] High peak-power laser pulses are used to almost instantaneously deposit energy into a small-surface volume of a target. Within a few nanoseconds, the irradiated layer is brought to temperatures of $\geqslant$20 000 °C. The heated material is ejected at high speeds and may be collected on a suitable substrate. If the substrate is held above a certain temperature and subsequently cooled at a proper rate, then a high quality crystalline thin film results. Under different conditions, a thin amorphous layer is produced. Optical materials and certain phosphor-related materials such as ZnS, CdS, and Y_2O_3 have been deposited via laser ablation.[83,84]

C. Measurement strategy

The physical variables most typically measured when characterizing the temperature dependence of thermographic phosphors are the intensity, lifetime, and line shift of se-

TABLE III. Intensities and fractional survival of three different phosphors. (Note: Each phosphor was bonded by rf sputtering, chemical agent, and e-beam deposition.)

Sample/binder (μm)	Relative intensity[a]	% remaining
Y_2O_3:Eu		
Sputtered (1–2)	0.029	33
Sputtered (3–5)	0.16	56
Binder (<35)	0.089	24
Binder (≈ 35)	0.58	0.6
e-beam (9–13)	0.37	62
e-beam (24–27)	0.44	61
YVO_4:Eu		
Sputtered (1–2)	0.80	42
Sputtered (3–5)	1.01	52
Binder (<35)	1.9	49
Binder (≈ 35)	0.72	43
e-beam (9–13)	1.1	32
e-beam (24–27)	0.72	52
YAG:Tb		
Sputtered (1–2)	0.04	51
Sputtered (3–5)	0.097	58
Binder (<35)	0.56	5.4
Binder (≈ 35)	0.32	28
e-beam (9–13)	0.29	86
e-beam (24–27)	0.29	35

[a]The intensities were measured relative to the luminescence-peak heights of a hot-pressed sample of Y_2O_3:Eu that was used as a standard (after Ref. 80). Comparisons were made using a laboratory spectrophotometer.

lected spectral features. Any particular one of these may offer the best measurement strategy in a given application.

Intensity-based approaches generally require the simplest instrumentation and, therefore, tend to be the least expensive to implement. Their disadvantage lies in the difficulties associated with maintaining calibration, since this class of experimental arrangement requires mechanical, electrical, and environmental stability. When possible, the signal is normalized to a temperature-independent optical signal at another wavelength. Even when this is done, however, the chromatic differences of optical elements will make changes in element positions, thermal expansion, etc., significant sources of error. An example would be a temperature dependence of the chromatic dispersion of lenses used for fluorescence collection.

Fluorescence lifetime approaches do not suffer this disadvantage. On the other hand, analysis of the decay rate data is generally more complex. Economy-of-scale has made it inexpensive to obtain simple analog-to-digital electronic components of the kind needed to measure fluorescence intensities. However, fast multichannel devices such as the transient digitizer are needed for lifetime measurements, and they are still relatively costly. In any case, the decay rates are measured in terms of time and frequency, and the method therefore offers comparatively less uncertainty since these quantities can generally be determined with greater accuracy than can, e.g., optical intensities.

Methods based on changes in spectral features, such as shifts in line position or variation of linewidths, do not suffer

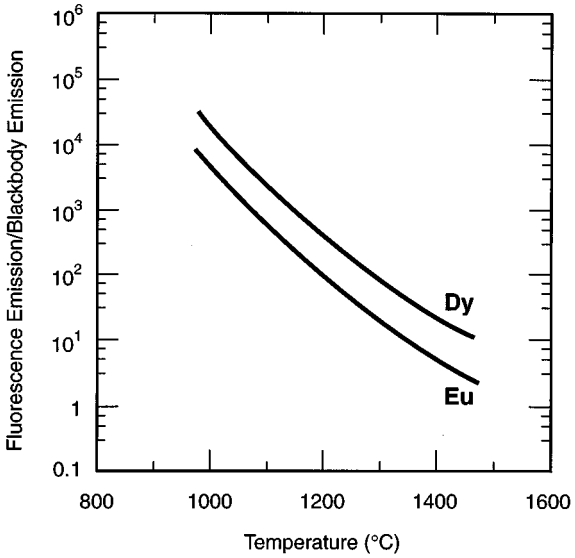

FIG. 14. The ratio of fluorescence to blackbody for Eu and Dy emission lines vs temperature.

the calibration problems of amplitude-based approaches. However, their principal drawback is that the thermal sensitivity of such effects is usually quite low relative to either the intensity or the lifetime approaches.

The decay time method is preferred when making high temperature measurements in situations where there is either a significant flame or combustion background, or where the blackbody emission is bright compared to the phosphor fluorescence. For measurement of moving surfaces, decay time methods do not require recalibration except at very high surface speeds. Measurements on a high speed motor are discussed later in this article, and in full detail elsewhere.[72] Figure 14 shows expected temperature dependence of the ratio of fluorescence to blackbody emission for two of the dopants most commonly used in phosphor thermometry, based on reasonable assumptions. This kind of (dc) background can be discriminated against quite effectively by spectral and temporal filtering. Clearly, in these situations, phosphors producing narrow-band emissions have an advantage over those that have a broader emission spectrum.

D. Particle size versus decay rate

There is a change in fluorescence lifetime with a change in the size of the phosphor particles. An example of this for small particles is cited by Christensen *et al.*,[85] where they observed an increase from 436 to 598 μs for a decrease in particle size from 0.42 to 0.11 μm. Because of this and other effects, the fluorescence decay time of virtually any phosphor sample may actually be a composite of the individual decay lifetimes arising from the distribution of particle sizes. From the purely practical standpoint, then, since some phosphor preparation methods yield large agglomerated particles, simply grinding the phosphor to a fine powder will affect the lifetime. This should not be overlooked during bonding studies and calibration procedures.

An explanation for this observation can be found in the quantum theory of the decay rates of electric-dipole emis-

sions. It predicts that the spontaneous lifetime of fluorescence is inversely proportional to the index of refraction of a fluorescent material.[85] Specifically, the refractive index n_c in the vicinity of an ion isolated in a crystal will be different from the index n_s in the vicinity of the same ion when it is located in a small (e.g., <600 nm) particle. The relationship between the indices and the lifetimes is

$$\tau_s = n_c \tau_c / n_s = \tau_0 / n_s, \tag{6}$$

where the τ_s, τ_c, and τ_0 are the lifetime values for the ionic emission in the small particle, crystal and vacuum cases, respectively. For small particles immersed in a liquid, the lifetime scales as the inverse of the index of refraction of the liquid.

E. Magnetic field effects

Only very large magnetic fields have a significant effect on the emission characteristics of thermographic phosphors. Mannik *et al.*[86] obtained calibration curves of decay time versus temperature for the 514 nm emission line of Y_2O_2S:Eu between 70 and 120 °C, first without an applied field and then in the presence of a 0.8 T field. They found no apparent change. At sufficiently high field strengths, of course, the degenerate energy levels will be split and, hence, the spectrum will change. This is the well-known Zeeman effect, a standard tool in spectroscopy for making energy level assignments and understanding spectra. As an example of the field strengths required to exhibit it, however, Alves *et al.*[26,27,87] needed a 5 T field to produce splitting of less than 0.5 nm for europium and terbium in some oxysulfides. Line broadening was an even smaller effect. Their experiments were done at liquid nitrogen and liquid helium temperatures to insure that the emission linewidths themselves were narrow enough to permit resolution of the effects.

F. Estimation of signal strength

Quantum yield is the ratio of the number of fluorescence photons produced in a particular emission band to the number of photons incident on the sample. Once the quantum yield is known or determined experimentally, signal levels may be estimated. The quantum yield may be measured by using an optical source to illuminate a phosphor sample at normal incidence. The resulting fluorescence is then monitored at some angle with respect to normal using a detector of known diameter so that the solid angle of collection is determined. It is assumed that the phosphor acts as a Lambertian source where, following Noel *et al.*:[88]

$$(A_0/A_1)\cdot I = I_0 \cos\theta, \tag{7}$$

Here A_0 is the area of the hemisphere defined by the distance of the detector surface from the phosphor, A_1 is the area of the detector surface, I_0 is the total amount of fluorescence emitted into the 2π-steradian hemisphere, and I is the fluorescence measured by the detector. This relation is used to determine I_0. The quantum yield, Q_y, is then simply

$$Q_y = I_0 / I_i, \tag{8}$$

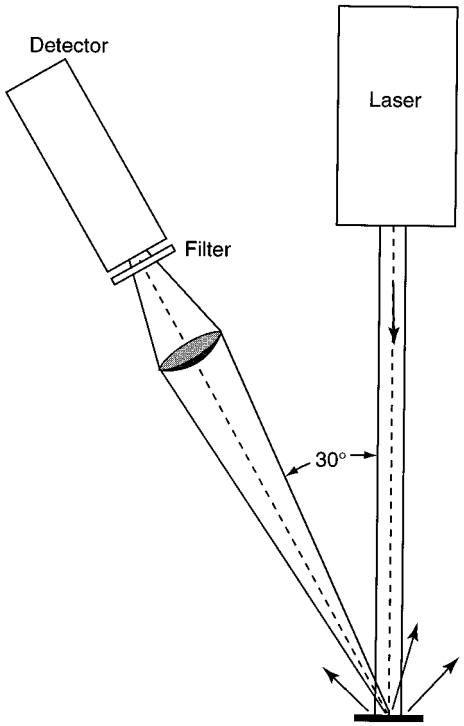

FIG. 15. The experimental arrangement for determining the fluorescence signal strength.

where I_i is the intensity of the source which strikes the phosphor. Noel *et al.*[88] followed this procedure to determine the quantum yield of the different emission bands of Gd_2O_2S:Tb, finding that $1\% < Q_y < 6\%$.

Knowing the quantum yield, the number of fluorescence photons striking a detector surface for any geometry can be calculated from the intensity of the incident source, the collection solid angle, and the losses introduced by intervening optical elements (such as lenses and filters), scatterers, and absorbers. The signal strength is subsequently a function of the detector sensitivity and the properties of the associated electronics.

An example is illustrated in Fig. 15 where a 3 mJ impulse of collimated light illuminates a phosphor layer, while a photomultiplier tube with an intervening lens and filter detect the fluorescence. Assuming that $Q_y = 5\%$, one can calculate the number of photons, F, detected and the size of the resulting signal:

$$F = (E/h\nu)\cdot Q_y \cdot \eta \cdot \Omega \cdot \cos\theta, \tag{9}$$

where $\Omega = \pi a^2/2\pi r^2$ is the solid angle subtended by the lens of radius a at distance r, η is the combined transmission efficiency of the lens and filter, and θ is the angle at which the fluorescence is observed with respect to the normal. Inserting the reasonable values of $E = 3\times10^{-3}$ J, $Q_y = 0.05$, $\eta = 0.3$, $a = 2.5$ cm, $r = 25$ cm, and $\theta = 30°$, we find that $F \cong 5\times10^{11}$ photons.

The efficiency, ϵ, with which a photocathode converts incoming photons to electrons is nominally 0.25. The liberated electron is multiplied by sequential collisions with the photomultiplier dynodes such that a gain, G, of between 10^4 and 10^7 is obtained. (The exact value of G will depend

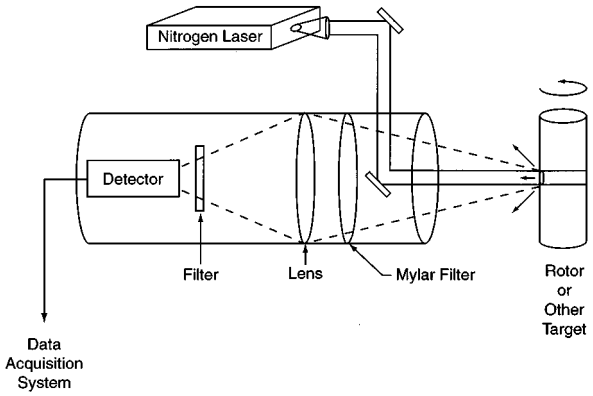

FIG. 16. The fundamental elements of a remote fluorescence thermometry system.

on the design of the photomultiplier tube, but the manufacturers typically list it in the specification sheets.)

The total charge, Q, that is detected is therefore

$$Q = F \cdot \epsilon \cdot G \cdot e, \tag{10}$$

where $e = 1.602 \times 10^{-19}$ C, the charge of the electron. For $G = 10^6$ and with 3 mJ of illumination, the total charge accumulated would thus be $Q \cong 2.8 \times 10^{-2}$ C. The temporal signature of the resulting detector current will be the familiar decaying exponential wave form of the laser-induced fluorescence process. The value of the detector current averaged over a 1 s period under conditions of continuous illumination in the present example would therefore be 2.8×10^{-2} C/s, i.e., 28 mA. This is, of course, a huge number and virtually any type of photodetector would be saturated or overdriven well before this. On the other hand, the example does illustrate that large numbers of photons (and, therefore, large signal levels) can be obtained rather straightforwardly.

IV. INSTRUMENTATION AND EXPERIMENTAL TECHNIQUES

A. The generic thermometry system

A phosphor-based optical thermometry system will generally consist of at least the following components: (1) a source of excitation energy, (2) a means to deliver the energy to the target (typically beam-steering elements or a fiberoptic bundle if the energy is in the optical spectrum), (3) a fluorescing medium that is bonded to the target and illuminated by the incident flux, (4) an optical system to collect and transport the fluorescence that is subsequently generated, (5) a detector or an array of detectors to monitor the fluorescence signal, and (6) a data acquisition and analysis system that ultimately yields the target's temperature. Figure 16 shows an elementary yet interesting illustrative example of this general arrangement. (The particular system depicted was designed to demonstrate the feasibility of making remote, noncontact measurements of the temperatures of and strains in high voltage devices such as transformers and other components in electrical substations in the Tennessee Valley Authority's power grid.)

In this arrangement, the energy source is a pulsed N_2 laser of 3 ns pulse length, emitting in the ultraviolet at 337 nm. Many other sources, either continuous or pulsed, can also be used to produce fluorescence. These include filament and arc lamps, various lasers and flashtubes and even flames, as well as beams of electrons, neutrons, ions, and other particles. In the present example, the laser light is guided to the fluorescent target by two mirrors. The first is front surfaced for beam steering, and the second is dichroic and hence able to reflect ultraviolet light while transmitting visible light. The excitation beam strikes a band of phosphor that is bonded onto a heated cylindrical brass target mounted on the shaft of a motor so that either static or dynamic measurements can be made. The fluorescence emanates from each illuminated point on the surface of the target into a solid angle of 2π steradians. A significant fraction of this light thus falls within the acceptance angle of the collection optics, in this case shown as a single plastic Fresnel lens of 15 cm diameter. Often, a more complex optical arrangement of lenses and/or fiberoptics is required for pulse delivery and fluorescence collection. The details depend on the particular experimental situation that must be addressed. The La_2O_2S:Eu phosphor used here produces simultaneous, bright emissions at several wavelengths across the visible spectrum. Because the temperature dependence of the lines varies, a narrow band pass filter is used to allow the desired wavelength to reach the detector, in this case a photomultiplier tube (PMT). The PMT, of course, transduces the fluorescence decay signal into an electrical wave form, which is then digitized, acquired, and analyzed. In this particular example, the computer-based analysis system averages the data, takes the logarithms of the averaged values, and calculates the slope of the resulting (presumably straight) line to arrive at the fluorescence decay time. The temperature of the targeted surface is subsequently revealed by access to a look-up table of decay times versus temperatures that is stored in memory.

For phosphors quenching at extremely high temperatures, the fluorescence pulses are typically quite fast, sometimes only nanoseconds in length. Moreover, the pulse heights will be very small if the fluorescence signal is weak. Because of these factors, PMTs are often the detectors of choice in phosphor thermography systems. The avalanche photodetector (APD) has been considered as an alternative to the PMT,[89] since it is equally fast in some applications.[90,91] It is not unusual, however, to find silicon photodiodes (photovoltaic mode), charge-coupled devices (CCDs) and other electro-optic detectors used in applications where the fluorescence signals are slower and stronger.

The source of illumination and the requisite detection equipment can typically be located at line-of-sight distances of up to ≈ 10 m from the target surface. For surfaces not accessible by a line-of-sight path, optical fibers may be used to convey the illumination and fluorescence signals. Moreover, the use of fibers opens the possibility of multiplexing of the excitation and decay pulses, thus increasing the number of regions on the target that can be monitored at the same time.

The equipment can be configured in a portable arrangement for field applications and, as mentioned above, temperatures of either static or moving surfaces can be determined. A general advantage of this and related remote

optical techniques is the freedom from electrical interference offered by the elimination of electromagnetically sensitive transducers at (and leads to and from) the target's location.

B. Calibration methodology

To provide valid thermometric data, the response of a phosphor-based temperature sensor must be calibrated against a known standard. At the very least, this requires that the quantity of interest (line intensity, lifetime, etc.) be measured as a function of temperature under known and repeatable conditions, with a stable and well-characterized thermometer serving as the reference. Ideally, the calibration measurements are carried out with a transfer standard. If so, and if the resulting data are taken under an appropriate protocol, traceability of the measurements to the International Temperature Scale[92] (ITS-90), as maintained by the various national standards laboratories,[93,94] can be established. Since these general features of the calibration process are largely the same for all the different fundamental methods of phosphor thermometry, we shall concentrate in what follows on just one of them, fluorescence lifetime versus temperature. Moreover, as per the defined scope of this review, most of the discussion is aimed at those experimental arrangements that are *noncontact* in nature. There remains, however, substantial overlap with the calibration processes applied to those systems that are not (e.g., a fiberoptic probe with phosphor bonded onto the tip, which is then touched to a surface or inserted into a volume).

Table V in Sec. VII A includes estimates of the postcalibration measurement errors claimed for several of the different phosphor thermometry systems that have been described in the recent literature. The sources of error that contribute to the overall error budget in the general case are discussed in the remainder of the text here.

1. General approach and thermal considerations

As discussed above, many different workers have investigated the temperature dependence of phosphor fluorescence lifetimes. The establishment of that dependence within the context of a quantitative calibration procedure calls for appropriate attention to details, many of which are not of particular interest in other measurement arrangements.

The overall scheme of a relatively generic calibration system[95] is shown representatively in Fig. 17. As might be expected, it constitutes a special case of the arrangement shown in Fig. 16. The phosphor to be evaluated is either bonded onto a substrate with a high-temperature adhesive, or a small amount of it is spread into a ceramic boat. This sample is then centered inside an oven or furnace and silica-clad optical fibers are used to convey the luminous signals into and out of the high-temperature cavity. The fibers are inserted into the cavity either through a viewport (if available) or directly through the thermal insulation of the walls. A dye laser driven by a pulsed nitrogen laser is used to tune the excitation signal to the wavelength of interest. The decaying-exponential fluorescence wave forms are gleaned from the optical background with a narrow band filter and converted to an electrical pulse train by a PMT. A useful variation involves substitution of a monochromater for the optical filter, thus extending the flexibility of the arrangement. A digital sampling oscilloscope or some other wave form acquisition device is used to collect the fluorescence signals, which are then analyzed by computer to yield the fluorescence lifetime. A signal derived from the laser pulse is used to trigger the data acquisition sweep of the oscilloscope, or otherwise enable a synchronous detection technique. The probe of the reference thermometer (e.g., a platinum resistance thermometer or a well-characterized thermocouple) is placed in direct contact with the phosphor sample inside the high-temperature cavity and its readings are stored in the computer, along with the decay time measurements, as the cavity is ramped up and down in temperature. In that way, a look-up table of decay times versus reference temperatures can be generated for use in the field.

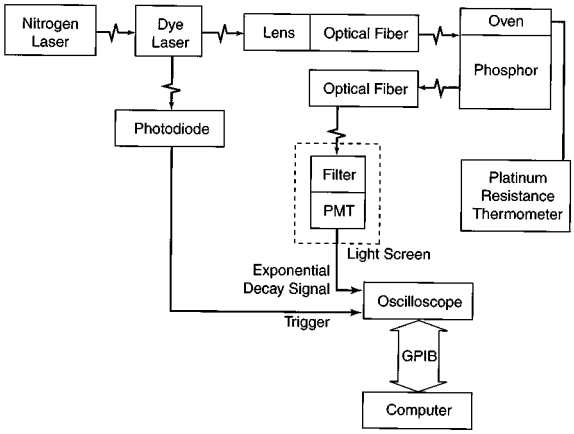

FIG. 17. The characteristic experimental arrangement used to calibrate the temperature dependence of fluorescence.

The overall accuracy and repeatability of the calibration depend critically on the quality and robustness of the reference standard and the stability and uniformity of the high-temperature cavity's thermal field. As a practical matter, then, the reference thermometer must typically be encased in an armored probe or it must have a surface passivation layer to minimize the effects of corrosion due to the oxidation that occurs during cycling to high temperatures. Bare-wire thermocouple junctions are particularly prone to a variety of well-known ''aging'' effects that degrade their measurement accuracy. For example, one study of type K thermocouples carried out in our laboratories[96] showed that shifts averaging 2% can arise in the temperature readings of thermocouples cycled even once between room temperature and 950 °C. Because of their ubiquity, however, few types of instrumentation have been studied as carefully as thermocouples and platinum resistance thermometers. As a result, there is a vast literature that describes them and provides guidelines for their (repeated) use in high-temperature environments.

A more insidious problem is that created by thermal gradients in the high-temperature cavity. The lack of a totally uniform distribution of temperatures within the oven or furnace means that it is generally necessary to keep the phosphor target and the reference thermometer fixed in place and in physical contact with each other during a calibration run. Moreover, the location of the target and the reference ther-

mometer within the thermal cavity should be noted so that they can be repositioned to those points during any subsequent recalibrations. To investigate this problem, Lutz developed a computer-aided data acquisition system that monitored an array of NIST-traceable thermocouples. It was used to map the thermal gradients of a Lindberg model 51442 box furnace driven by a model 59344 digital controller.[97] (This particular furnace was subsequently used in investigations of the metrological aspects of phosphor thermometry.[98]) The planar array of nine thermocouples was moved from the front to the back of the 19.05 cm×13.34 cm×35.56 cm furnace cavity with data then acquired at 15 mm intervals over the range from 50 to 1200 °C. The maximum measured gradients[99] at 100 and 1000 °C, respectively, were 0.11 and 0.73 °C/mm, with a measurement resolution of 0.02 °C/mm. A 12.5 mm (≈0.5 in.) uncertainty in the repositioning of the phosphor target relative to the reference thermometer could thus lead to an error of ≈1% at temperatures of 1000 °C, but the error can obviously be reduced if care is taken in repositioning the target.

One remedy to the thermal gradient problem (at least at relatively low temperatures) was devised by Crovini and Fernicola[100] at the Colonnetti Institute. They custom built an oven that was subsequently used in calibration studies of fluorescence decay thermometers. Their system is smaller in scale than the furnace described above, in that it has a temperature-regulated inner chamber ≈80 mm in length. The components inside this chamber consists of a phosphor-holder block and a mating piece in which are mounted the optical fibers used for illumination and observation. These blocks can be either fixed in place to insure positional repeatability or moved with precision relative to each other by a bellows-coupled drive to simulate noncontact thermometry conditions. The temperature uniformity over the specimen of phosphor under study is ±0.03 °C. This makes it possible to achieve resolution in temperature as sensed with their Nd:glass samples (Schott, type LG-760) of ±0.2 °C over the range from −20 to 100 °C. Circulating thermostatted fluid and an integral electrical heating coil are used to establish the oven's operating temperature over this range and even beyond (up to 200 °C, with a stability of ±0.03 °C). Further details of their work are available elsewhere.[101]

Other relevant studies include one in which a precursor to the prototypical calibration system shown in Fig. 17 was developed by Cates *et al.*[102] One of the more recent furnace-based calibration systems for Y_2O_3:Eu and YAG:Tb phosphor thermometers was described by Alaruri *et al.*[103] They used an alignment laser to adjust the positions of the beam-steering and collection optics relative to the phosphor target. Further discussion of thermal influences on the calibration methodology has been provided by Dowell *et al.*[95] and Gillies *et al.*[104]

2. Optical considerations

Several optical components are typically needed to handle the excitation and fluorescence pulses in a phosphor thermometry system. Thermal and mechanical instabilities in the optical fibers used in such systems include dopant migration, silica devitrification, and variation of the material's index of refraction, all produced by exposure to high temperature. At high enough temperatures, the small but finite absorption coefficients of some optical materials can even make them emitters, although typically in the infrared. These effects and related phenomena produce variations in the flux-guiding properties of the optical fibers, leading to loss of signal strength and/or resultant degradation of the measurement's signal-to-noise ratio (SNR).

Milcent and colleagues[105] have previously presented and discussed these problems and carried out a careful investigation of the way in which the properties of optical fibers used in thermometry systems change with temperature. In particular, they studied the response of both unclad and metal-clad silica fibers to thermal cycling and heating-rate variations. The fibers were part of an optical pyrometer that had a measurement range of 100–1000 °C. They found that heating the metal-clad fiber to ≈900 °C led to variations of up to 20 °C in the measured temperatures, i.e., deviations of ≈2.2%. When the silica-clad fibers were heated to 700 °C, the resulting variations in the measured temperatures were roughly the same, but the total power guided by the fiber decreased by about 4%.

Another source of thermomechanical damage to optical fibers that can affect the calibration (or even limit the usability) of remote thermometry systems is that resulting from the internal focusing of high energy pulses emitted by the excitation laser. Allison *et al.*[106] reviewed the work of others and explored this problem within the context of laser-induced fluorescence. They used a Nd:YAG laser to drive pulses of up to 8 mJ with 5 ns durations through fibers having core diameters ranging from 400 to 1000 μm. They found that the damage threshold for the fiber under study varied with the focal length of the coupling lens, the structure and composition of the fiber, and the nature of the fiber's surface preparation. They noted in particular that careful alignment of the input beam with the axis of the fiber is necessary to minimize the optical energy density at the first internal reflection point. Their results provide guidelines for the fluences that can be sustained at the input faces of both plastic-clad and hard-clad silica fibers. These findings become particularly significant when attempts are made to increase laser power in order to offset the rolloff in signal strength associated with either saturation phenomena or quenching of a particular phosphor at the high end of its useful temperature-sensing range. An extension of their study that assesses other attenuating mechanisms, such as those due to nonlinear optical effects in fiber materials, environmental influences, and ionizing radiation, is available elsewhere.[107] (As an aside, we note that the work on pulsed laser damage to optical fibers[106] led to the development of a method for generating self-imaging effects in such waveguides and the resulting conceptualization of a new potential means of sensing temperature.[108])

Maintaining careful alignment between components at points downstream from the input coupling face of the fiber is also an important consideration in maximizing the excitation intensity delivered to the phosphor target. In particular, reduction of the lateral offset between any two butt splices in the optical fiber pathway is of particular importance. Dowell *et al.*[109,110] measured the lateral offset power losses of a va-

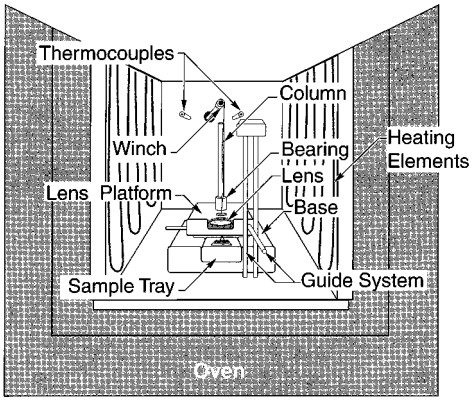

FIG. 18. A kinematic lens displacement device used to adjust the position of optical elements within high-temperature furnace cavities.

riety of step-index optical fibers scanning point sources in order to quantify this problem. Their results are presented as graphical mappings of the attenuation in transmitted power versus the size of the lateral offset. Quantitative estimates of the residual misalignment that can be tolerated in a given experimental arrangement can thus be made, and all of this allows inference of how the SNR is affected by misalignment.

In many situations a lens is used to focus the light emerging from the optical fiber onto the phosphor target, and also to collect the fluorescence signal and couple it into the return fiber. Should the lens be inside the high-temperature cavity, its figure may change due to thermal expansion, as will the dimensions of the standoffs or other structural elements that hold it. If these changes produce large enough shifts in the position of the excitation beam's focal point relative to the phosphor target, then the level of excitation energy density at the surface of the target will begin to decrease. At very high temperatures, the fluorescence signals for most phosphors are typically quite weak due to quenching, whereas the background glow due to blackbody emission is relatively strong. Since a decrease in the available excitation energy results in a weaker fluorescence signal, thermomechanically driven shifts in the position of the focal point of the coupling lens may thus limit the range over which the phosphor thermometry system can be fully calibrated.

To deal with the problem of obtaining precise positioning of a lens inside a high-temperature cavity, Hanft *et al.*[111] developed the kinematic lens displacement device shown in Fig. 18. It is in essence a high-temperature translation stage, consisting of alumina and ceramic-foam components. The lens is placed into a holder that can be maneuvered up and down along a linear slide rod by turning a winch that plays out an alumina thread that is attached to the holder. The shaft of the winch extends through the insulated walls of the furnace and can thus be rotated from outside the high-temperature cavity. The phosphor sample to be calibrated is placed in a removable tray located in the base of the device. As shown in Fig. 18, a set of vertical guides (seen mounted on the base) is provided in order to keep the lens holder from rotating about the axis of the linear slide rod. In this arrangement, one rotation of the winch corresponds to ≈ 2.4 cm of travel by the lens holder. The overall positional repeatability of the device is better than 1 mm and, when at temperature, the system can be adjusted at a maximum rate of ≈ 12 rotations per min. This relatively simple mechanism provides a very satisfactory means of adjusting the position of the lens placed inside a phosphor thermometry calibration furnace.

As discussed in Sec. IV A, the transducer of choice in most phosphor thermometry systems is a photomultiplier tube, although avalanche photodiodes and other kinds of detectors are also employed. The types of noise, drift, and other uncertainties that arise when making measurements with such devices are well understood and will not be dwelt upon here. We note only that Dowell carefully investigated the performance characteristics of the PMTs used in his metrological-grade phosphor thermometry systems, and detailed discussions (including error assessments) of his findings are available elsewhere.[98,110]

3. Signal processing considerations

When making fluorescence lifetime measurements, a decaying exponential wave form with noise and dc offset is typically presented to the signal processing system. Composite signals consisting of multiexponential wave forms are encountered for some phosphors (see Sec, II C/2a), and this can complicate the calibration process. The more routine problem, though, is that of measuring the parameters of a single-exponential wave form.

Two broad central issues that arise in synthesizing an appropriate signal processing system are (1) the choice of the data acquisition and signal averaging devices and (2) the choice of the algorithm used to analyze and reduce the data. These issues have been faced many times in the physical, biological, and engineering sciences with the result that a vast effort has gone into the creation of methodologies that permit the precise estimation of the $1/e$ lifetimes of exponentially decaying signals. An overall assessment of the general problem is far beyond the scope of this article, and we instead comment briefly on only those parameter estimation techniques that have been developed and used within the context of calibrating phosphor thermometry systems. Guides to the extensive literature on the more general problem are available elsewhere.[98,112]

As an introductory historical note, we mention some of the early work done on laser-induced fluorescence at ORNL. That effort focused on the development of synchronous detection techniques for making precise measurements of the heights of exponential pulses in the presence of background noise. Lock-in amplifiers are the standard class of instrument used for this purpose. They have output measurement errors[113] that are inversely proportional to the SNR of the raw signal over the range $10^{-3} < \mathrm{SNR} < 1$, i.e., over the ''worst case'' range of highly corrupted signals, a consequence of their function as a bandwidth reduction filter.[114] Several workers, both before and since that time, have incorporated phase-sensitive detection and frequency domain techniques into phosphor thermometry systems, and a few representative examples are mentioned elsewhere in this article.

Calibration studies of some of the various lifetime measurement techniques benefited from this early work at ORNL in that the methodology of summing noise onto known signals,[113] while certainly not a novel idea, nevertheless allowed for the identification of many types of systematic errors in the instrumentation chains used to measure the fluorescence signals. For instance, when a Tektronix 7854 digital sampling oscilloscope (DSO) was used to acquire the fluorescence signal, average it, and then calculate the exponential decay time constant, the resulting measurement errors were found to decrease with continued averaging, but not without limit.[115] Exploration of this point led to the establishment of an optimal sampling strategy for this DSO as a function of the SNR at the input of the instrument. Similar studies were carried out with an EG&G/PARC Corp. model 162 boxcar averager[110] and a novel phase-locked digital filter[116] for the purpose of evaluating the measurement errors intrinsic to these devices. The general conclusion of this line of work was that, while it was possible to characterize the systematic errors in any of the devices used to recover a wave form from noisy data, the most accurate overall system calibrations required postrecovery assessment of the computational errors in the time-constant estimation algorithm as well.

To that end, a series of studies examining the errors in a variety of algorithms running on the thermometry system's host computer (see Fig. 17) was undertaken. This series began with a preliminary empirical investigation of the problems encountered in making a simple least-squares fit of a two-parameter exponential curve to the phosphor fluorescence data.[117] A more sophisticated subsequent study involved numerical Monte Carlo testing of both two-point and nonlinear least-squares algorithms, with Gaussian-distributed noise added onto the simulated signals.[118] Comparing the two algorithms at a simulation SNR of $\sim 40{:}1$, the two-datapoint estimation had an uncertainty of about 4%, while that of the least-squared error estimation was only 0.1%. The comparison of the theoretical predictions with actual measurements made on Y_2O_3:Eu was favorable.[119] The use of Marquardt least-squared error algorithms and Kullback–Leibler stochastic distance analysis allowed for ever more precise modeling and validation studies,[98,120] including those incorporating the dc offset of the wave form into the model being tested. The final results were similar in nature to those found in the experimental evaluations of the various wave form-acquisition instruments: one can establish an optimum observation time that should be used in measuring the exponential decay in order to minimize the lifetime-estimation error caused by the noise.[119] More recently Zhang *et al.*[121] implemented Prony's method for improving computational speed, achieving a 98% decrease in run time. Sun *et al.*[122] extended this approach for the double exponential fluorescence decay process.

4. Low temperature arrangements

The discussion so far has focused on the calibration of phosphor thermometers over the range from room temperature through 1000 °C and above. There have been several attempts at making fluorescence-based thermometers that work at cryogenic temperatures as well, and we describe the measurement and calibration features of some of those systems in what follows.

The main instrumentational difference encountered in working at low temperatures, of course, is the change from a furnace-based to a cryostatic experimental arrangement, with the concomitant presence of liquid cryogens. Selection of the phosphor is also an important issue, as many of these materials exhibit little or no temperature dependence in their lifetimes and intensities at low temperatures. As an example, Dowell and Gillies[123] found that the fluorescence lifetime of Y_2O_3:Eu (6.8%) changed by less than 3% between room temperature and 77.5 K. (The phosphor and optical fibers had been mounted in a Teflon holder and submerged in a bath of liquid nitrogen. The temperature standard in this case was a Cryogenic Consultants model DTG 200 resistance thermometer.)

Simmons *et al.*,[124] however, found in a calibration study of La_2O_2S:Eu that the $^5D_3$ transition line (434 nm) of this material exhibited a strong temperature dependence down to liquid nitrogen temperatures. They extended their study to include observations of the 657 nm emission line of $Mg_4(F)GeO_6$:Mn and built a cryostatic sample holder that was used to make noncontact temperature measurements of both materials over the range from 4 to ≈ 140 K, with the cooling provided by liquid helium.[125] A photo of the experimental apparatus is shown in Fig. 19(a) and a cross-sectional view of the sample holder immersed in the helium bath is shown in Fig. 19(b). The data taken during calibration runs with this system established that the relationships between the temperature, T, of the phosphors and their emission lifetimes, τ, are given by

$$T(\tau) = 194.00(2.36 - \log\ \tau),\ \ La_2O_2S{:}Eu,$$
$$4\ \ \mathrm{K} < T < 80\ \ \mathrm{K}, \tag{11a}$$
$$T(\tau) = 38.3(4.05 - \log\ \tau),\ \ La_2O_2S{:}Eu,$$
$$80\ \ \mathrm{K} < T < 125\ \ \mathrm{K}, \tag{11b}$$
$$T(\tau) = 2341.0(0.74 - \log\ \tau),\ \ Mg_4(F)GeO_6{:}Mn,$$
$$4\ \ \mathrm{K} < T < 140\ \ \mathrm{K}, \tag{11c}$$

where T is in degrees kelvin and τ is in microseconds.

Krauss *et al.*[126] also studied La_2O_2S:Eu at low temperatures (over the range from 193 to 293 K). They measured the ratio of the $^5D_3$ and $^5D_1$ lines of a sample bonded on a liquid-nitrogen-cooled copper plate that was mounted in an evacuated test cell, and achieved a resolution of 0.25 K in their calibration runs.

The performance of several other types of fluorescence thermometry systems has also been characterized at low temperatures. One example is the attenuation-based, holmium-doped optical fiber sensor of Yataghene *et al.*,[127] which was designed for use at liquid nitrogen temperatures. Another is the molecular luminescence cryothermometer of Petrin and Maki[128] that employed photoexcitation of thioketones to measure temperatures at 20 K and below. A ruby crystal thermometer described by Anghel *et al.*[129] was calibrated against a type-K thermocouple to a precision of ± 0.3 K over

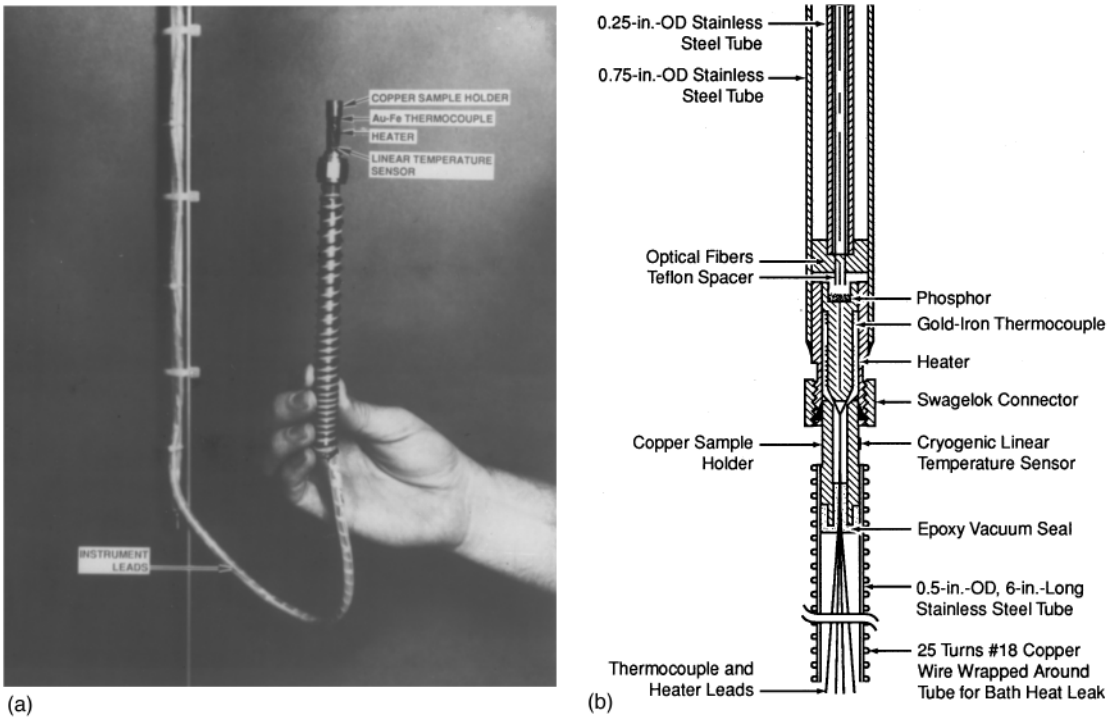

FIG. 19. Low temperature calibration system. (a) Photograph of the cryostatic sample holder. (b) Thermography system diagram.

the range from 200 to 300 K. The fluorescence of the crystal was excited by a green light-emitting diode (LED), and the decay lifetime was the quantity of interest. Zhang *et al.*[130] reviewed the various types of Cr^{3+}-doped thermometric schemes. In particular, they evaluated YAG:Cr^{3+} as a fluorescence lifetime-based thermal sensor material over the range from 77 to 900 K using their own data and that of others. They developed a very useful calibration formula that takes into account the energetics of the atomic transitions that occur during the fluorescence process. The general conclusion of their effort was that sensors of this type should thus be satisfactory in meeting a variety of industrial thermometry needs. In addition, this same research group[131] demonstrated that the size of a ruby crystal affects the calibration when used in the cryogenic region. This is due to fluorescence reabsorption.

C. Thermometry of moving surfaces

A phosphor target mounted on a surface moving at high speeds may translate or rotate by nonnegligible amounts during the period required to make a decay time-based measurement of its temperature. Virtually any kind of light delivery and collection scheme used in the measurement system will have a limited field of view. As a result, the fluorescing region may move significantly within the field of view, perhaps even completely into and then out of it, during the measurement period. This possibility is depicted in Fig. 20 which illustrates how measurements were made on the armature of a high-speed motor, using only a single optical fiber to collect the emission.[72] The total amount of light reaching the detector will change with time as the fluorescing spot sweeps through the acceptance numerical aperture of the collection fiber. The efficiency of light collection will vary as a function of rotation angle, being a maximum on the fiber axis and dropping to zero at points sufficiently far off the axis. The time dependence of the signal will be given by the product of the exponential time dependence and the (changing) optical collection efficiency factor. This time-dependent efficiency factor, F, may be determined in several ways. For example, a temperature independent fluorescence line may be observed. Allison *et al.*[72] noted that the 538 nm emission lifetime of the phosphor used in that study was temperature independent over the expected range of interest (room temperature to 100 °C). The point-to-point intensity ratio of the moving signal, I_v, to the stationary signal, I_s, both at 538 nm, yields the functional dependence of the efficiency factor at that particular speed. Thus,

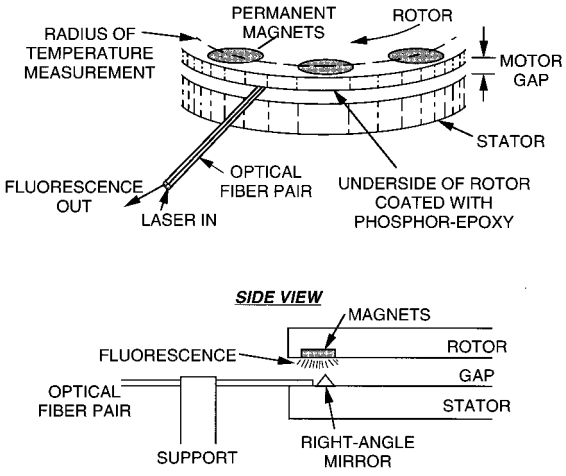

FIG. 20. The experimental arrangement used to measure the armature temperature of an operating, high-speed, permanent-magnet motor.

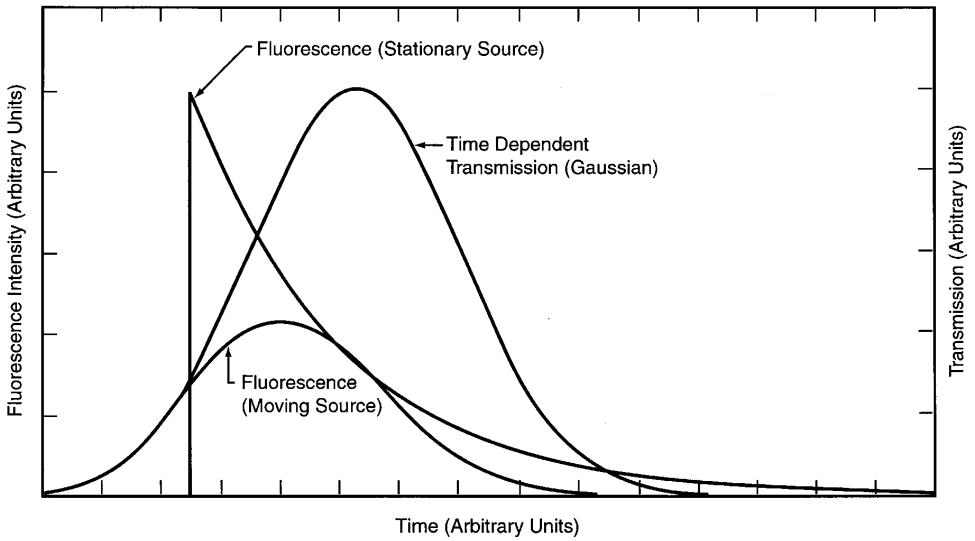

FIG. 21. Illustration of the effect of motion on the fluorescence signal.

$$F = I_v / I_s . \tag{12}$$

Two such idealized signals are depicted in Fig. 21. When this function is used to normalize the acquired temperature-dependent signal, $I_v(t)$, which for Allison *et al.* was at a wavelength of 514 nm, the intrinsic time dependence, $I_c(t)$, is revealed. If the logarithm of the curve fit through the resulting data turns out to be a straight line, then the operation has most likely been carried out properly, since this result would match the static case. The relationships should be

$$I_c(t) = I_v(t)/F, \tag{13}$$

$$\log(I_c(t)) = -t/\tau + A, \tag{14}$$

where τ is the characteristic decay time and A is a constant.

A different approach to thermometry of moving surfaces was developed by Leroux and Taboué[132] within the context of a broader study of the thermometric properties of the ZnS class of phosphors. In their work, a cylindrical spindle was rotated about its axis at speeds up to 400 rps while being convectively and radiatively heated. A circumferential band of phosphor and, separately, a spot of phosphor on the conical tip of the rotor's axis were illuminated with UV light, and the shift in wavelength (i.e., the change in color) of the phosphor patterns was observed while the shaft was spinning. Measurements of the rotor's surface temperature over the range from 20 to 200 °C could be made with uncertainties no larger than those obtained in similar measurements on static surfaces, viz., $\approx 2\%$ at 200 °C.

D. Transient thermometry

Because of the very low ''thermal mass'' or heat capacity of a thin film of phosphor, and the fact that the temperature-dependent processes occur over periods governed by the atomic vibrations in the host lattice, i.e., <1 ns, phosphor thermometry can measure rapidly changing temperatures. As discussed above, Turley *et al.*[76] used a pulsed CO_2 laser to produce temperature rises that were probably in excess of 100 °C/ms.

A different approach was taken by Tobin *et al.*[133] In their case, a nichrome wire coated with YVO_4:Eu was continuously illuminated with an ultraviolet lamp. A fast-acting mechanical switch connected the wire to a capacitor to achieve a temperature rise requiring only a few milliseconds to equilibrate. By following the ratio of two of the emission lines having different temperature responses, heating rates of about 100 °C/ms were tracked and determined.

E. Surface and volumetric thermography

As conceived originally, phosphor thermography was intended foremost to be a means of depicting two-dimensional temperature patterns on surfaces. In fact, over its first three decades of existence, the predominant use of the technique was in imaging applications in aerodynamics. The method was termed, ''contact thermometry'' since the phosphor was in contact with the surface to be monitored.

An alternate approach suggested by Urbach called ''projection thermography'' involved the optical transfer and projection of a thermal image onto a phosphor screen for subsequent analysis.[11,12] Figure 22 shows the calibration curves obtained by Byler and Hays[16] of the four phosphors derived from Urbach's work as being useful for this purpose. They were applied to the surface of interest by either spraying them on or by painting them while in a phosphor/acetate mixture. At least one manufacturer prepared and marketed a tape consisting of a phosphor backing on a thermoplastic resin that provided adhesion.[16] Generally, the data acquisition system was simply a photographic camera. Using Polaroid™ ASA 3000 film, Dixon and Czysz[21–23] at the AEDC noted that, under their conditions of illumination, the phosphors emit 10^{-6}–10^{-5} W/cm^2 before the onset of quenching. Quantitative analysis was performed by point-to-point densitometry measurements of the transmission of the photographic film. They resolved temperature differences of

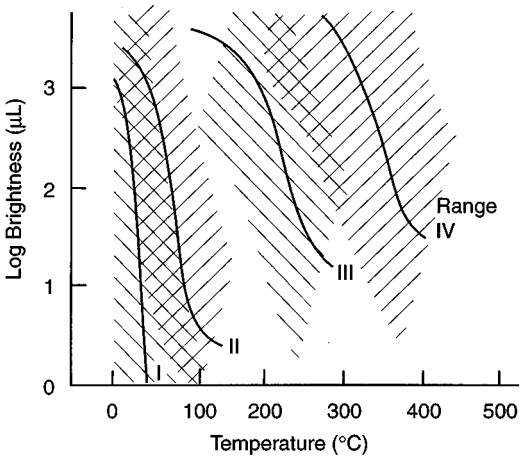

FIG. 22. Some phosphors used for thermometry in the 1960s. Range I: ZnCdS:Ag:Ni; range II: ZnCdS:Ag:Ni; range III: ZnS:Cu:Ni; and range IV: ZnS:Cu (from Ref. 16, reprinted with permission of the American Society for Nondestructive Testing).

$\approx$0.2 °C. It is important to note that these applications were intensity- rather than decay-rate-based approaches. This general technique has been and continues to be a standard tool used in aerodynamic heating studies in wind tunnels. The overall approach, however, has largely been overshadowed by the introduction of modern infrared thermal imaging techniques, several of which have evolved into commercial products that are used in a wide range of industrial and scientific applications.

Buck developed a phosphor imaging system for transient aerodynamic measurements made in a hypersonic wind tunnel at NASA's Langley Research Center.[134–136] His approach used a three-color video camera to view a fluorescing phosphor mixture. The ratio of the intensity of the blue part of the emission band to that of the green provided the signal of interest, as it was a function of temperature for the Radelin 2090 and 3003 phosphors that were used. The technique called for the collection of several dozen images during a 30 s transient heating test, a task made possible with computer-aided data acquisition.

Bizzak and Chyu[137,138] noted that the more conventional thermometry methods are not satisfactory for temperature and heat transfer measurements that must be made in the rapidly fluctuating conditions peculiar to the microscale environment. They suggested that thermal equilibrium on the atomic level might be achieved within 30 ns, and, therefore, to be useful in performing microscale thermometry the instrumentation system must have a very rapid response time. Moreover, its spatial resolution should approach the size of an individual phosphor particle, typically just a fraction of a micron. In their effort to develop a phosphor imaging system based on La_2O_2S:Eu, they used a frequency-tripled Nd:YAG laser. The image was split and the individual beams were directed along equal-length paths to an intensified CCD detector, a technique similar to that of Goss *et al.*[139] The gate duration was 40 μs and the ratio of the $^5D_2$ to $^5D_0$ line intensities yielded the temperature. Significantly, they were able to determine how the measurement accuracy varied with measurement area. The maximum error found for a surface the size of which was represented by a 1×1 pixel in their video system was 1.37 °C, with an average error of only 0.09 °C.

Taliaferro *et al.*[140] used an image-intensified Cohu model 012A03 CCD camera to monitor the fluorescence intensity profiles of La_2O_2S:Eu- and Y_2O_2S:Eu-coated surfaces over the range from room temperature to 200 °C. The excitation source was an ultraviolet lamp, having peak emission at 254 nm and producing an irradiation intensity of 9 mW/cm^2 at a distance of 2.5 cm. Narrow band pass optical filters blocked undesired wavelengths from the camera. The images were stored and processed by computer, with the temperature-dependent surface brightnesses subsequently translated into false-color thermograms for ease of visual interpretation. The precision of the imaging system was such that thermal gradients of 0.02 °C/pixel (at nominal temperatures of 35 °C) could be resolved over the surface. Noel *et al.*[141] report the results of related experimental studies of two-dimensional phosphor thermography.

It has often been suggested that combustion flames could be diagnosed by seeding them volumetrically with phosphor particles. In fact, the flames themselves can in some instances serve to excite the luminescence. Sweet and White[142] describe phosphor excitation in a hydrogen diffusion flame and note that this method for producing optical emissions received considerable attention in the early part of the 20th century. Their experiment involved coating a surface with the phosphor to be tested, and then placing it in the flame. The particular materials under study were Y_2O_3, La_2O_3, Gd_2O_3, and Lu_2O_3 doped with either Tb or Eu. A conclusion of their work was that the excitation mechanism involved collisions with excited neutral OH molecules.

By the 1980s, the performance of video cameras, segmented detectors, CCD array detectors, and laboratory computers provided greater data acquisition power and experimental design flexibility, leading to several new developments. A particularly clever conception by Goss *et al.*[143–145] at System Development Laboratories involved the visualization of the condensed-phase combustion of solid rocket propellant. They impregnated the fuel under test with YAG:Dy, and used the ratio of an F-level band at 496 nm to a G-level band at 467 nm as the signal of interest. Because of thermalization, the intensity of the 467 nm band increased in comparison with the 496 nm band over the range from ambient to the highest temperature they were able to attain, 1673 K. At that temperature, the blackbody emission introduced a significant background component into the signal, even within the narrow pass band of the spectrometer that was employed. For this reason, they used a Q-switched Nd:YAG laser (frequency tripled to 355 nm). The detectors in this arrangement included an intensified (1024-element) diode array which was gated on for a period of 10 μs. They also used an intensified CCD detector,[139] perhaps the first use of such a device for phosphor thermometry. To simulate combustion in the laboratory, the phosphor was mixed with a low melting point (400 K) plastic and the resulting blend was heated with a focused CO_2 laser which ignited a flame that eroded the surface. A time history of the disintegrating plas-

tic surface was then obtained with the measurement system. Because of the short duration of the fluorescence, the power of the laser, and the gating of the detector, they were able to measure temperature profiles in the presence of the flame.

F. Optical fiber fluorescence thermometry

It has been a general goal of this review to concentrate on noncontact methods of phosphor thermometry. However, there have been instances above (and some to follow below) where it has been useful and appropriate to incorporate some discussion of the various phosphor-tipped fiberoptic temperature sensors and the physical principles underlying them. It is outside the scope of this review, though, to provide an extensive survey of such devices, especially since others have done so already.[1] Therefore, the additional commentary in this subsection will be limited to a brief overview of this general class of instrumentation.

Grattan, Palmer, and colleagues in the U.K. have reported the results of studies on several different kinds of decay-time-based fiberoptic thermometers. Some of the papers in their long series of articles describe sensors in which the tip of the fiberoptic probe consists of a fluorescing element made of either ruby,[19,146] alexandrite,[147] YAG:Nd,[148,149] or YAG:Cr^{3+},[130,150] among other materials. These devices have been used with visible[151] and infrared[152] excitation, with fluorescence reference channels,[153,154] and in narrow low-temperature bands[130] and higher wide-temperature bands.[155] A review of early developments in the field was published by Grattan[156] in 1987, and the recent book by Grattan and Zhang[1] provides a very thorough and up-to-date discussion of the field as a whole.

The background research underpinning what was to become another well-known effort within the field of fiberoptic thermometry was begun by Wickersheim, Buchanan, and colleagues in the 1960s. They studied the luminescence of several rare-earth-doped oxides and oxysulfides,[24–28,87,157–161] many of which would prove to be useful in phosphor thermometry. Subsequently, Luxtron Corp.[162] developed techniques for making robust fiberoptic probes with thermal phosphor tips. Wickersheim, Sun, and others[13,14,163–166] have described the general operating principles of the thermometric instrumentation systems that incorporate these transducers. Many applications have been found for this kind of system, including various uses in clinical medicine (Sec. V A) and in the maintenance of electrical machinery (Sec. V B). A variation of the prototypical Luxtron design allows the phosphor target to be mounted remotely on the surface to be measured, rather than fixed directly onto the tip of the optical fiber.[14,165,166] When used in this manner, noncontact determinations of the temperature of a moving or otherwise difficult-to-access surface can be made in largely the same fashion as would be done with the ''generic'' system described earlier (Sec. IV A). A series of technical notes[167–170] outlines some probe configurations and experimental arrangements useful in making noncontact measurements.

There may be circumstances where fluorescence thermometers based on visible-light excitation may have some advantages over competing methods in terms of both ease of design and practicality of the source. Bosselmann *et al.*[18] and Fernicola and Crovini[171–172] have investigated this using YAG:Cr crystals on fibers illuminated with a laser diode emitting in the red. In both cases, the excitation wavelength was 636 nm, and the emission was from the well-known R lines which in this host are at 687 nm. There were slight variations in their four samples, but the lifetimes were ≈ 2 ms at ambient temperature, and decreased by about an order of magnitude at 300 °C. Their common interest in this technique stemmed from various automotive applications.

One final example of fiber-based thermometry is the work of Maurice *et al.*[173] In their technique, the ratio of intensities of the ${}^4S_{3/2} \rightarrow {}^4I_{15/2}$ and ${}^2H_{11/2} \rightarrow {}^4I_{15/2}$ transitions is monitored in a segment of Er-doped fiber pumped by an argon ion laser beam passed through a dichroic mirror. They found that the intensity ratio varied by about a factor of 10 over the range from 300 to 1000 K, thus making this a potentially useful method around which to design thermometer.

V. APPLICATIONS

A. Biophysical and biomedical uses

Many workers over the past several decades have investigated the properties of organic materials via fluorimetry of various kinds, and the general technique is now a standard tool in science and engineering. A few of the specific efforts within this broad field that have focused on improving measurements of fluorescence decay lifetimes include the use of mode-locked lasers to study extremely fast fluorescence processes (Wild *et al.*[174]), the development of cross-correlation phase and modulation fluorimetry (Alcala *et al.*[175,176]), and the use of digital electronics to synthesize parallel phase-fluorimetry systems (Feddersen *et al.*;[177] see also the discussion of limitations of this technique given by Alcala[178]). All of this work has been ongoing while noncontact phosphor thermometry has been under development, with the cross-over region being the incorporation of phosphors into optical fibers to make fluorescence-based sensors. Some background on the general features of this class of sensor is provided above, and a thorough discussion is available elsewhere.[1]

The resulting instrumentation has been very useful in monitoring physiological variables. For instance, Alcala, Yu, and Yeh[179] describe a digital phosphorimeter with frequency-domain data processing that is able to extract the values of the partial pressure of oxygen in blood. The device has a drift of less than 1% per 100 h of use. At about the same time, Alcala, Liao, and Zheng[180] designed and built a phosphorescence lifetime thermometer that has alexandrite crystals bonded to the tip of an optical fiber. It operates over the range from 15 to 45 °C, has an accuracy of better than 0.2 °C, and measures the lifetime of the alexandrite's He–Ne stimulated phosphorescence with a reproducibility of 0.3%.

The commercially available FLUOROPTIC™ thermometers of Luxtron Corp. (see Sec. IV F) have found many uses in the biomedical arena since their introduction. One particularly significant medical application of these instruments has been in clinical hyperthermia.[181,182] The small outer diameter of the optical fiber (<1 mm) allows for insertion of the probe into standard catheters, and the established precision

of measurement (<0.1 °C) is obtainable in the presence of large electromagnetic fields.[183] This makes the instruments compatible with rf induction and other hyperthermia systems, with minimal perturbation of the electromagnetic fields.[184] (In fact, others[185] have also taken advantage of the nonperturbative nature of thermoluminescent phosphors by making dosimeters for microwave fields.) A Luxtron 2000B thermometer was used in the first *in vivo* studies of dynamic boundary hyperthermia,[186] in which the uncertainty in the boundary of thermally driven cell death in porcine brain was found to be controllable to within <0.6 mm. Samulski has written a succinct, useful review[187] that includes discussion of the role of photoluminescent thermometry in clinical and biomedical research.

Ikeda, Sun, and Phillips[188,189] designed a blood flow-rate sensor that incorporated a FLUOROPTIC™ thermometer. This device inferred the flow rate from direct measurement of temperature change due to heat transfer through the sensor, in analogy to hot-wire anemometry. A variety of other fiber-optic-based blood flow sensors has been described in the literature (see Tjin *et al.*[190] for a review), but they are typically based on Doppler anemometry rather than on heat transfer.

Shrum and colleagues[191] have devised a molecular fluorescence thermometry technique that derives its signal from the shift in wavelength with temperature of the fluid in which an organic compound (BTBP) is dissolved. The sensitivity of the method is ≈ 0.05 nm/°C, and they used it to measure temperature changes in both associated and nonpolar fluids to within ± 2 °C over the range from 15 to 70 °C. This technique can be thought of as a liquid-based equivalent of solid-state phosphor thermometry: low concentrations of BTBP (as little as 10^{-7} M) can seed the host fluid and produce detectable temperature-sensitive fluorescence in somewhat the same way as small concentrations of the rare-earth dopant function in thermographic phosphors.

Finally, within the realm of biomedical applications of temperature-dependent phosphors, Shearer and Kimball[192] have noted that the temperature dependence of the phosphor screens used in medical x-ray fluoroscopy systems can affect the quality of the images. They examined several types of screens that were illuminated by typical levels of x-ray flux to quantify the effect on overall emission efficiency. A $BaPbSO_4$ sample at 50 °C exhibited a 60% decrease in total efficiency relative to a sample held at 0 °C. A similar result was found by Morgan[193] for calcium tungstate and by Trout and Kelly,[194] who studied zinc cadmium sulfide. Rare-earth screens made from LaBrO:Tb and La_2O_2S/Gd_2O_2S:Tb exhibited efficiency changes of $<5\%$ over this range. We note here that a greater temperature dependence would be expected for some emission lines of the terbium-doped oxysulfides, particularly at low terbium-dopant concentrations. Buchanan and colleagues[195] have also investigated rare-earth-doped phosphors for use in x-ray transduction.

B. Electrical machinery

The immunity of optical signals to electromagnetic interference makes phosphor thermometry very useful in diagnostic studies of electrical machinery. For instance, Mannik and colleagues at Ontario Hydro have developed a phosphor-based technique for monitoring the temperature of the rotor in a large turbogenerator.[86,196,197] The motivation for doing this is to seek out any ''hot spots'' that might develop in the rotor of the generator as a result of several possible causes, including overheated insulation. They used a pulsed nitrogen laser as the optical source, and conveyed its light along an all-silica optical fiber having a core diameter of 600 μm. (Silica fibers are generally preferred over plastic-clad fibers because of their higher pulsed-power damage threshold and their superior transmission characteristics in the ultraviolet.) A plastic-clad fiber collected the fluorescence and conveyed it to a photomultiplier tube. They used a microprocessor-based, custom-designed data analysis system[196] to determine the fluorescence decay times. A silicone binder, mixed 50% by weight with phosphor, was painted in a 5-cm-wide stripe around the circumference of the rotor, with a gap in the stripe that functioned as a fiducial line. As noted above, their calibration and characterization studies established that external magnetic fields did not affect the phosphor lifetimes. The presence of a thin film of oil arising from the lubricants used in this kind of machinery was found to marginally degrade the signal, but measurements were still possible. In field tests[197,198] involving a 540 MW generator, they used the 514 nm lines of the phosphors Y_2O_2S:Eu (1%), Gd_2O_2S:Eu (0.5%), and La_2O_2S:Eu (1%). While the first two materials exhibited a strong signal and a marked temperature dependence from 60 to 150 °C, they were also subject to saturation. The last material did not saturate, however, and measurements were made with it up to temperatures of between 70 and 80 °C. Above that level, the signals were weak and the associated lifetimes were very short, i.e., <1 μs. The surface velocity of the rotor was ≈ 207 m/s. The spatial resolution of the measurements was 4 mm, and their accuracy was ± 2 °C.

Hot spots also develop in electrical transformers, and FLUOROPTIC™ thermometers have been used to determine the temperatures of the windings,[199,200] the leads,[201] and the transformer tank.[202] Other applications that call for the sensor to function in the presence of large electromagnetic fields include fiber optic thermometry-based measurements of microwave power[183,203,204] and rf susceptibility.[205]

C. Gas centrifuges

During the 1980s, workers from several institutions first began using phosphor thermometry for making noncontact measurements on the gas centrifuges being developed for the U.S. Department of Energy's uranium enrichment program. These devices are large right circular cylinders driven at very high speeds. Their function is to separate U^{235} from the natural isotopic distribution in UF_6 gas to create enriched fuel for nuclear power reactors. The flow pattern inside the machine and, hence, the separative efficiency of the centrifuge are affected by thermal variations on the rotor surface. The goal of maximizing separative work performance provided the impetus for developing a remote thermometry system compatible with a high speed mechanism of this type.

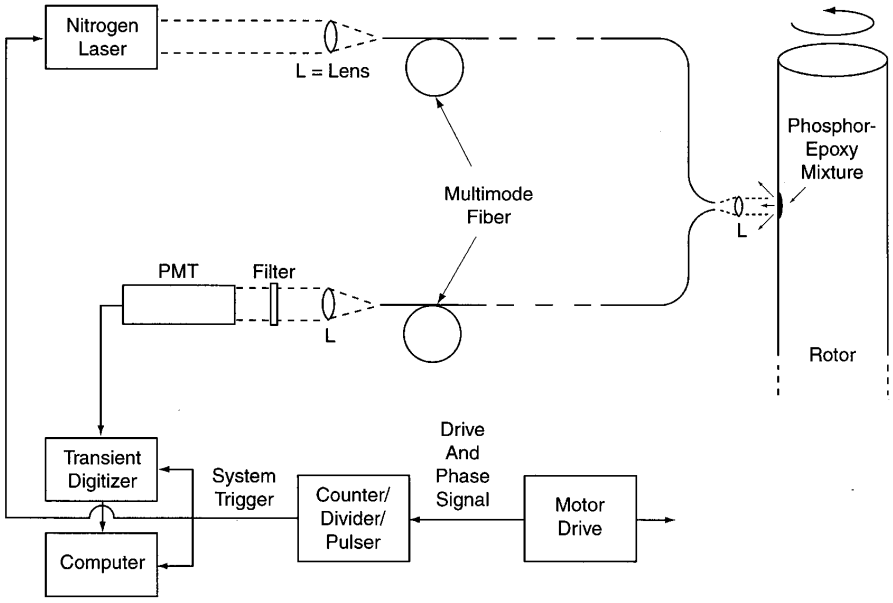

FIG. 23. Schematic diagram of the phosphor thermography system developed for measuring the wall temperature at points around the periphery of a full-sized gas centrifuge.

Making the measurement by taking the ratio of line intensities was the first approach considered, but the high speed of the centrifuge surface complicated the calibration of the phosphor. In addition, mechanical concerns dictated a spacing of several centimeters between the tips of the optical fibers used for delivery/collection of the light, and the measurement surface. This latter point meant that beam spread would be non-negligible, and implied that a bright source of illumination would be needed to counter the falloff of intensity with distance. A portable nitrogen laser was incorporated into the experimental arrangement and emission lifetime measurements were made on La_2O_2S:Eu. This phosphor had already been studied by others, and it exhibited thermally sensitive emission lines in the temperature range of interest. Benchtop tests on low speed rotors demonstrated feasibility by establishing the technique's precision (1/3 °C) and confirming the utility of the fiberoptic, timing, and signal synchronization[206,207] components of the apparatus.

Figure 23 presents a schematic diagram of the experimental arrangement developed for use with a full-sized gas centrifuge. Circumferential strips of phosphor were painted on the rotor at various locations along its axis. The pulse jitter in the trigger circuit for the laser was in the worst case a few hundred nanoseconds, enabling excellent spatial resolution of the temperature measurements made on the phosphor bands.

D. Gas turbines

The useful results obtained by applying phosphor thermometry to high speed gas centrifuges led to efforts aimed at measuring the temperatures of surfaces and structures inside turbine engines, particularly those of the rotating blades and stationary vanes. The history of that work is documented in a series of papers by Noel *et al.*[208–215] and colleagues,[216] which includes a review of the results obtained through 1993.[217] Several other groups have also independently applied phosphor thermometry to turbomachinery, and in what follows we provide a synopsis of the work that has been done in this field.

One of the original intents of the ORNL phosphor thermometry program was to provide a means of sensing the temperatures of objects within the combustion-flame environment. The first experimental tests of the technique were carried out inside a high-altitude simulation wind-tunnel at the AEDC.[218] In these tests, the exhaust from the aft end of a Pratt & Whitney (PW) F100 engine impinged on a variable-area extractor (VAE), a cone-shaped centerbody that aids in pressure recovery and the pumping process. Measurements were made of the VAE surface temperature, both with and without an afterburner plume intervening between the surface and detection optics. The VAE was water cooled, though, so its temperature was consequently rather low, typically 150 °C. The laser-induced fluorescence signals from the phosphor layer bonded on the VAE surface were successfully detected despite the optical background created by the plume. This is shown in Figure 24 which is a print made from a 16 mm film of the afterburner and VAE. The white spot is the phosphor luminescence. The resulting data made it possible to track the temperature change of the VAE during the course of afterburner ignition transients.

Subsequent engine experiments were performed at a burner-rig installation, i.e., a test cell capable of exposing turbine blades to an engine-simulating environment. The usual arrangement involves mounting several blades on a mechanical carousel which is then rotated at relatively low speeds through a jet flame. Phosphor thermometry tests by Tobin *et al.*[219] in one such installation demonstrated the workability of the technique up to 1100 °C. Other studies have been carried out in spin pits, where the higher rotational speeds and the intermediate-range temperatures encountered

in operating turbine engines can be simulated, albeit without the exhaust flame present.

A number of *in situ* experiments have also been carried out, including measurements made on first-stage stator vanes inside a PW 2037 engine,[220] on the vanes of a turbine disk running near full speed (14 600 rpm) in an advanced turbine-engine gas generator (ATEGG) system,[214] on the components of a PW joint technology developmental engine (JTDE),[217] and inside an experimental turbine engine at Virginia Polytechnic Institute and State University.[220] Collectively, these tests have demonstrated that phosphors based on materials such as yttrium oxide, yttrium vanadate, and yttrium aluminum garnet (YAG) can survive for extended periods, even when bonded in place in the first stage of a turbine where the blades are adjacent to the burner. Useful optical signals were obtained at temperatures well in excess of 1000 °C, and separate calibration studies[221,222] showed that the fluorescence decay parameters of some of the phosphors were still readily measurable at 1200 °C. The preferred design of the optical probe consisted of a two-fiber configuration with internal optical elements coated so as to minimize stray reflections, laser-induced damage to the input fiber, and the optical background due to blackbody radiation. On a related note, studies of the heat transfer through combustion engine components have also been undertaken with thermographic phosphors.[223]

Several others have also explored turbine engine and other aerospace applications of phosphor thermometry. For instance, Alaruri and colleagues[103,224] exposed samples of Y_2O_3:Eu to the combustion flows in a burner rig. The gas velocities in the rig ranged from 245 to 407 m/s at roughly atmospheric pressure. Data were taken over the range of 400–1000 °C, with the overall accuracy of the measurements estimated to be $\pm 3\%$. They noted that the phosphor's fluorescence was easily distinguishable from the luminescence due to the fuel pulses (JP-5 aviation fuel was used).

Phillips and Tilstra[225] describe a ruggedized, thermographic phosphor temperature sensor based on the decay-time approach and designed using a 200 μm optical fiber to convey the fluorescence signals. It was tested over the range from -75 to 350 °C, at altitude simulations of up to 21.3 km (70 000 feet), and under accelerative loadings equivalent to 20 G over the range of 5–2000 Hz. It can be used for measuring engine inlet total temperature, fuselage total temperature, and engine inlet immersion temperature, all without being subject to the effects of electromagnetic interference.

Simons *et al.*[226] describe calibrations of additional phosphor materials of use for moderately high temperature measurements.

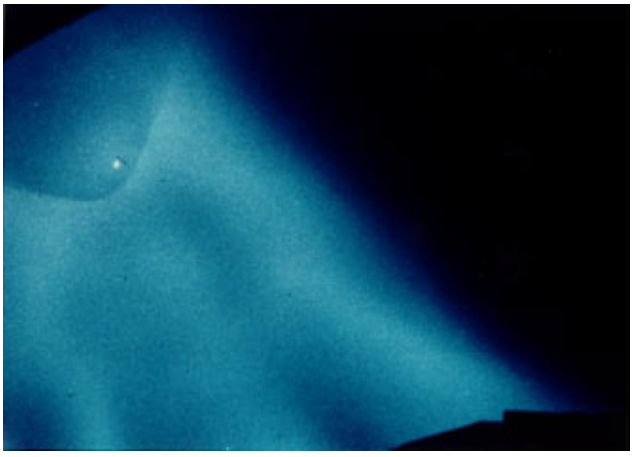

FIG. 24. Afterburner flame impinging on the variable-area extractor. The white spot is phosphor luminescence viewed through the flame.

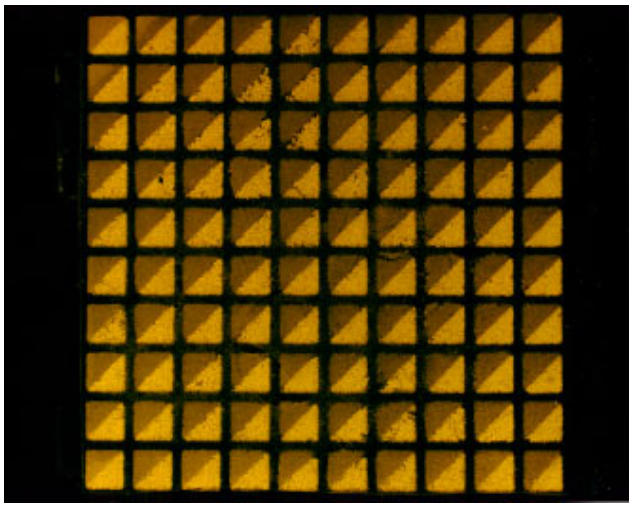

FIG. 25. Photograph of the fluorescing heat-flux gauge.

VI. MEASUREMENT OF OTHER QUANTITIES

A. Heat flux

The determination of the heat flux through a surface is important in a variety of scientific and engineering applications. Noel *et al.*[88,227] and Turley *et al.*[228] pursued development of several embodiments of thermal phosphor-based heat flux gauges. A standard expression relates the heat flux, q, to the insulator thickness, d, thermal conductivity, K, and temperature difference, ΔT, across an insulating barrier:

$$q = K \cdot \Delta T / d. \tag{15}$$

FIG. 26. Photograph of the heat-flux range gauge attached to a turbine blade.

As originally conceived, a phosphor-based heat flux gauge would consist of a sandwich of two different types of phosphors separated by a UV-transparent insulator. The first realization of such a device incorporated Gd_2O_2S:Tb, in which the ratio of the D_3 state at 415 nm to the D_4 state at 490 nm served to provide the temperature of the top surface. The bottom surface was made of La_2O_2S:Eu, and its temperature was derived from the ratio of the emission of the D_2 band at 514 nm to that of the D_0 band at 614 nm. A demonstration arrangement utilized a hot-air stream to apply heat to one such gauge bonded onto a water-cooled aluminum container. Levels of heat flux up to 40 kW/m^2 could be measured in this way.

A second realization of this method consisted of an array of discrete circular and triangular spots of phosphor. This made it possible to obtain a two-dimensional determination of heat flux through the surface of interest. Also, only one phosphor is required when, for instance, one-half of a semicircle of it is deposited on the top of the insulator with the matching half bonded onto the bottom. Figure 25 is a close-up photograph of a fluorescing heat-flux gauge with matching triangular phosphor layers. Figure 26 depicts the gauge attached to a turbine blade. Figure 27 shows the experimental arrangement for this type of heat-flux gauge.

Baumann[33] has also made heat-flux measurements using thermographic phosphors. Wind tunnel models made of three different materials (steel, Macor™ glass ceramic, and Norcoat™ 4000 silicone elastomer), all of which had thin coatings of Y_2O_2S:Eu (0.15%) applied, were monitored during blow-down tests in a hypersonic flow facility. The response time of the measurement system was typically less than 200 ms, and the values of the heat flux measurements obtained with his technique compared well with the standard spot-gauge methods.

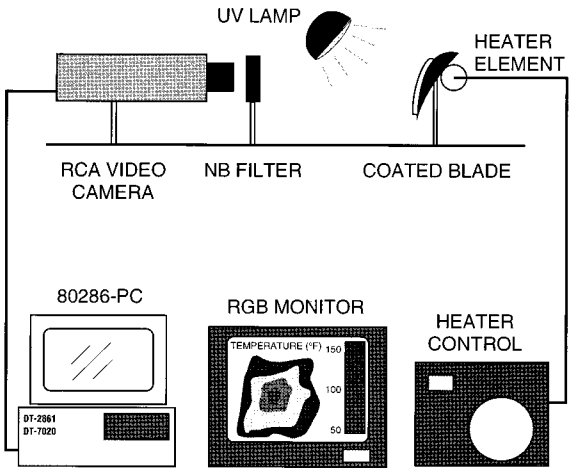

FIG. 27. Laboratory heat-flux gauge system.

As a practical point, we note that the oxysulfide-based phosphors begin to degrade chemically in air at about 450 °C. However, other phosphors may be used for this application when higher temperatures will be involved. Another limitation encountered in developing this concept for use at high temperatures is the difficulty in finding a suitable insulator. To circumvent this, Noel has developed a theory and a resulting design that eliminates the need for an intervening insulator in the gauge.[88] As a related matter, we note that a detailed calculation of the heat flow through a thin film subjected to laser heating has been carried out by Abraham and Halley.[229]

B. Pressure and strain

Pressure will generally affect a material's luminescence and spectral absorption properties. However, the nature of this effect is not as well studied or understood as are the effects of temperature on luminescence. The application of pressure may be viewed as the imposition of compressive strain from all directions. Hence, knowledge of a material's pressure dependence also lends insight into its strain dependence. On the atomic level, strain results in a change in chemical bond lengths and atomic orbital configurations. This perturbs the electric and magnetic fields seen by the activator and, hence, the spectral energy level manifold. These environmental changes modify the fluorescence properties, but the precise mechanism will vary from one phosphor to another. For the case of La_2O_2S:Eu, the application of pressure (compressive strain) has the effect of increasing the energy of the CTS. The CTS parabola as seen in Fig. 2 would be placed higher and, consequently, the value of the difference between the excited electronic state and the level where the CTS intersects the ground state would be increased. In this case, assuming a constant ambient temperature, the increased pressure has an effect similar to that of cooling the phosphor, i.e., certain of the lines, e.g., the $^5D_2$ lines for La_2O_2S:Eu, get brighter and the decay times get longer. Tensile strain will have the reverse effect for the same emission line of this phosphor.

Table IV presents a survey of the existing data on the pressure dependence of various phosphor, glass, and crystalline materials. The effect of pressure on fluorescence decay lifetime (at constant temperature) is more pronounced in the oxysulfides than it is in other materials. Webster and Drickamer[230,231] have a theory that appears to explain the pressure dependence of the luminescence of these oxysulfides; it involves the CTS discussed earlier. Most authors, though, have been more concerned with the effects of pressure on line shifts. For example, Haugen[232] discusses the use of line shifts of ruby for making pressure measurements. In fact these line shifts are often used for pressure calibration of diamond anvil cells. Also suggested are the trivalent ions, Ce^{+3}, Pr^{+3}, Eu^{+3}, and Er^{+3}, possibly in fluoride hosts since they have transitions that can be transmitted by optical fibers. The pressure dependence of the emission intensities, linewidths, and peak locations for ZnS:Eu^{+2} and Y_2O_2S:Eu^{+3} is given by Zhizhong *et al.*[233] For the last, the emission frequency changed by about 30 cm^{-1} in going from 0 to 4 GPa,

TABLE IV. Survey of the effects of high pressure on the luminescence characteristics of several fluorescent materials.

Material	Reference	Pressure range	Fluorescence line(s)	Sensitivity $\Delta\lambda/\Delta P$	Sensitivity $\Delta I/\Delta P$	Sensitivity $\Delta\tau/\Delta P$	Temperature effects	Comments
Gd_2O_2S:Tb	243, 244	5 GPa	$^5D_3$	⋯	100% decrease	$\tau\times0.1$ over 2 GPa	⋯	Maximum $\Delta\tau/\Delta P$
			$^5D_4$	2 cm^{-1}/GPa	25% decrease 0–5 GPa	<5% change 0–5 GPa	⋯	⋯
$La_2O_2S:Eu^{3+}$	231, 243, 244	12 GPa	$^5D_2$	5 cm^{-1}/GPa	$\times10$ in 3.5 GPa	$\tau\times10$ in 3.5 GPa	See the text	Shift of CTS important
			$^5D_1$	6 cm^{-1}/GPa	Mild decrease	No change		
			$^5D_0$	4 cm^{-1}/GPa	Mild decrease	No change		
La_2O_2S:Tb	244	5 GPa	$^5D_4$	3 cm^{-1}/GPa	100% increase in 5 GPa	No change	⋯	$^5D_3$ lines weak in this host
YVO_4:Eu	244	5 GPa	$^5D_0$	3 cm^{-1}/GPa	10% decrease in 5 GPa	$\tau\times0.9$ in 5 GPa	⋯	⋯
			$^5D_1$	7 cm^{-1}/GPa	50% decrease in 5 GPa	$\tau\times0.67$ in 5 GPa	⋯	⋯
			$^5D_2$	9 cm^{-1}/GPa	No change	No change	⋯	⋯
YVO_4:Dy	243, 244	5 GPa	$^4F_{9/2}-{}^6H_{13/2}$	7 cm^{-1}/GPa	6% decrease 0–5 GPa	$\tau\times0.9$ in 5 GPa	See the text	⋯
			$^4F_{9/2}-{}^6H_{15/2}$	10 cm^{-1}/GPa	45% decrease 0–5 GPa	Mild decrease		⋯
$Y_2O_2S:Eu^{3+}$	233	7 GPa	$^5D_0$ and $^5D_1$	5 cm^{-1}/GPa	−0.24/GPa	⋯	⋯	⋯
Gd_2O_2S:Tb	243, 244	5 GPa	$^5D_3$	⋯	100% decrease 0–5 GPa	$\tau\times0.1$ in 2 GPa	⋯	Maximum $\Delta\tau/\Delta P$
			$^5D_4$	2 cm^{-1}/GPa	25% decrease 0–5 GPa	<5% change 0–5 GPa	⋯	⋯
$CaWO_4:Nd^{3+}$	237	7 GPa	$^4I_{11/2}$	0.727 nm/GPa at 290 K (7 cm^{-1}/GPa)	⋯	⋯	$d\lambda/dT=-4\times10^{-4}$ nm/K	4.5 times softer than Al_2O_3; small crystals used
$YAG:Eu^{3+}$	240	7 GPa	591 nm	0.197 nm/GPa (6 cm^{-1}/GPa)	⋯	⋯	to 973 K, -5×10^{-4} nm/K	Expression derived for $\Delta\lambda=f(P,T)$
$LaOCl:Eu^{3+}$	238	14 GPa	Many	1–10 cm^{-1}/GPa	⋯	⋯	⋯	Ar ion laser excitation
$YAG:Tb^{3+}$	228	8 GPa	$^5D_4\rightarrow{}^7F_J$	1–10 cm^{-1}/GPa	⋯	⋯	⋯	Ar ion laser excitation
Al_2O_3:Cr	234	10 GPa	R_1	0.366 nm/GPa (8 cm^{-1}/GPa)	⋯	⋯	⋯	⋯
Al_2O_3:Cr	235	1 GPa	R_1	⋯	30% increase 0–0.8 GPa	3.4 ms at 0.8 GPa	⋯	Tensile stress

while the intensity decreased tenfold over the same range. Their results complement those obtained by Webster.[230]

More recent work on ruby has been done by Gupta and Shen,[234] who include a review of the literature in their article. They found the pressure sensitivity of ruby to be slightly less than 10 cm^{-1}/GPa. Liu *et al.*[235] measured the effects of tensile stress on ruby emission, finding a shift of 2 cm^{-1}/GPa, i.e., roughly a third of the shift due to pressure. Vos and Schouten[236] have investigated the temperature dependence of the pressure response of the ruby absorption lines R_1 and R_2. Beales and Goodman,[237] meanwhile, have explored the temperature and pressure dependence of lines in the spectrum of $CaWO_4$:Nd, finding $d\lambda/dT=-4\times10^{-4}$ nm/K and a pressure sensitivity of 7 cm^{-1}/GPa for emission at 1.06 nm. They note that the results are similar for other rare-earth-doped crystals, and that they chose this material because it is not as hard as sapphire and, therefore, should exhibit a larger pressure dependence. Chi and colleagues[238] found line shifts of up to 10 cm^{-1}/GPa for $LaOCl:Eu^{+3}$ and similar results[239] for YAG:Tb. Arashi and Ishigane[240] tested the pressure dependence of $YAG:Eu^{3+}$ finding that it exhibited a sensitivity of 6 cm^{-1}/GPa in its 591 nm fluorescence, a value only slightly less than the sensitivity of ruby. Doped alkali halides show a pronounced change in absorption position and shape, especially in

the 2–4 GPa range of pressures. (Other materials Arashi and Ishigane tested but did not describe include Al_2O_3:Eu^{3+}, $YAlO_3$:Eu^{3+}, Gd_2O_3:Eu^{3+}, YbAG:Eu^{3+}, and GdAG:Eu^{3+}.) Drotning and Drickamer[241] considered Tl^+ and In^+ in particular. In contrast to the rare-earth phosphors, the spectral properties of these materials are rather broad. Seals *et al.*[242] have also studied the pressure and temperature sensitivities of certain inorganic phosphors.

Allison *et al.*,[243] in conjunction with Gleason,[244] used a diamond anvil cell to study the possibility of employing the pressure sensitivity of thermographic phosphors as the mechanism that would underlie a new class of strain gauges. In particular, the pressure dependence of the fluorescence properties of YVO_4:Dy, Y_2O_3:Dy, and Gd_2O_2S:Tb were investigated. For YVO_4:Dy, the fluorescence lifetime changes little with either pressure or temperature below 300 °C. However the relative intensities of narrow emission lines that comprise the emission band centered at 575 nm do change with temperature. The ratio of emission at 575.3 nm to that at 572.3 nm is constant up to a threshold value of pressure where there is an increase to a new level. The value of this threshold varies from 4.5 GPa at 20 °C to 0.3 GPa at 150 °C.

Measurements of the pressure dependence of the lifetime of Gd_2O_2S:Tb were made and compared with La_2O_2S:Eu. These two phosphors exhibit the strongest pressure dependence of all the materials surveyed. The former decreases in decay time by an order of magnitude with an application of only 2 GPa, while the europium phosphor increases by an order of magnitude with an application of 3.5 GPa. Also, a tapered sapphire rod was used to apply force to a La_2O_2S:Eu sample. As expected, the set of lines between 510 and 515 nm increased in intensity and the emission lines at 537 and 538 nm decreased. The applied pressure was estimated to be between 0.5 and 1 GPa. The response of the materials clearly demonstrates that these oxysulfides are good candidates for further study of strain-induced effects, with potential for practical measurement of strain in industrial situations. (A survey of some possible applications is available elsewhere.[245]) There may be other molecular species that have even greater pressure sensitivities.

Work that is closely related to the pressure- and strain-sensing studies described above includes that of Prins and colleagues.[246,247] They employ thermographic phosphors and a digital imaging technique to make simultaneous measurements of surface temperatures and strain fields. The temperature measurements are derived from the fluorescence intensity of the phosphor. The strain, meanwhile, is measured via geometric interference: a set of lines etched onto the phosphor is imaged under different strain conditions, and the images are superimposed to reveal a strain-dependent moiré pattern. Comparisons with strain gauges reveal an uncertainty of $\pm 0.05\%$ over a 1.8% strain dynamic range. (Simpson and Welch[248] also developed a noncontact, optoelectronic method for strain measurement based on a different principle of operation. In it, the shape changes of a multilobed geometric form on the surface of a rotating target were monitored and analyzed, with the results yielding the parameters of the strain field.) Gallery *et al.*[249] have used temperature- and pressure-sensitive paints based on rhodamine B and platinum octaethylporphyrin, respectively, to characterize the behavior of an airfoil model in a wind tunnel operated at Mach numbers of up to 0.56. Their imaging system used a Pulnix model TM-745 CCD camera to record the luminescence signals. This method of pressure sensing for aerodynamic applications via fluorescent materials has grown rapidly the past five years. Finally, we note that the characteristics of optical fibers change as a function of applied pressure. For example, tensile stresses in the range of 0.05–4 GPa will significantly change the transmission at 325 nm for a 125-μm-diam fiber of $\approx$20 m length. Furthermore, for this excitation, the ratio of emission bands at 400 and 620 nm changes.[250] (Pure silica optical fibers have a mechanical strength of about 5 GPa at room temperature, in practice, as compared with a theoretically predicted value of 22 GPa.) Allison *et al.*[251] have investigated various experimental arrangements aimed at exploiting this effect in the design of optomechanical sensors, while Egalon and Rogowski[252] have studied how the modal patterns in a fiber vary with axial strain.

C. Flow tracing

Nakatani *et al.*[253–255] developed techniques for using phosphor particles as tracers to aid in visualizing the flows of liquids. Both continuous ultraviolet lamps and a nitrogen laser served as sources of illumination for the different configurations of this method. The phosphors with which they worked included various combinations of ZnS, CdS, and CaS. The last material has a lifetime of $\approx$1.5 s, making it particularly well suited for measuring the flow of slowly moving liquids. Streak photographs were used to track the seeded fluid, yielding distance versus time relationships that made it possible to resolve the flow's velocity and direction. Their experimental results and analyses revealed the wide variety of conditions over which the phosphor particles could be used to make high fidelity mappings of the flow field.

Keyes and Sartory[256] have also used the luminescence properties of thermographic phosphors in fluid dynamics experiments. Their goal was to evaluate the Ludwieg model via determinations of local fluid drag.

D. Particle beam characteristics

Phosphors and other scintillating materials can be used to study the structure of high energy ion and electron beams, indicating the position, profile, and flux density of the beam as a function of phosphor brightness. Also, if the beam current is large enough to heat the material, then an appropriate method of phosphor-based thermometry can be used to diagnose the beam. Over time, as a significant dose accumulates, the phosphor's efficiency will deteriorate due to radiation damage. This process, which manifests itself as a decrease in brightness, was first noted by Birks and Black.[257,258] They established the relationship between phosphor intensity, I, and total accumulated dose, N:

$$I/I_0 = 1/[1 + (N/N_{1/2})]. \tag{16}$$

Here, I_0 is the original zero-dose brightness and $N_{1/2}$ is the characteristic dose at which the brightness decreases to one-

TABLE V. Performance characteristics of several relatively recent, representative thermographic phosphor temperature measurement systems.

Author(s)	Application	Phosphor/method	Design features	Range/uncertainty	References
Mannik *et al.*	Noncontact thermometry of 540 MW electrical generator rotor surfaces	Gd_2O_2S:Eu, Y_2O_2S:Eu and La_2O_2S:Eu, decay lifetime	Ambient magnetic field of the generator was ≈ 1 T; measurement had spatial resolution of 4 mm	41–73 °C $\Delta T = \pm 2.0$ °C	1987; 86, 196, 197, 198
Dowell	Design and evaluation of a thermal phosphor-based temperature standard	Y_2O_3:Eu (single crystals), decay lifetime	Fluorescence lifetimes were measured relative to a cesium-beam atomic clock	$\approx$30–800 °C $\Delta T = 6.4$ °C (at $\approx$800 °C)	1989; 98
Noel *et al.*	Remote measurement of vane and blade temperatures in an operating turbine engine	YVO_4:Eu, Y_2O_3:Eu and YAG:Tb, decay lifetime	Phosphor layers from 4 to 35 μm thick applied by rf sputtering, e-beam deposition, chemical binder	450–1300 °C relative error $\approx \pm 2\%$	1991; 212–214
Draina and Anderson	Temperature control of IC wafers during plasma etch and chemical vapor deposition processes	Luxtron MIH probes and custom-designed SEMATECH probe	Measurements made in vacuum and at low pressures relative to a type-K thermocouple or a PRT	25–400 °C $\Delta T \approx \pm 10$ °C	1992; 262
Alaruri *et al.*	Monitoring temperatures of turbine engine parts in a burner rig	Y_2O_3:Eu (4.52%) and YAG:Tb (5%), decay lifetime	Air-cooled fiberoptic probe with sapphire lens was developed; its damage threshold was 3.5 J/cm^2	27–1095 °C accuracy quoted as $\pm 3\%$ for Y_2O_3:Eu	1993; 103, 244
Chyu and Bizzak	2D surface temperature measurements/general heat transfer studies	$La_2O_2S:Eu^{+3}$, intensity ratio of 512–620 nm lines	80 mJ excitation energy supplied by laser beam of 6.4-mm-diam during 8 ns pulses	18–60 °C $\Delta T = \pm 0.5$ °C	1994; 137, 263
Luxtron Corp.	Commercially available apparatus used in a wide variety of measurements	MFG2 phosphor-tipped fiberoptic probes, decay lifetime	Excitation and fluorescence return pulses transmitted over the same optical fiber (model 790 systems)	-200–450 °C $\Delta T = \pm 0.1$ °C rms, at calibration point	1993; 166
Anghel *et al.*	Development of probes useful in low temperature industrial applications	Ruby crystal with fiberoptic couplings, decay lifetime	Green LED used to excite sensor, overall size of probe 4×10 mm, calibrated with type-K thermocouple	≈ -70–30 °C $\Delta T = \pm 0.3$ °C	1995; 129

half of its original level. Hence, $N_{1/2}$ is an indicator of a phosphor's susceptibility to radiation damage. In recent work, Hollerman *et al.*[259,260] studied the proton-beam-induced damage of several common phosphor materials at 3 and 60 MeV, and found that the dose associated with one-half decay ranged from $(1-20)\times 10^{15}$ protons/cm^2. One of the interesting results was that raising the temperature from ambient to 150 °C actually increased $N_{1/2}$ somewhat. Evidently, the higher temperatures promoted some healing of atomic-level damage sites. Such information may be of significance in assessing the use of phosphors in nuclear reactor as well as particle beam applications.

Hollerman and colleagues[261] have already explored the possible use of Gd_2O_2S:Tb for this class of application, with the specific goal being to develop a beam-positioning system for high energy accelerators. They used a 45 MeV proton beam to irradiate a surface painted with this material in order to determine the change in the total integrated intensity of the fluorescence as a function of temperature. Their measurements showed that the intensity dropped by a factor of 2 in going from 113 to 133 °C, thus indicating the potential importance of thermal effects in selecting a phosphor for use in beam positioning systems.

VII. DISCUSSION

A. Performance characteristics

Phosphor thermometry systems can be divided roughly into two broad categories: those designed for laboratory investigations and those designed for field applications. While there are many performance characteristics that are mutually important to both general classes of apparatus, a number of significant differences also exists between them. The laboratory systems are typically used to explore the performance limits of the technique under highly controlled conditions, for instance, varying only one experimental or environmental parameter at a time during calibration studies. On the other hand, field-grade systems must be very robust in nature, with the phosphor target in particular being able to withstand extreme levels of thermal and mechanical shock, as occurs when measurements are taken, for example, on surfaces impinged by high speed, combusting flows.

Because of the diverse range of situations over which phosphor thermometry has been employed, it is instructive to intercompare several recent realizations of the technique to establish a sense of the overall performance limits of modern systems. To that end, Table V presents a summary of the characteristics of several different but largely representative experimental arrangements, including laboratory-grade and field-deployed setups. From Table V, and a perusal of the discussions in the preceding sections, it is evident that the temperature-dependent characteristics of a wide variety of phosphors have been studied to date. These include single-crystal and powdered materials, ceramic oxides and oxysulfides, and many others as well. The thermometric properties of these materials have been exploited over the range from 4 to over 1800 K. The fluorescence lifetime approach to determining the sample's temperature is preferred to alternative methods in many types of field applications, especially those where large and broadband optical background signals (e.g., blackbody radiation) are present. Of course, ratios of temperature-dependent line intensities, or simply measurements of the individual line intensities as a function of temperature, also provide useful thermometric data. This is par-

ticularly the case for those phosphors used in the range of 100–300 °C which, when operated below their quenching temperature, exhibit relatively bright optical lines. The phosphor target can be interrogated on the surface to which it is bonded by light channeled through optical fibers, the tips of which may be placed arbitrarily close to the surface of interest. Alternatively, a laser beam can be steered onto the target by mirrors, over paths of up to 10 m. Phosphor thermography is generally capable of spatial resolutions on the order of 1 μm, and the phosphors typically exhibit no sensitivity in their fluorescence parameters to ambient magnetic fields of at least 1 T. (Extremely fine spatial resolutions, 0.7 μm, have been reported by Kolodner and colleagues,[264,265] who used rare-earth chelate films to make fluorescently imaged surface temperature profiles of metal–oxide–semiconductor field effect transistor MOSFET circuits. They have used similar compounds to make noncontact temperature measurements of a glass resin undergoing reactive-ion etching.[266])

The measurement uncertainties found in this class of thermometry system range from approximately 0.1% to 5% of the temperature reading, with some authors reporting smaller uncertainties in particular experimental arrangements. While the development of an error budget is only meaningful within the context of a given apparatus, factors that generally contribute to the overall measurement error include, for example, the chemical purity of the phosphor (contaminant dopants may make the decay time multiexponential in nature), the presence of uncharacterized nonlinearities in the transducer and signal conditioning electronics (e.g., rectification errors), and mathematical or computational peculiarities in the algorithm and processor used to reduce the data (e.g., baseline offset error and other modeling inadequacies). In addition to these types of systematic error, there are also several sources of random error (phototube shot noise, etc.) that introduce statistical uncertainty into the results. Section IV B contains detailed discussions of several of the sources of experimental error and signal-to-noise ratio degradation that have to be dealt with during calibration of a phosphor thermography system.

Ultimately, of course, the quantity of interest is the temperature of the phosphor target itself, which is presumably almost identical to that of the substrate to which it is bonded. In many experimental arrangements, the level of breakdown in the exactness of this presumption constitutes the limiting factor on the final accuracy with which the temperature of the substrate can be determined. This is because the phosphor coating (no matter how thin) may have enough heat capacity and thermal conductivity to alter its thermal environment. If so, then the temperature of the substrate may be different from that of the coating and, of importance, from what it would be in the absence of the coating. This is usually not a problem at ambient temperatures where the heat fluxes are small and both emissivity and blackbody radiation play only a negligible role. However, at higher temperatures, and especially in applications calling for measurements inside of turbine engines, high temperature wind tunnels, etc., it may be necessary to make a thermal model of the measurement zone to determine whether or not the heat transfer process will impose a limit on the ultimate accuracy of the measurement.

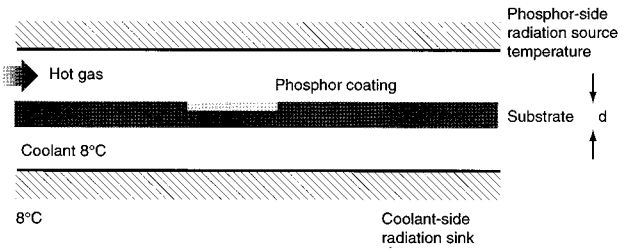

FIG. 28. Simplified thermal model geometry.

For the idealized situation shown in Fig. 28, a simple model was developed for use in estimating the size of the uncertainties introduced by this effect into high temperature aerospace applications.[267] It relies on a perturbative solution of the steady-state heat conduction problem. The emissivities and thermal conductivities for a given coating and substrate may not always be known but, as seen in Table VI, rough estimates suffice to bracket the error. The baseline case and a parametric sensitivity analysis of it are depicted in Table VI.

B. Comparison with other techniques

One of the primary virtues of any type of noncontact thermometry is the elimination of electrical leads and/or other interconnections between the object under study and the sensor element(s) and associated read-out instrumentation. In fact, in many cases the presence of leads introduces insurmountable mechanical roadblocks, e.g., making thermocouples, thermistors, noise thermometers, etc., seldom used for measuring the surface temperatures of moving objects. While sliprings are sometimes employed as an interface between the sensor leads and the read-out device in such situations, they are typically limited in maximum speed of operation. Also, the relative motions of the slipring components can generate electrical noise that can corrupt the signal. From a broader perspective, *any* measurement environment that has a high EMI/RFI background can lead to inductive coupling of electrical noise into thermocouple and resistive-temperature-device leads, whether the sensor is static or moving. This latter point is a well-known problem and a great deal of effort has gone into the design of signal conditioning circuits that have high levels of common-mode rejection and other electronic features that work to maximize the signal-to-noise ratio. Even so, electrical pickup can place severe constraints on a variety of measurement circumstances.

Robinson and Beams[268] attempted to address the measurement of temperatures on high speed rotors by designing a miniature radio telemetry system that was able to transmit a temperature-dependent signal. With it, they could resolve temperature differences of 0.01 °C on rotors spinning at speeds of up to 300 rotations per second. However, on-board circuitry and battery power were required, and an array of the devices would have been needed to obtain even an approximate mapping of the surface temperature of the rotor.

In contrast to all of these limitations, phosphor thermography is a leadless, completely noncontact technique, and the photo-optical nature of the signal makes it unsusceptible to

TABLE VI. Thermal model error analysis.

Parameter	Base case	Increased spot diameter	Thicker coating	Thinner substrate	Increased coating emissivity	Increased substrate emissivity	Decreased coating thermal conductivity	Decreased substrate thermal conductivity	Increased gas temperature
Coating diameter	12 mm	25 mm	⋯	⋯	⋯	⋯	⋯	⋯	⋯
Coating thickness	0.15 mm	⋯	1.5 mm	⋯	⋯	⋯	⋯	⋯	⋯
Substrate thickness	6 mm	⋯	⋯	3 mm	⋯	⋯	⋯	⋯	⋯
Coating emissivity	0.33	⋯	⋯	⋯	0.9	⋯	⋯	⋯	⋯
Substrate emissivity	0.5	⋯	⋯	⋯	⋯	0.9	⋯	⋯	⋯
Coating thermal conductivity	2.76 W/mK	⋯	⋯	⋯	⋯	⋯	0.276	⋯	⋯
Substrate thermal conductivity	45 W/mK	⋯	⋯	⋯	⋯	⋯	⋯	18	⋯
Hot gas temperature	920 K	⋯	⋯	⋯	⋯	⋯	⋯	⋯	1250 K
Thermal radiation source	920 K	⋯	⋯	⋯	⋯	⋯	⋯	⋯	⋯
Estimated error	+1%	+0.8%	+10%	+1%	2%	−0.7%	10%	0.7%	0.8%

EMI/RFI pickup. Only a thin film of phosphor is needed on the surface under study, and no on-board circuitry is required for interrogation. Although most phosphor thermography systems do use optical fibers to launch and recover the incident and fluorescence pulses in proximity to the target, refractive and reflective components have been used to steer beams along free-space paths of up to 10 m without difficulty.[218]

Competing noncontact techniques include radiometric IR thermography and optical pyrometry. Very sophisticated and highly developed versions of both classes of instrumentation are commercially available, and a substantial manufacturer's literature describes the performance characteristics of the pertinent devices. The thermometric resolution presently obtained via either technique is typically 0.1 °C.

Some IR thermography systems require liquid nitrogen cooling of the detector array, while others use solid-state devices to accomplish this. They can thermally image objects at distances both near and far from the camera, with the spatial resolution of the resulting thermograms governed in either case by the granularity of the detector's pixelation. In some measurement situations, it may be useful and perhaps even necessary to interchange with the thermal target being imaged a blackbody source that is peaked at the proper temperature. This could help to normalize the response of the camera to the thermal background against which it must operate. On the other hand, measurements of a phosphor's fluorescence lifetime can be made in the presence of substantial amounts of blackbody background, and with good spatial resolution even when the target is distantly located.

Optical pyrometry is a well-established technique that has found many applications in science and industry. When attempting to use a pyrometer that is not located in close proximity of its target, though, any intervening haze or other obscuring atmospheric effect can mask the signal, thus making this technique relatively sensitive to the environment in which it must function. Moreover, for maximum accuracy, it is important to know how the emissivity of the surface under observation varies with temperature. Phosphor thermography is largely immune to both of these limitations, thus allowing it to be of use in certain of the situations where parametric measurements of temperature are either difficult or impractical. Of course, advances are always being made in pyrometry too, and improved instrumentation that can overcome various measurement hurdles is now becoming available.[269,270]

C. Suggestions for further research

1. Recommendations for improvement

As new applications for phosphor thermometry arise, there will be a concomitant need for target materials that have luminescence characteristics appropriate to the measurement being undertaken. For instance, although many of the phosphors that have been studied to date emit at the longer visible wavelengths, i.e., at the yellow-to-red end of the spectrum, some color-sensitive applications might call for a phosphor that emits at shorter wavelengths, near the blue-to-violet end of the spectrum. Cunningham *et al.*[271] have made preliminary measurements of the temperature dependence of the excitation and emission spectra of eight different phosphors that emit in the blue region when excited by ultraviolet light. Their study covered the temperatures from 20 to 350 °C. It would be beneficial to explore the decay lifetime dependence on temperature of these materials, and to extend the overall study to a higher range of temperatures.

Similarly, Allison *et al.*[272] have recently observed that $LuPO_4$ codoped with Dy (1%) and Eu (2%) has six different spectral lines with temperature-dependent intensities. Moreover, each of these lines has a different thermal sensitivity. (One of them, at 453 nm, actually increases in intensity as the temperature of the material rises.) The simultaneous availability of these multiple fluorescence signals suggests the possibility of using two or more of them to make differential measurements of temperature. Such an arrangement might introduce a certain amount of ''optical common-mode rejection'' into the measurement. This could potentially improve the signal-to-noise ratio in situations where intensity-based remote thermometry is made difficult by the presence of a large blackbody background. More extensive studies will be needed to determine the optimum ratio of dopants for this material, to fully characterize the temperature sensitivity

of its fluorescence, and to evaluate its robustness. The fluorescence properties of other codoped phosphors should be investigated as well.

At temperatures in the range of 1000 °C and above, the fluorescence lifetimes of virtually all phosphors are very short. Once the lifetime drops below about 100 μs, the speed, resolution, and accuracy requirements placed on the data acquisition system typically call for the use of sophisticated transient digitizers and fast pulse analyzers. Equipment of this type is used routinely in nuclear, particle, and laser physics laboratories. If more were done to adapt it for use in phosphor thermometry systems, then the range over which temperature measurements could be made with this technique might be extended.

Improvements in the methods of phosphor bonding would also be welcome. A particularly valuable advance would arise from the development of a technique that would produce thin, durable, spray-on coatings like those created by flame and plasma deposition, but without the need for high-temperature combusting gases and expensive apparatus.

Finally, the potential of thermographic phosphors to sense still other physical quantities should continue to be explored. Interesting steps along this line have been taken by Egalon, Rogowski and colleagues.[273–275] They investigated the possible use in chemical sensing applications of thin films of fluorescent material placed at the core/cladding interface of fiberoptic probes. Their publications review the literature that is relevant to this effort and describe the results of a preliminary experiment done with large diameter (9 mm) glass tubing coated with Y_2O_3:Eu^{3+} powder that was mixed into a polymer binder.

2. Thermographic phosphor temperature standards

The kelvin stands apart from the other base units of the Système International d'Unités (SI) in that it is not realized in terms of universally reproducible atomic quantities. (The kilogram, too, is still defined in terms of an artifactual standard.) The intriguing possibility of establishing a temperature scale based on the atomic transitions of luminescing phosphors has been suggested as a means of addressing this situation.[110] In such a scheme, the relationship between the decay lifetime of a particular excited state of a given phosphor and its temperature would have to be predicted reliably from an appropriate quantum mechanical model. Moreover, the fluorescence lifetime of the phosphor must be measured in terms of the ''ticks'' of an atomic clock and the systematic errors of the measurement system must be well understood. If these conditions could be met, then one could establish in principle an absolute scale of temperature based on atomic transitions over the range for which the phosphor in use has temperature-dependent fluorescence.

This would be an ambitious undertaking, of course, and it would ultimately require the resolution of many important metrological issues. (Even the existing realization of the kelvin via the ITS-90, which has been studied carefully for many years,[93,94] remains the subject of close metrological scrutiny.[276]) The intermediate step of investigating single-crystal thermal phosphors as temperature transfer standards has already been taken[277] though, with $LaPO_4$:Eu having been studied for this purpose over the range from room temperature through 650 °C. $LuPO_4$:Eu has also been studied.[278] Dowell[98] developed a NIST-traceable thermometry system based on single crystals of Y_2O_3:Eu, with the goal in mind of exploring the metrological issues of its use in absolute thermometry. In fact, the time base for his data collection and analysis system was calibrated with a Frequency and Time Systems model FTS 4050 cesium-beam atomic clock buffered by a Spectracom 8140 distribution amplifier. His work demonstrated that precision of 0.6% relative to existing standards could be obtained with phosphor thermometry at temperatures of up to $\approx$1060 °C. It also revealed several interesting sources of systematic uncertainty that can contribute to the error budget of such systems. Meanwhile others, notably Zhang, Grattan, and colleagues (including workers at the Colonnetti Institute),[130,150] have developed very useful models of the theoretical dependence of the lifetime of YAG:Cr^{3+} on temperature, and confirmed them with experimental measurements taken through 900 K. Some other theoretical work that interrelates fluorescence lifetime and temperature was discussed in Sec. II C1.

The results of these efforts, along with those of related studies by various others, suggest that phosphor thermometry may make it possible to realize the kelvin over a continuous range of temperatures (perhaps through 1300 K and above) without the need for interpolation between fixed points. (An interesting aside is that some work has already been done on using the melting points of refractory ceramics, i.e., undoped phosphors, as secondary high-temperature standards,[279] thus making these materials potential contributors to a future version of the existing variety of temperature scale as well.) A very significant effort would be required to bring a phosphor-based, atomic-transition realization of the kelvin into existence, but interest in the possibility has prompted research on the subject at a growing number of standards laboratories.[280,281]

ACKNOWLEDGMENTS

The authors acknowledge the efforts of the many graduate students from the University of Virginia, the University of Tennessee, and various other colleges and universities who have done much to establish the scientific and engineering foundations of phosphor thermography over the past decade. They also thank the large number of colleagues at the Oak Ridge National Laboratory, the Los Alamos National Laboratory, Wright-Patterson Air Force Base, the University of Virginia, the University of Tennessee, EG&G Energy Measurements, Inc., and the International Bureau of Weights and Measures for their interest in this work, for many stimulating and useful discussions, and/or for their ongoing research efforts in this area. The authors give special acknowledgement to W. A. (Bill) Stange of Wright Laboratory for his continued support of much of the effort described above for well over a decade. His influence has made possible the development of the method for important aerospace and turbine engine applications. Finally, the authors thank the workers at the Science and Engineering Library of the University of Virginia (Physics Branch Librarian James Shea in particular), and those at the Oak Ridge National Laboratory Library

(Jon Arrowood in particular) for much valuable assistance in obtaining several of the references cited in this review. The Oak Ridge National Laboratory is operated by Lockheed-Martin Energy Research, Inc. under Contract No. DE-AC05-84OR21400 with the U.S. Department of Energy. The National Technical Information Service of the U.S. Department of Commerce (5285 Port Royal Road, Springfield, VA 22161) is a useful point of contact for obtaining information about the availability and distribution of U.S. Government technical reports.

[1] K. T. V. Grattan and Z. Y. Zhang, *Fiber Optic Fluorescence Thermometry* (Chapman and Hall, London, 1995).
[2] P. Pringsheim, *Fluorescence and Phosphorescence* (Interscience, New York, 1949), pp. 1–5.
[3] K. H. Butler, *Fluorescent Lamp Phosphors* (Pennsylvania State University Press, University Park, PA, 1980).
[4] R. C. Ropp, *Luminescence and the Solid State*, Studies in Inorganic Chemistry Vol. 12 (Elsevier, Amsterdam, 1991).
[5] R. C. Ropp, *The Chemistry of Artificial Lighting Devices: Lamps, Phosphors and Cathode Ray Tubes*, Studies in Inorganic Chemistry Vol. 17 (Elsevier, Amsterdam, 1993).
[6] R. H. Hoskins and B. H. Soffer, US Patent No. 3,496,482 (31 December 1963).
[7] P. N. Yocom, *Proceedings of the 6th Rare Earth Research Conference* (Oak Ridge National Laboratory, Oak Ridge, TN, 1967), pp. 228–237.
[8] C. Greskovich and J. P. Chernoch, J. Appl. Phys. **44**, 4599 (1973).
[9] M. J. Weber, in *The Handbook on the Physics and Chemistry of Rare Earths*, edited by K. A. Gschneidner, Jr. and L. Eyring (North-Holland, Amsterdam, 1979), Chap. 35, pp. 275–315.
[10] Neubert, US Patent No. 2,071,471 (1937).
[11] F. Urbach, N. R. Nail, and D. Pearlman, J. Opt. Soc. Am. **39**, 1011 (1949).
[12] F. Urbach, US Patent No. 2,551,650 (8 May 1951).
[13] K. Wickersheim and R. Alves, Ind. Res. Dev. **21**, 82 (1979).
[14] K. Wickersheim and M. Sun, Res. Dev. **27**, 114 (1985).
[15] L. C. Bradley III, Rev. Sci. Instrum. **24**, 219 (1953).
[16] W. H. Byler and F. R. Hays, Nondestr. Test. **19**, 177 (1961).
[17] R. R. Sholes and J. G. Small, Rev. Sci. Instrum. **51**, 692 (1980).
[18] T. Bosselmann, A. Reule, and J. Schroeder, Proc. SPIE **514**, 151 (1984).
[19] K. T. V. Grattan, R. K. Selli, and A. W. Palmer, Rev. Sci. Instrum. **59**, 1328 (1988).
[20] N. C. Chang, J. Appl. Phys. **34**, 3500 (1963).
[21] P. A. Czysz and D. N. Kendall, McDonnell Company Technical Report No. F 938, April 1968.
[22] P. A. Czysz and W. P. Dixon, SPIE J. **7**, 77 (1969).
[23] P. A. Czysz and W. P. Dixon, Instrum. Control Syst. **41**, 71 (1968).
[24] K. A. Wickersheim, R. A. Buchanan, L. E. Sobon, R. V. Alves, and J. J. Pearson, Lockheed Missiles & Space Company, Third Annual Report No. 4-17-69-1, June 1969.
[25] K. A. Wickersheim, R. V. Alves, and R. A. Buchanan, IEEE Trans. Nucl. Sci. **NS-17**, 57 (1970).
[26] R. V. Alves and R. A. Buchanan, IEEE Trans. Nucl. Sci. **NS-20**, 415 (1973).
[27] R. V. Alves, R. A. Buchanan, K. A. Wickersheim, and E. A. C. Yates, J. Appl. Phys. **42**, 3043 (1971).
[28] L. E. Sobon, K. A. Wichersheim, R. A. Buchanan, and R. V. Alves, J. Appl. Phys. **42**, 3049 (1971).
[29] H. Kusama, O. J. Sovers, and T. Yoshioka, Jpn. J. Appl. Phys. **15**, 2349 (1976).
[30] J. P. Leroux and R. Taboue, Societe Francaise des Thermiciens, Rencontre annuelle, La Baule 5, 6, 7 May 1975.
[31] J. P. Leroux, Publications Scientifiques et Techniques du Ministere de l'Air, NT No. 119, 1962.
[32] J. P. Leroux, G. Blanc, M. Delisee, P. Coppolani, R. Taboue, Cahiers de la Thermique (I.F.C.E. Paris), cahiers No. 3 Ser. A, March 1973, p. IV. 1 a IV.55.
[33] P. Baumann, Rech. Aérosp. (5), 29 (1993).
[34] K. A. James, W. H. Quick, and V. H. Strahan, Control Eng. **26**, 30 (1979).
[35] T. Samulski and P. K. Shrivastava, Science **208**, 193 (1980).
[36] T. Samulski and P. K. Shrivastava, Phys. Med. Biol. **27**, 107 (1982).
[37] J. S. McCormack, Electron. Lett. **17**, 630 (1981).
[38] G. E. Gross, Midwest Research Institute Final Report (M.R.I. Project No. 2300-P), June 1960.
[39] J. C. Gravitt, G. E. Gross, J. E. Beachy, and W. E. McAllum, Midwest Research Institute Final Report (M.R.I. Project No. 2423 P), June 1963.
[40] D. J. Brenner, National Bureau of Standards (U.S.) Technical Note No. 591, July 1971.
[41] E. M. Fry, *Temperature: Its Measurement and Control in Science and Industry*, (Instrument Society of America, Research Triangle Park, NC, 1971), Vol. 4, pp. 577–583.
[42] R. J. D. Pattison, UK Patent No. 1, 480, 583 (20 July 1977).
[43] L. J. Dowell, Appl. Mech. Rev. **45**, 253 (1992).
[44] L. J. Dowell, G. T. Gillies, S. W. Allison, and M. R. Cates, Martin Marietta Energy Systems, Inc., Technical Report No. K/TS-11, 771, July 1986.
[45] L. J. Dowell and G. T. Gillies, University of Virginia Technical Report No. UVA/640419/NEEP89/102, April 1989.
[46] L. J. Dowell, G. T. Gillies, S. W. Allison, and M. R. Cates, J. Lumin. **36**, 375 (1987).
[47] W. C. B. Peatman, M.Sc. thesis, University of Virginia, 1987.
[48] G. H. Dieke and H. M. Crosswhite, Appl. Opt. **2**, 675 (1963).
[49] W. H. Fonger and C. W. Struck, J. Chem. Phys. **52**, 6364 (1970).
[50] C. W. Struck and W. H. Fonger, J. Appl. Phys. **42**, 4515 (1971).
[51] G. Blasse, Prog. Solid State Chem. **18**, 79 (1988).
[52] M. J. Weber, Phys. Rev. B **8**, 54 (1973).
[53] D. J. Robbins, B. Cockayne, B. Lent, C. N. Duckworth, and J. L. Glasper, Phys. Rev. B **19**, 1254 (1979).
[54] D. J. Robbins, B. Cockayne, J. L. Glasper, and B. Lent, J. Electrochem. Soc. **126**, 1213 (1979).
[55] D. J. Robbins, B. Cockayne, J. L. Glasper, and B. Lent, J. Electrochem. Soc. **126**, 1221 (1979).
[56] D. J. Robbins, B. Cockayne, B. Lent, and J. L. Glasper, J. Electrochem. Soc. **126**, 1556 (1979).
[57] L. Ozawa and P. M. Jaffe, J. Electrochem. Soc. **118**, 1678 (1971).
[58] J. L. Sommerdijk and A. Bril, J. Electrochem. Soc. **122**, 952 (1975).
[59] W. F. van der Weg, T. J. A. Popma, and A. T. Vink, J. Appl. Phys. **57**, 5450 (1985).
[60] L. J. Dowell, Los Alamos National Laboratory Technical Report No. LA-11873-MS, August 1990.
[61] L. J. Dowell, J. Laser Appl. **3**, 27 (1991).
[62] S. W. Allison, M. R. Cates, L. A. Franks, H. M. Borella, S. S. Lutz, W. D. Turley, B. W. Noel, and A. Beasley, Martin Marietta Energy Systems, Inc., Report No. ORNL/ATD-12, April 1989.
[63] R. G. Hellier, Jr., M.Sc. thesis, University of Virginia, 1992.
[64] A. T. Rhys-Williams and M. J. Fuller, Comput. Enhanced Spectrosc. **1**, 145 (1983).
[65] D. M. de Leeuw and G. W. 't Hooft, J. Lumin. **28**, 275 (1983).
[66] S. Imanaga, S. Yokono, and T. Hoshima, Jpn. J. Appl. Phys. **19**, 41 (1980).
[67] H. Yamamoto and T. Kano, J. Electrochem. Soc. **126**, 305 (1979).
[68] P. H. Dowling and J. R. Sewell, J. Electrochem. Soc. **100**, 22 (1953).
[69] R. Raue, K. Nieuwesteeg, and W. Busselt, J. Lumin. **48&49**, 485 (1991).
[70] J. L. Ferri and J. E. Mathers, US Patent No. 3,639,932 (8 February 1972).
[71] S. S. Lutz, W. D. Turley, H. M. Borella, B. W. Noel, M. R. Cates, and M. R. Probert, *Proceedings of the 34th International Instrumentation Symposium: Instrumentation for the Aerospace Industry* (Instrument Society of America, Research Triangle Park, NC, 1988), pp. 217–229.
[72] S. W. Allison, M. R. Cates, B. W. Noel, and G. T. Gillies, IEEE Trans. Instrum. Meas. **37**, 637 (1988).
[73] Guo Chang-Xin, Zhang Wei-Ping, and Shi Chao-Shu, J. Lumin. **24–25**, 297 (1981).
[74] A. R. Bugos, M.Sc. thesis, University of Tennessee, 1989.
[75] A. R. Bugos, S. W. Allison, D. L. Beshears, and M. R. Cates, in *Proceedings of the IEEE Southeastcon Conference* (IEEE, New York, 1988), pp. 228–233.
[76] W. D. Turley, C. E. Iverson, S. S. Lutz, R. L. Flurer, J. R. Schaub, S. W. Allison, J. S. Ladish, and S. E. Caldwell, Proc. SPIE **1172**, 27 (1989).
[77] S. W. Allison, M. A. Abraham, L. A. Boatner, M. R. Cates, D. L. Beshears, K. W. Tobin, B. W. Noel, and W. D. Turley, *Technical Digest of the Eleventh International Congress on Lasers & Electro-Optics* (Laser Institute of America, Anaheim, CA, 1992).
[78] D. L. Beshears, H. M. Henderson, T. J. Henson, M. J. Bridges, R. M. Sadler, M. A. Cyr, Martin Marietta Energy Systems, Inc. Report No. K/ETAC-59, July 1988.
[79] H. M. Borella, EG&G Energy Measurements Inc. Technical Report No. M-2657, March 14, 1986.

[80] W. D. Turley, H. M. Borella, and D. L. Beshears; EG&G Energy Measurements, Inc. Technical Report No. EGG 10617-2133, March 1992.
[81] T. G. Maple and R. A. Buchanan, J. Vac. Sci. Technol. **10**, 616 (1973).
[82] C. Sella, J. C. Martin, and Y. Charreire, Thin Solid Films **90**, 181 (1982).
[83] K. L. Saenger, in *Pulsed Laser Deposition of Thin Films*, edited by D. B. Chrisey and G. K. Hubler (Wiley, New York, 1994), pp. 581–604.
[84] S. Metev, in Ref. 83, pp. 255–264.
[85] H. P. Christensen, D. R. Gabbe, and H. P. Jenssen, Phys. Rev. B **25**, 1467 (1982).
[86] L. Mannik, S. K. Brown, and S. R. Campbell, Appl. Opt. **26**, 4014 (1987).
[87] R. V. Alves, J. J. Pearson, K. A. Wickersheim and R. A. Buchanan, Proceedings of the Tenth Rare Earth Conference, Carefree, AZ, 1970, Vol. 2, pp. 703–713.
[88] B. W. Noel, D. L. Beshears, H. M. Borella, W. K. Sartory, K. W. Tobin, W. D. Turley, and R. K. Williams, Los Alamos National Laboratory, Technical Report No. LA-12129-MS, July 1991.
[89] L. J. Dowell and G. T. Gillies, University of Virginia Technical Report No. UVA/538033/NEEP89/101, September 1988.
[90] A. Lacaita, S. Cova, and M. Ghioni, Rev. Sci. Instrum. **59**, 1115 (1988).
[91] T. Louis, G. H. Schatz, P. Klein-Bölting, A. R. Holzwarth, G. Ripamonti, and S. Cova, Rev. Sci. Instrum. **59**, 1148 (1988).
[92] H. Preston-Thomas, Metrologia **27**, 3 (1990).
[93] Comité Consultatif de Thermométrie, *Techniques for Approximating the International Temperature Scale of 1990* (Bureau International des Poids et Mesures, Sèvres, France, 1990).
[94] Comité Consultatif de Thermométrie, *Supplementary Information for the International Temperature Scale of 1990* (Bureau International des Poids et Mesures, Sèvres, France, 1990).
[95] L. J. Dowell, W. N. Lutz, G. T. Gillies, R. C. Ritter, S. W. Allison, and M. R. Cates, Proc. Laser Inst. Am. **57**, 135 (1987).
[96] W. N. Lutz, G. T. Gillies, and S. W. Allison, Ind. Heat. **54**, 36 (1987).
[97] W. N. Lutz, M.Sc. thesis, University of Virginia, 1987.
[98] L. J. Dowell, Ph.D. dissertation, University of Virginia, 1989.
[99] W. N. Lutz, G. T. Gillies, and S. W. Allison, Rev. Sci. Instrum. **60**, 673 (1989).
[100] L. Crovini and V. Fernicola, Sens. Actuators B **7**, 529 (1992).
[101] V. Fernicola and L. Crovini, in *Temperature: Its Measurement and Control in Science and Industry*, edited by J. F. Schooley (American Institute of Physics, New York, 1992), Vol. 6, Part 2, pp. 725–730.
[102] M. R. Cates, S. W. Allison, L. A. Franks, H. M. Borella, B. R. Marshall, and B. W. Noel, Proc. Laser Inst. Am. **49–51**, 142 (1985).
[103] S. D. Alaruri, A. J. Brewington, M. A. Thomas and J. A. Miller, IEEE Trans. Instrum. Meas. **42**, 735 (1993).
[104] G. T. Gillies, L. J. Dowell, W. N. Lutz, S. W. Allison, M. R. Cates, B. W. Noel, L. A. Franks, and H. M. Borella, Proc. Laser Inst. Am. **63**, 15 (1988).
[105] E. Milcent, G. Olalde, J. F. Robert, D. Hernandez, and M. Clement, Appl. Opt. **33**, 5882 (1994).
[106] S. W. Allison, G. T. Gillies, D. W. Magnusson, and T. S. Pagano, Appl. Opt. **24**, 3140 (1985).
[107] S. W. Allison, M. R. Cates, G. T. Gillies, and B. W. Noel, Opt. Eng. (Bellingham) **26**, 538 (1987).
[108] S. W. Allison and G. T. Gillies, Appl. Opt. **33**, 1802 (1994).
[109] L. J. Dowell, G. T. Gillies, and S. W. Allison, Opt. Eng. (Bellingham) **26**, 547 (1987).
[110] L. J. Dowell, M.Sc. thesis, University of Virginia, 1987.
[111] T. A. Hanft, S. W. Allison, J. V. Laforge, and G. T. Gillies, Ind. Heat. **62**, 39 (1995).
[112] J. N. Demas, *Excited State Lifetime Measurements* (Academic, New York, 1983).
[113] G. T. Gillies and S. W. Allison, Rev. Sci. Instrum. **57**, 268 (1986).
[114] D. M. Gualtieri, Rev. Sci. Instrum. **58**, 299 (1987).
[115] L. J. Dowell, G. T. Gillies, M. R. Cates and S. W. Allison, Rev. Sci. Instrum. **58**, 1245 (1987).
[116] G. T. Gillies, M. B. Scudiere, and S. W. Allison, Rev. Sci. Instrum. **60**, 3762 (1989).
[117] W. N. Lutz, L. J. Dowell, and G. T. Gillies, University of Virginia Technical Report No. UVA/532705/NEEP87/101, September 1986.
[118] L. J. Dowell and G. T. Gillies, Rev. Sci. Instrum. **59**, 1310 (1988).
[119] L. J. Dowell and G. T. Gillies, Rev. Sci. Instrum. **62**, 242 (1991).
[120] L. J. Dowell and G. T. Gillies, Los Alamos National Laboratory Technical Report No. LA-UR-90-2621, August 1990.
[121] Z. Y. Zhang, K. T. V. Grattan, Y. Hu, A. W. Palmer, and B. T. Meggitt, Rev. Sci. Instrum. **67**, 2590 (1996).
[122] T. Sun, Z. Y. Zhang, K. T. V. Grattan, and A. W. Palmer, Rev. Sci. Instrum. **68**, 58 (1997).
[123] L. J. Dowell and G. T. Gillies, University of Virginia Technical Report No. UVA/532866/NEEP89/101, October 1988.
[124] C. M. Simmons, D. L. Beshears, and M. R. Cates, Martin Marietta Energy Systems, Inc. Technical Report No. ORNL/ATD-25, February 1990.
[125] D. L. Beshears, G. J. Capps, M. R. Cates, and C. M. Simmons, Martin Marietta Energy Systems, Inc. Technical Report No. ORNL/ATD-44, October 1990.
[126] R. H. Krauss, R. G. Hellier, and J. C. McDaniel, Appl. Opt. **33**, 3901 (1994).
[127] A. Yataghene, M. Himbert, and A. Tardy, Rev. Sci. Instrum. **66**, 3894 (1995).
[128] M. Petrin and A. H. Maki, Rev. Sci. Instrum. **58**, 69 (1987).
[129] F. Anghel, C. Iliescu, K. T. V. Grattan, A. W. Palmer, and Z. Y. Zhang, Rev. Sci. Instrum. **66**, 2611 (1995).
[130] Z. Y. Zhang, K. T. V. Grattan, A. W. Palmer, V. Fernicola, and L. Crovini, Phys. Rev. B **51**, 2656 (1995).
[131] Y. L. Hu, Z. Y. Zhang, K. T. V. Grattan, A. W. Palmer, and B. T. Meggitt, Rev. Sci. Instrum. **67**, 2394 (1996).
[132] J. P. Leroux and R. Taboué, Mes. Regulation, Automat. **40**, 49 (1975).
[133] K. W. Tobin, G. J. Capps, J. D. Muhs, D. B. Smith, and M. R. Cates, Martin Marietta Energy Systems, Inc. Report No. ORNL/ATD-43, August 1990.
[134] G. M. Buck, US Patent No. 4,885,633 (5 December 1989).
[135] G. M. Buck, in Ref. 71, pp. 655–663.
[136] G. M. Buck, American Institute of Aeronautics and Astronautics Paper No. AIAA 91-0064, Burlingame, CA 1991).
[137] D. J. Bizzak and M. K. Chyu, Rev. Sci. Instrum. **65**, 102 (1994).
[138] D. J. Bizzak, Ph.D. dissertation, Carnegie Mellon University, 1993.
[139] L. P. Goss and M. E. Post, U.S. Air Force Office of Scientific Research Technical Report No. 88-0765, April 1, 1988.
[140] J. M. Taliaferro, S. W. Allison, and K. W. Tobin, Martin Marietta Energy Systems, Inc. Technical Report No. ORNL/ATD-61, November 1991.
[141] B. W. Noel, W. D. Turley, M. R. Cates, and K. W. Tobin, Los Alamos National Laboratory Technical Report No. LA-UR-90-1534, May 1990.
[142] J. R. Sweet and W. B. White, Proceedings of the Ninth Rare Earth Conference, Virginia Polytechnic Institute and State University, Blacksburg, VA, 1971, pp. 452–464.
[143] L. P. Goss and A. A. Smith, *Solid-Fuel Propellants: Proceedings of the 21st JANNAF Combustion Meeting* (Chemical Propulsion Information Agency, Johns Hopkins University, Laurel, MD, 1984), pp. 241–249.
[144] L. P. Goss and A. A. Smith, U.S. Air Force Office of Scientific Research Technical Report No. AFOSR-85-0560TR, February 1985.
[145] L. P. Goss, A. A. Smith, and M. E. Post, Rev. Sci. Instrum. **60**, 3702 (1989).
[146] Z. Ghassemlooy, K. T. V. Grattan, and D. Lynch, Rev. Sci. Instr. **60**, 87 (1989).
[147] A. T. Augousti, K. T. V. Grattan, and A. W. Palmer, J. Lightwave Technol. **LT-5**, 759 (1987).
[148] K. T. V. Grattan, J. D. Manwell, S. M. L. Sim, and C. A. Willson, Opt. Commun. **62**, 104 (1987).
[149] K. T. V. Grattan, A. W. Palmer, and C. A. Wilson, J. Phys. E **20**, 1201 (1987).
[150] Z. Y. Zhang and K. T. V. Grattan, J. Lumin. **62**, 263 (1994).
[151] A. T. Augousti, K. T. V. Grattan, and A. W. Palmer, IEEE Trans Instrum. Meas. **37**, 470 (1988).
[152] K. T. V. Grattan and A. W. Palmer, Rev. Sci. Instrum. **56**, 1784 (1985).
[153] K. T. V. Grattan, R. K. Selli, and A. W. Palmer, Rev. Sci. Instrum. **57**, 1175 (1986).
[154] K. T. V. Grattan, R. K. Selli, and A. W. Palmer, Rev. Sci. Instrum. **59**, 256 (1988).
[155] K. T. V. Grattan, J. D. Manwell, S. M. L. Sim, and C. A. Wilson, Proc. IEE **134**, 291 (1987).
[156] K. T. V. Grattan, Measurement **5**, 123 (1987).
[157] R. V. Alves, R. A. Buchanan, and T. G. Maple, Appl. Phys. Lett. **21**, 530 (1972).
[158] W. I. Dobrov and R. A. Buchanan, Appl. Phys. Lett. **21**, 201 (1972).
[159] K. A. Wickersheim and R. A. Buchanan, Appl. Phys. Lett. **17**, 184 (1970).
[160] R. A. Buchanan, K. A. Wickersheim, J. L. Weaver, and L. E. Sobon, Proceedings of the Sixth Rare Earth Research Conference, (Oak Ridge National Laboratory, Oak Ridge, TN, 1967), pp. 271–282.
[161] K. A. Wickersheim, R. A. Buchanan, and E. C. Yates, Proceedings of the

Seventh Rare Earth Research Conference, Clearinghouse for Federal Scientific and Technical Information Document No. CONF-681020 (U.S. Department of Commerce, Washington, DC, 1968), Vol. II, pp. 835–846.
[162] Luxtron Corp., 2775 Northwestern Parkway, Santa Clara, CA 95051-0941.
[163] K. A. Wickersheim, in Ref. 101, Vol. 6, Part 2, pp. 711–714.
[164] M. Sun, in Ref. 101, Vol. 6, Part 2, pp. 715–719.
[165] M. H. Sun, J. H. Kim, and C. L. Sandberg, *Digital Solutions for Industry Science and Technology* (Instrument Society of America, Research Triangle Park, North Carolina, 1985), pp. 79–85.
[166] Fiberoptic Probes and Accessories for Model 790 Systems, Luxtron Corp., Santa Clara, CA, March 1993.
[167] Luxtron Corp., Santa Clara, CA, Technical Note No. TN 86-4, 1986.
[168] Luxtron Corp., Santa Clara, CA, Technical Note No. TN 86-6, 1986.
[169] Luxtron Corp., Santa Clara, CA, Technical Note No. TN 86-7, 1986.
[170] Luxtron Corp., Santa Clara, CA, Technical Note No. TN 86-8, 1986.
[171] V. Fernicola and L. Crovini, Proc. SPIE **2070**, 472 (1994).
[172] V. Fernicola and L. Crovini, Proc. SPIE **2360**, 211 (1994).
[173] E. Maurice, G. Monnom, D. B. Ostrowsky, and G. Baxter, Proc. SPIE **2360**, 219 (1994).
[174] U. P. Wild, A. R. Holzwarth, and H. P. Good, Rev. Sci. Instrum. **48**, 1621 (1977).
[175] J. R. Alcala, E. Grattan and D. M. Jameson, Anal. Instrum. **14**, 225 (1985).
[176] J. R. Alcala, E. Grattan, and F. G. Pendergast, Biophys. J. **51**, 587 (1987).
[177] B. A. Feddersen, D. W. Piston, and E. Grattan, Rev. Sci. Instrum. **60**, 2929 (1989).
[178] J. R. Alcala, Rev. Sci. Instrum. **62**, 1672 (1991).
[179] J. R. Alcala, C. Yu and G. J. Yeh, Rev. Sci. Instrum. **64**, 1554 (1993).
[180] J. R. Alcala, S.-C. Liao, and J. Zheng, IEEE Trans. Biomed. Eng. **42**, 471 (1995).
[181] K. A. Wickersheim, Proc. SPIE **713**, 150 (1987).
[182] K. A. Wickersheim and W. D. Hyatt, Proc. SPIE **1267**, 84 (1990).
[183] K. A. Wickersheim and M. H. Sun, J. Microwave Power **22**, 85 (1987).
[184] K. W. Chan, C. K. Chou, J. A. McDougall, and K. H. Luk, Int. J. Hyperthermia **4**, 699 (1988).
[185] J. S. Nagpal, G. Varadharajan, and P. Gangadharan, Phys. Med. Biol. **27**, 145 (1982).
[186] J. A. Molloy, R. C. Ritter, W. C. Broaddus, M. S. Grady, M. A. Howard III, E. G. Quate, and G. T. Gillies, Med. Phys. **18**, 794 (1991).
[187] T. V. Samulski, in Ref. 101, Vol. 6, Part 2, pp. 1185–1190.
[188] M. H. Ideda, M. H. Sun, and S. R. Phillips, Proc. SPIE **904**, 47 (1988).
[189] M. H. Ideda, M. H. Sun, and S. R. Phillips, Tech. Dig. Ser. **2**, 438 (1988).
[190] S. C. Tjin, D. Kilpatrick, and P. R. Johnston, Opt. Eng. (Bellingham) **34**, 460 (1995).
[191] K. F. Schrum, A. M. Williams, S. A. Haerther, and D. Ben-Amotz, Anal. Chem. **66**, 2788 (1994).
[192] D. R. Shearer and S. Kimball, Proc. SPIE **454**, 169 (1984).
[193] R. H. Morgan, Radiology **43**, 256 (1944).
[194] E. D. Trout and J. P. Kelly, Radiology **110**, 103 (1974).
[195] R. A. Buchanan, M. Tecotzky, and K. A. Wickersheim, U S Patent No. 3, 829, 700 (13 August 1974).
[196] L. Mannik, S. K. Brown, and S. R. Campbell, Proc. Laser Inst. Am. **63**, 23 (1988).
[197] L. Mannik, S. K. Brown, and S. R. Campbell, Appl. Opt. **30**, 2670 (1991).
[198] L. Mannik and S. K. Brown, in Ref. 101, Vol. 6, Part 2, pp. 1243–1248.
[199] J. W. McNutt, J. C. McIver, G. E. Leibinger, D. J. Fallon, and K. A. Wickersheim, IEEE Trans. Power Apparatus Syst. **PAS-103**, 1155 (1984).
[200] K. A. Wickersheim, Proc. SPIE **1584**, 3 (1991).
[201] Luxtron Corp., Santa Clara, CA Applications Note No. AN 86-HV1, 1986.
[202] Luxtron Corp., Santa Clara, CA Applications Note No. AN 86-HV2, 1986.
[203] V. M. Martin, R. M. Sega, and R. Durham, Opt. Lett. Eng (Bellingham) **26**, 170 (1987).
[204] K. Wickersheim, M. Sun, and A. Kamal, J. Microwave Power Electron. Ener. **25**, 141 (1990).
[205] S. Gibes, E. Jensen, M. Sun, and K. Wickersheim, EMC Technol. **6**, 45 (1987).
[206] M. R. Cates, S. W. Allison, L. A. Franks, M. A. Nelson, T. J. Davies, and B. W. Noel, Proc. Laser Inst. Am. **39**, 50 (1984).
[207] M. R. Cates, S. W. Allison, B. R. Marshall, L. A. Franks, T. J. Davies, M. A. Nelson, B. W. Noel, Proc. Laser Inst. Am. **45**, 4 (1985).
[208] B. W. Noel, H. M. Borella, L. A. Franks, B. R. Marshall, S. W. Allison, and M. R. Cates, AIAA J. Propulsion Power **2**, 565 (1986).
[209] B. W. Noel, H. M. Borella, L. A. Franks, B. R. Marshall, S. W. Allison, and M. R. Cates, American Institute of Aeronautics and Astronautics Paper No. AIAA 85-1468, Burlingame, CA, 1985.
[210] B. W. Noel, S. W. Allison, D. L. Beshears, M. R. Cates, H. M. Borella, L. A. Franks, C. E. Iverson, S. S. Lutz, B. R. Marshall, M. B. Thomas, W. D. Turley, L. J. Dowell, G. T. Gillies, and W. N. Lutz, American Institute of Aeronautics and Astronautics Paper No. AIAA 87–1861, Burlingame, CA, 1987.
[211] B. W. Noel, M. C. Bibby, H. M. Borella, S. E. Woodruff, C. L. Hudson, S. S. Lutz, W. D. Turley, S. W. Allison, D. L. Beshears, M. R. Cates, J. D. Muhs, and K. W. Tobin, American Institute of Aeronautics and Astronautics Paper No. AIAA 89-2913, Burlingame, CA, 1989.
[212] B. W. Noel, H. M. Borella, W. Lewis, W. D. Turley, D. L. Beshears, G. J. Capps, M. R. Cates, J. D. Muhs, and K. W. Tobin, ASME J. Eng. Gas Turbines Power **113**, 242 (1991).
[213] B. W. Noel and W. D. Turley, Los Alamos National Laboratory Technical Report No. LA-CP-91-0350, October 1991.
[214] B. W. Noel, W. D. Turley, W. Lewis, K. W. Tobin, and D. L. Beshears, in Ref. 101, Vol. 6, Part 2, pp. 1249–1254.
[215] B. W. Noel, W. D. Turley, and W. Lewis, Los Alamos National Laboratory Report No. LA-UR-92-4227, 1993.
[216] K. W. Tobin, S. W. Allison, M. R. Cates, G. J. Capps, D. L. Beshears, and M. Cyr, American Institute of Aeronautics and Astronautics Paper No. AIAA 88-3143, Burlingame, CA, 1989.
[217] B. W. Noel, W. D. Turley, and S. W. Allison, *Proceedings of the 40th International Instrumentation Symposium* (Instrument Society of America, Research Triangle Park, NC, 1994), pp. 271–288.
[218] S. W. Allison, M. R. Cates, M. B. Scudiere, H. T. Bentley, H. M. Borella, and B. R. Marshall, Proc. SPIE **788**, 90 (1987).
[219] K. W. Tobin, S. W. Allison, M. R. Cates, G. J. Capps, D. L. Beshears, M. Cyr, and B. W. Noel, AIAA J. **28**, 1485 (1990).
[220] K. W. Tobin, M. R. Cates, D. L. Beshears, J. D. Muhs, G. J. Capps, D. B. Smith, W. D. Turley, H. M. Borella, W. F. O'Brian, R. J. Roby, and T. T. Anderson, Martin Marietta Energy Systems, Inc. Technical Report No. ORNL/ATD-31, May 1990.
[221] S. W. Allison, M. R. Cates, G. J. Pogatshnik, and A. R. Bugos, Martin Marietta Energy Systems, Inc. Technical Report No. ORNL/ATD-21, January 1990.
[222] W. Lewis, W. D. Turley, H. M. Borella, and B. W. Noel, *Proceedings of the 36th International Instrumentation Symposium: Instrumentation for the Aerospace Industry* (Instrument Society of America, Research Triangle Park, NC, 1990), pp. 23–27.
[223] N. Domingo, Martin Marietta Energy Systems, Inc. Technical Report No. ORNL/TM-11816, June 1991.
[224] S. Alaruri, D. McFarland, A. Brewington, M. Thomas, and N. Sallee, Opt. Lasers Eng. **22**, 17 (1995).
[225] R. W. Phillips and S. D. Tilstra, in Ref. 101, Vol. 6, Part 2, pp. 721–724.
[226] A. J. Simons, I. P. McClean, and R. Stevens, Electron. Lett. **32**, 253 (1996).
[227] B. W. Noel, W. D. Turley, and K. W. Tobin, Los Alamos National Laboratory Technical Report No. LA-CB-91-0182, April 1991.
[228] W. D. Turley, H. M. Borella, B. W. Noel, A. Beasley, W. K. Sartory, and M. R. Cates, Los Alamos National Laboratory Technical Report No. LA-11408-MS, January 1989.
[229] E. Abraham and J. M. Halley, Appl. Phys. A **42**, 279 (1987).
[230] G. A. Webster, Ph.D. dissertation, University of Illinois–Urbana, 1979.
[231] G. A. Webster and H. G. Drickamer, J. Chem. Phys. **72**, 3740 (1980).
[232] G. R. Haugen, Lawrence Livermore National Laboratory Technical Report No. UCID-20922, November 1986.
[233] W. Lizhong, Z. Zaixuan, C. Yuanbin, and L. Shensin, in *High Pressure in Science and Technology, Proceedings of the 9th AIRAPT International High Pressure Conference*, edited by C. Homan, R. K. MacCrone, and E. Whalley (North-Holland, New York, 1984), Part 3, pp. 345–348.
[234] Y. M. Gupta and X. A. Shen, Appl. Phys. Lett. **58**, 583 (1991).
[235] H. Liu, K. Lim, W. Jia, E. Strauss, and W. M. Yen, Opt. Lett. **13**, 931 (1988).
[236] W. L. Vos and J. A. Schouten, J. Appl. Phys. **69**, 6744 (1991).
[237] T. P. Beales and C. H. L. Goodman, High Temp.-High Press. **21**, 227 (1990).
[238] Y. Chi, S. Liu, W. Shen, L. Wang, G. Zou, Physica B & C **139&140**, 555 (1986).

[239] S. Liu, Y. Chi, L. Ma, L. Wang, and G. Zou, Physica B & C **139&140**, 559 (1986).
[240] H. Arashi and M. Ishigame, Jpn. J. Appl. Phys. 1 **21**, 1647 (1982).
[241] W. D. Drotning and H. G. Drickamer, Phys. Rev. B **13**, 4568 (1976).
[242] W. O. Seals, H. W. Offen, W. D. Turley, and H. M. Borella, in *The 24th JANNAF Combustion Meeting*, CPIE Publication No. 476, edited by D. L. Becker (Chemical Propulsion Information Agency, Johns Hopkins University, Laurel, MD, 1987), Vol. II, pp. 339–349.
[243] S. W. Allison, G. J. Capps, D. B. Smith, M. R. Cates, W. D. Turley, and J. Gleason, Electric Power Research Institute Technical Report No. TR-103867, June 1994.
[244] J. K. Gleason, M.Sc. thesis, University of California at Santa Barbara, 1992.
[245] S. W. Allison, M. R. Cates, M. L. Simpson, B. W. Noel, D. W. Turley and G. T. Gillies, Proc. Laser Inst. Am. **66**, 131 (1989).
[246] R. J. Prins, G. Laufer, R. H. Krauss, and S. Narasimhan, American Institute of Aeronautics and Astronautics Paper No. AIAA 95-0482 Burlingame, CA, 1995.
[247] R. J. Prins, M.Sc. thesis, University of Virginia, 1995.
[248] M. L. Simpson and D. E. Welch, Exp. Mech. **27**, 37 (1987).
[249] J. Gallery, M. Gouterman, J. Callis, G. Khalil, B. McLachlan, and J. Bell, Rev. Sci. Instrum. **65**, 712 (1994).
[250] H. Hoshinori and H. Hiroaki, J. Non-Cryst. Solids **107**, 23 (1988).
[251] S. W. Allison, J. D. Muhs, D. J. Adams, G. J. Capps, M. R. Cates, and B. L. Johnson, Proc. SPIE **987**, 20 (1988).
[252] C. O. Egalon and R. S. Rogowski, Opt. Eng. (Bellingham) **31**, 1332 (1992).
[253] N. Nakatani, K. Fujiwara, M. Matsumoto, and T. Yamada, J. Phys. E **8**, 1042 (1975).
[254] N. Nakatani, M. Matsumoto, Y. Ohmi, and T. Yamada, J. Phys. E **10**, 172 (1977).
[255] N. Nakatani and T. Yamada, in *Flow Visualization II: Proceedings of the Second International Symposium on Flow Visualization*, edited by W. Merzkirch (Hemisphere, New York, 1980), pp. 215–219.
[256] J. J. Keyes, Jr. and W. K. Sartory, Martin Marietta Energy Systems, Inc. Technical Report No. K-ETAC-80, 1988.
[257] J. B. Birks and F. A. Black, Proc. Phys. Soc. London, Sec. A **64**, 511 (1951).
[258] J. B. Birks, *Theory and Practice of Scintillation Counting* (Macmillan, New York, 1964).
[259] W. A. Hollerman, J. H. Fisher, G. A. Shelby, L. R. Holland, and G. M. Jenkins, IEEE Trans. Nucl. Sci. **38**, 184 (1991).
[260] W. A. Hollerman, J. H. Fisher, G. A. Shelby, L. R. Holland, and G. M. Jenkins, IEEE Trans. Nucl. Sci. **39**, 2295 (1992).
[261] W. A. Hollerman, G. M. Jenkins, J. H. Fisher, L. R. Holland, E. K. Williams, H. Maleki, and C. C. Foster, J. Nucl. Mater. **224**, 314 (1995).
[262] J. M. Draina and R. L. Anderson, in Ref. 101, Vol. 6, Part 2, pp. 1135–1138.
[263] M. K. Chyu and D. J. Bizzak, J. Heat Transfer **116**, 263 (1994).
[264] P. Kolodner and J. A. Tyson, Appl. Phys. Lett. **40**, 782 (1982).
[265] P. Kolodner and J. A. Tyson, Appl. Phys. Lett. **42**, 117 (1983).
[266] P. Kolodner, A. Katzir, and N. Hartsough, Appl. Phys. Lett. **42**, 49 (1983).
[267] S. W. Allison, Martin Marietta Energy Systems, Inc. Technical Report No. K/ETAC-38, October 1987.
[268] T. K. Robinson and J. W. Beams, Rev. Sci. Instrum. **34**, 63 (1963).
[269] R. A. Felice, Ind. Heat. **62**, 74 (1995).
[270] U. Anselmi-Tamburini, G. Campari, and G. Spinolo, Rev. Sci. Instrum. **66**, 5006 (1995).
[271] D. M. Cunningham, S. W. Allison, and D. B. Smith, Martin Marietta Energy Systems, Inc. Technical Report No. ORNL/ATD-70, January 1993.
[272] S. W. Allison, L. A. Boatner, and G. T. Gillies, Appl. Opt. **34**, 5624 (1995).
[273] C. O. Egalon and R. S. Rogowski, Opt. Eng. (Bellingham) **31**, 237 (1992).
[274] C. O. Egalon, R. S. Rogowski, and A. C. Tal, Opt. Eng. (Bellingham) **31**, 1328 (1992).
[275] S. Albin, A. L. Bryant, C. O. Egalon, and R. S. Rogowski, Opt. Eng. (Bellingham) **33**, 1172 (1994).
[276] C. K. Ma, Rev. Sci. Instrum. **66**, 4233 (1995).
[277] L. J. Dowell, G. T. Gillies, A. R. Bugos, and S. W. Allison, Proc. Laser Inst. Am. **66**, 122 (1989).
[278] A. R. Bugos, S. W. Allison, and M. R. Cates, *IEEE Southeastern: Energy and Information Technologies in the Southeast* (IEEE, New York, 1989), pp. 361–365.
[279] F. Cabannes, V. T. Loc, J. P. Coutures, and M. Foex, High Temp.-High Press. **8**, 391 (1976).
[280] T. P. Jones, National Measurement Laboratory of Australia (private communication, 1993).
[281] D. E. Holcomb and R. L. Shepard, Oak Ridge National Laboratory (private communication, 1994).